INSTITUTUL
DE
MATEMATICA

INSTITUTUL NATIONAL
PENTRU CREATIE
STIINTIFICA SI TEHNICA

ISSN 0250 3638

SOME DEVELOPEMENTS AND APPLICATIONS OF THE BEM

with the contribution of

D.Homentcovschi, R.Magureanu, D.Cocora,
L.Kreindler, N.Vasile, M.Tiba,
A.Manolescu and A.M.Manolescu

NO. 25 / 1987

BUCURESTI

SOME DEVELOPEMENTS AND APPLICATIONS OF THE BEM

with the contribution of

D.Homentcovschi*), R.Magureanu*), D.Cocora***),
L.Kreindler*), N.Vasile**), M.Tiba**),
A.Manolescu*) and A.M.Manolescu*)

June 1987

*) Polytechnic Institute of Bucharest,
313 Splaiul Independentei, Bucharest, ROMANIA

**) I C P E Bucharest, 45-47 T. Vladimirescu,
Bucharest, ROMANIA

***) I P C T Bucharest, 21 T. Arghezi,
Bucharest, ROMANIA

1. An Introduction to BEM by Integral Transforms

D. Homentcovschi

2. An Interactive Programme for Solving Mixed BVP for the 2D - Laplace Equation by CVBEM

D. Homentcovschi, D. Cocora, R. Magureanu

3. Complex Variable Spline Boundary Element Method

D. Homentcovschi, L.Kreindler

4. An Analytic Solution to the Poisson Equation in some plane Domains

D.Homentcovschi

5. An Analytical Solution for the coupled Stripline-like Microstrip Lines Problem

D. Homentcovschi, A. Manolescu, A.M. Manolescu, L.Kreindler

6. Calculation of the magnetic field and parameters of synchronous motors with ceramic permanent magnets using the BEM

R.Magureanu, N.Vasile, M.Tiba

AN INTRODUCTION TO BEM BY INTEGRAL TRANSFORMS

Dorel Homentcovschi

Polytechnic Institute of Bucharest,
Department of Mathematics,
313 Splaiul Independentei,
Bucharest, Romania

An Introduction to BEM by Integral Transforms

The paper gives a new method for obtaining the fundamental integral setting used in BEM. The method is based on integral transforms and can be applied to all linear differential equations with constant coefficients.

1. Introduction

The BEM proved to be a very efficient tool in solving boundary-value problems involved in engineerig. The key-point of the method is the fundamental integral representation of the solution $u(\vec{x})$ inside the domain D by means of the boundary values $u(x')$ and of the 'flux values' $q(x')$. By means of this formula the boundary integral equation of the problem is written. Further on, the system of algebraic equations obtained by discretization of the integral equation is solved. The solution at points inside D is obtained by using the fundamental integral representation once more.

We are pointing out two ways of obtaining the fundamental integral formulation for a given partial differential equation. The classical way is based on reciprocity relationships established for some differential operators. The second method was given by Brebbia /1/ and is justified by weighted residual arguments. This latter method is more general and permits a straightforward extension to more complex differential equations.

In this paper we give a new method for obtaining the fundamental integral representation based on integral transforms.

The integral transforms are often used by electrical engineers (and not only by them) to solve ordinary differential equations and partial differential equations for regular boundary domains: the halfspace, the halfplane, the strip, etc. We shall show that in the case of irregular boundary domains the Fourier transform straightforwardly provides the integral representation formula for the solution in terms of the boundary values. The advantages of applying this approach to boundary-value problems are the simplicity of the method (especially for the people in the electrical engineering field who are familiar with operational methods) and its applicability to all linear partial differential equations with constant coefficients.

In what follows in order to show how our method operates the presentation of three worked examples is preferred to the general theory.

2. The Fourier Transform in Two and Three Variables

The one-dimensional Fourier transform can be generalised to the case of three independent variables by the relation

$$\hat{f}(\vec{k}) \equiv \mathcal{F}\{f(\vec{x})\} = \iiint f(\vec{x})\, e^{-i\vec{k}\cdot\vec{x}}\, d^3\vec{x} \qquad (2.1)$$

where $\vec{x} = x\vec{i} + y\vec{j} + z\vec{k}$, $\vec{k} = k_1\vec{i} + k_2\vec{j} + k_3\vec{k}$, $d^3x = dx\,dy\,dz$ and $\vec{k}\cdot\vec{x}$ is the scalar product of the two vectors. If the function $f(\vec{x})$ complies with some Dirichlet-type requirements in every bounded domain and is absolutely integrable in the whole space, we also have the inversion formula

(2.2)

valid at all points where the function $f(\vec{x})$ is continuous. In case $\vec{x} \in \Sigma$ where Σ is a surface of discontinuity of the function $f(\vec{x})$, the left-hand side of relation (2.2) must be replaced by the Dirichlet sum

$$\frac{f(\vec{x}+0) + f(\vec{x}-0)}{2}$$

where $f(\vec{x}+0)$, $f(\vec{x}-0)$ are the two limit values of the function $f(\vec{x})$ at point $\vec{x}$ when approaching this point from different sides of the surface of discontinuity.

Now let $f(\vec{x})$ be zero outside the domain D, bounded by the surface Σ, and differentiable at every point inside D. We have

$$\mathcal{F}\left\{\frac{\partial f}{\partial x}\right\} = \iiint \frac{\partial f}{\partial x} e^{-i\vec{k}\cdot\vec{x}}\, d^3\vec{x} = \iiint_D \frac{\partial}{\partial x}\left(f(\vec{x})\, e^{-i\vec{k}\cdot\vec{x}}\right) d^3\vec{x} + \\ + ik_1 \iiint_D f(\vec{x})\, e^{-i\vec{k}\cdot\vec{x}}\, d^3\vec{x} \qquad (2.3)$$

By appplying the divergence formula, we have

$$\iiint_D \frac{\partial}{\partial x}\left(f e^{-i\vec{k}\cdot\vec{x}}\right) d^3\vec{x} = \iint_\Sigma n_x f(\vec{x})\, e^{-i\vec{k}\cdot\vec{x}}\, d\sigma$$

Relation (2.3) becomes

$$\mathcal{F}\left\{\frac{\partial f}{\partial x}\right\} = ik_1\, \mathcal{F}\{f\} + \iint_\Sigma n_x f(\vec{x})\, e^{-i\vec{k}\cdot\vec{x}}\, d\sigma \qquad (2.4)$$

By means of this relation we can prove the following formulae

$$\mathcal{F}\{\operatorname{grad} f\} = i\vec{k}\cdot\hat{f} + \iint_\Sigma \vec{n} f(\vec{x})\, e^{-i\vec{k}\cdot\vec{x}}\, d\sigma$$
$$\mathcal{F}\{\operatorname{div}\vec{V}\} = i\vec{k}\cdot\hat{\vec{V}} + \iint_\Sigma \vec{n}\cdot\vec{V}\, e^{-i\vec{k}\cdot\vec{x}}\, d\sigma \qquad (2.5)$$
$$\mathcal{F}\{\operatorname{rot}\vec{V}\} = i\vec{k}\times\hat{\vec{V}} + \iint_\Sigma \vec{n}\times\vec{V}\, e^{-i\vec{k}\cdot\vec{x}}\, d\sigma$$

Here $\vec{V}$ is a vector field vanishing outside D and belonging to the class $C^{(1)}$ in the domain.

Now let us define the convolution product

$$f*g = \iiint f(\vec{x}')\, g(\vec{x}-\vec{x}')\, d^3\vec{x}'$$

It can be easily proved that we have

$$\mathcal{F}\{f*g\} = \mathcal{F}\{f\}\cdot\mathcal{F}\{g\} \qquad (2.6)$$

Next we shall consider two examples.

i) Let $k^2 = k_1^2 + k_2^2 + k_3^2$. We have

$$\mathcal{F}^{-1}\left\{\frac{1}{k^2}\right\} = \frac{1}{(2\pi)^3}\iiint \frac{1}{k^2}\, e^{i\vec{k}\cdot\vec{x}}\, d^3\vec{k}$$

To calculate this integral we shall use a spherical system of coordinates with a polar axis in the direction of the vector $\vec{x}$. Therefore we have

$$\vec{k}\cdot\vec{x} = kr\cos\theta, \qquad r^2 = x^2 + y^2 + z^2$$

$$d^3\vec{k} = k^2 \sin\theta\, dk d\theta d\varphi$$

and the above integral becomes

$$\mathcal{F}^{-1}\left\{\frac{1}{k^2}\right\} = \frac{1}{(2\pi)^2}\int_0^\infty dk \int_0^\pi \exp\{ikz\cos\theta\}\sin\theta\, d\theta =$$

$$= \frac{1}{(2\pi)^2}\int_0^\infty \frac{e^{ikz} - e^{-ikz}}{ikz}\, dk = \frac{1}{4\pi^2 z}\int_0^\infty \frac{\sin kz}{k}\, dk$$

But we have

$$\int_0^\infty \frac{\sin x}{x}\, dx = \pi$$

Finally we obtain

$$\mathcal{F}^{-1}\left\{\frac{1}{k^2}\right\} = \frac{1}{4\pi z} = \frac{1}{4\pi|\vec{x}|} \qquad (2.7)$$

ii) As a second example we shall determine the inverse Fourier transform (in two variables) of the function

$$\hat{f}(k_1, k_2) = \frac{1}{k_1 + i k_2}$$

We have

$$f(x,y) = \frac{1}{(2\pi)^2} \int_{-\infty}^{+\infty} e^{ik_2 y}\, dk_2 \int_{-\infty}^{\infty} \frac{e^{ik_1 x}}{k_1 + i k_2}\, dk_1$$

The inner integral is

$$\frac{1}{2\pi} \int_{-\infty}^{+\infty} \frac{e^{ik_1 x}}{k_1 + i k_2}\, dk_1 = \begin{cases} i\, e^{k_2 x}\, h(x) & , \quad k_2 > 0 \\ -i\, e^{k_2 x}\, h(-x) & , \quad k_2 < 0 \end{cases}$$

where h(x) is the Heaviside function. This equality can be checked up directly by taking the Fourier transform of the function in the right-hand side (or alternatively by using the residue theorem). Further on, we have

$$f(x,y) = \frac{i}{2\pi} \left\{ \int_{-\infty}^{0} e^{k_2 x}\, e^{ik_2 y}\, h(x)\, dk_2 - \int_{0}^{\infty} e^{k_2 x}\, e^{ik_2 y}\, h(-x)\, dk_2 \right\}$$

$$= \frac{i}{2\pi} \frac{h(x) + h(-x)}{x + iy}$$

Finally we obtain

$$\mathcal{F}^{-1}\left\{ \frac{1}{k_1 + i k_2} \right\} = \frac{i}{2\pi z} \qquad (2.8)$$

where z = x + iy is a complex variable.

3. Green's Formula

We consider the Poisson equation

$$-\Delta u(x,y,z) = \rho(x,y,z), \quad (x,y,z) \in D \qquad (3.1)$$

where D is the domain bounded by the surface Σ. We can write

$$\mathcal{F}\{\Delta u\} = \mathcal{F}\{\operatorname{div}\operatorname{grad} u\} = i\vec{k} \cdot \mathcal{F}\{\operatorname{grad} u\} +$$

$$+ \iint_S \vec{n} \cdot \operatorname{grad} u\, e^{-i\vec{k}\cdot\vec{x}}\, d\sigma = i\vec{k} \cdot \{ i\vec{k} \cdot \hat{u} + \iint_\Sigma \vec{n} u\, e^{-i\vec{k}\cdot\vec{x}}\, d\sigma \}$$

$$+ \iint_\Sigma \frac{\partial u}{\partial n} e^{-i\vec{k}\cdot\vec{x}}\, d\sigma$$

The Fourier transform of equation (3.1) is

$$k^2 \hat{u} - i\vec{k} \cdot \iint_\Sigma \vec{n}\, u\, e^{-i\vec{k}\cdot\vec{x}}\, d\sigma - \iint_\Sigma \frac{\partial u}{\partial n} e^{-i\vec{k}\cdot\vec{x}}\, d\sigma = \hat{\rho}$$

Hence

$$\hat{u}(\vec{k}) = \frac{1}{k^2}\cdot\hat{\rho}(\vec{k}) + \frac{1}{k^2}\iint_\Sigma \frac{\partial u}{\partial n} e^{-i\vec{k}\cdot\vec{x}}\, d\sigma + \frac{i\vec{k}}{k^2}\iint_\Sigma \vec{n}\, u\, e^{-i\vec{k}\cdot\vec{x}}\, d\sigma \qquad (3.2)$$

The inverse Fourier transform of the first term in the right-hand side of relation (3.2) is the convolution product $\rho(\vec{x}) * (4\pi|\vec{x}|)^{-1}$.

We shall now determine the inverse transforms of the other terms

$$u^{(1)}(x,y,z) \equiv \mathcal{F}^{-1}\left\{ \frac{1}{k^2} \iint_\Sigma \frac{\partial u'}{\partial n'} e^{-i\vec{k}\cdot\vec{x}'}\, d\sigma' \right\} = \frac{1}{(2\pi)^3} \iiint \frac{e^{i\vec{k}\cdot\vec{x}}}{k^2}\, d^3\vec{k} \cdot$$

$$\cdot \iint_\Sigma \frac{\partial u'}{\partial n'} e^{-i\vec{k}\cdot\vec{x}'}\, d\sigma' = \iint_\Sigma \frac{\partial u'}{\partial n'} d\sigma' \cdot \frac{1}{(2\pi)^3} \iiint \frac{e^{i\vec{k}(\vec{x}-\vec{x}')}}{k^2}\, d^3\vec{k}$$

The last integral in this formula is given by relation (2.6) and therefore

$$u^{(1)}(x,y,z) = \frac{1}{4\pi} \iint_\Sigma \frac{\partial u'}{\partial n'} \frac{1}{|\vec{x}-\vec{x}'|}\, d\sigma'$$

Then we have

$$u^{(2)}(x,y,z) \equiv \frac{1}{(2\pi)^3} \iiint \frac{i\vec{k}}{k^2} e^{i\vec{k}\cdot\vec{x}}\, d^3\vec{k} \iint_\Sigma \vec{n}'\, u(\vec{x}')\, e^{-i\vec{k}\cdot\vec{x}'}\, d\sigma'$$

By changing the order of integration this relation becomes

$$u^{(2)}(x,y,z) = \iint_\Sigma \vec{n}'\, u'\, d\sigma' \; \frac{1}{(2\pi)^3} \iiint \frac{i\vec{k}}{k^2} e^{i\vec{k}(\vec{x}-\vec{x}')}\, d^3\vec{k}$$

We can write

$$\frac{1}{(2\pi)^3} \iiint \frac{i\vec{k}}{k^2} e^{i\vec{k}(\vec{x}-\vec{x}')}\, d^3\vec{k} = \operatorname{grad} \frac{1}{(2\pi)^3} \iiint \frac{e^{i\vec{k}(\vec{x}-\vec{x}')}}{k^2}\, d^3\vec{k}$$

$$= \operatorname{grad}\left(4\pi|\vec{x}-\vec{x}'| \right)^{-1}.$$

But

$$\text{grad } (|\vec{x} - \vec{x}'|)^{-1} = - \text{grad}' (|\vec{x} - \vec{x}'|)^{-1}$$

and therefore

$$u^{(2)}(x,y,z) = - \frac{1}{4\pi} \iint_{\Sigma} \mu' \frac{\partial}{\partial n'} \left(\frac{1}{|\vec{x} - \vec{x}'|} \right) d\sigma'$$

Finally, the inverse Fourier transform of relation (3.2) is

$$c\,u(x,y,z) = \frac{1}{4\pi} \iiint_{D} \frac{\rho(\vec{x}')}{|\vec{x} - \vec{x}'|} d^3\vec{x}' + \frac{1}{4\pi} \iint_{\Sigma} \frac{\partial u'}{\partial n'} \frac{1}{|\vec{x} - \vec{x}'|} d\sigma' -$$

$$- \frac{1}{4\pi} \iint_{\Sigma} \mu' \frac{\partial}{\partial n'} \left(\frac{1}{|\vec{x} - \vec{x}'|} \right) d\sigma' \qquad (3.3)$$

Here c=1 for points inside D. If we have the point $\vec{x}_0 \in \Sigma$, by the discussion in section 2, the left-hand side of relation (3.3) must be

$$\frac{u(\vec{x}_0 + 0) + u(\vec{x}_0 - 0)}{2} = \frac{1}{2} u(x_0)$$

Hence constant c equals 1/2 for points on q. If point x is outside D, we have c=0.

Relation (3.3) is just Green's formula of the three potentials.

4. A Vectorial Green Formula

Let us now consider the system of equations

$$\begin{cases} \text{div } \vec{V} = \rho \\ \text{rot } \vec{V} = \vec{J} \qquad \text{in D} \end{cases} \qquad (4.1)$$

where ρ and $\vec{J}$ are given functions. This system of equations occurs in many problems of steady-state fields in homogeneous and isotropic media.

By taking the Fourier transform of the system (3.1), we obtain

$$\begin{cases} i\vec{k}\cdot\hat{\vec{V}} + \iint_\Sigma \vec{n}\cdot\vec{V}\, e^{-i\vec{k}\cdot\vec{x}}\, d\sigma = \hat{\rho} \\ i\vec{k}\times\hat{\vec{V}} + \iint_\Sigma \vec{n}\times\vec{V}\, e^{-i\vec{k}\cdot\vec{x}}\, d\sigma = \hat{\vec{J}} \end{cases} \qquad (3.2)$$

The solution of this algebraic system can be obtained by means of the vectorial identity

$$i\vec{k}\times(i\vec{k}\times\hat{\vec{V}}) = i\vec{k}(i\vec{k}\cdot\hat{\vec{V}}) + k^2\hat{\vec{V}}$$

We obtain

$$\hat{\vec{V}}(\vec{k}) = -i\vec{k}\cdot\frac{1}{k^2}\left\{\hat{\rho} - \iint_\Sigma \vec{n}\cdot\vec{V}\, e^{-i\vec{k}\cdot\vec{x}}\, d\sigma\right\} + i\vec{k}\times\frac{1}{k^2}\left\{\vec{J} - \iint_\Sigma \vec{n}\times\vec{V}\, e^{-i\vec{k}\cdot\vec{x}}\, d\sigma\right\}$$

By using the Fourier transform properties given in section 2, we obtain

$$c\vec{V}(\vec{x}) = -\operatorname{grad}\left\{\frac{1}{4\pi}\iiint \frac{\rho(\vec{x}')}{|\vec{x}-\vec{x}'|}\, d^3\vec{x}' - \frac{1}{4\pi}\iint_\Sigma \vec{V}'\cdot\vec{n}'\, \frac{d\sigma'}{|\vec{x}-\vec{x}'|}\right\} + \operatorname{rot}\left\{\frac{1}{4\pi}\iiint \frac{\vec{J}(\vec{x}')}{|\vec{x}-\vec{x}'|}\, d^3\vec{x}' - \frac{1}{4\pi}\iint_\Sigma \vec{n}'\times\vec{V}'\, \frac{d\sigma'}{|\vec{x}-\vec{x}'|}\right\}$$

This formula was obtained by a different method by C.Jacob /2/. It gives a representation of the vectorial field $\vec{V}$ by means of the divergence and rotor values ρ and $\vec{J}$ and also by values of the normal and tangential components of $\vec{V}$ on the surface Σ. It can be used to obtain the boundary integral equations when the normal or the tangential component of $\vec{V}$ is given.

5. Pompei's Formula

Now let us consider the complex equation

$$\frac{\partial f(z,\bar{z})}{\partial \bar{z}} = g(z,\bar{z}) \qquad \text{in } D \qquad (5.1)$$

where $z = x + iy$, $\bar{z} = x - iy$, $g(z,\bar{z})$ are given functions and

$$\frac{\partial f}{\partial \bar{z}} = \frac{1}{2}\left(\frac{\partial f}{\partial x} + i\frac{\partial f}{\partial y}\right)$$

By taking the Fourier transform of the relation (5.1) (assuming zero values for f outside the domain D), we obtain

$$(ik_1 - k_2)\hat{f}(k_1,k_2) + \int_C (n_x + i n_y) f(z,\bar{z})\, e^{-i(k_1 x + k_2 y)}\, ds \equiv 2\pi \hat{g}(k_1,k_2) \qquad (5.2)$$

Here C is the boundary curve of the domain D.

We also have

$$n_x + i n_y = \frac{dx}{dn} + i\frac{dy}{dn} = \frac{dy}{ds} - i\frac{dx}{ds} = -i\left(\frac{dx}{ds} + i\frac{dy}{ds}\right) = -i\frac{dz}{ds}$$

Equation (4.2) gives

$$\hat{f}(k_1,k_2) = \frac{2}{i(k_1+ik_2)}\hat{g}(k_1,k_2) + \frac{1}{k_1+ik_2}\int_C f(z',\bar{z}')\, e^{-i(k_1x'+k_2y')}\, dz'$$

The inverse Fourier transform of the first term is $g*(i\pi z)^{-1}$. The other term gives

$$\mathcal{F}^{-1}\left\{\frac{1}{k_1+ik_2}\int_C f' e^{-i(k_1x'+k_2y')}\, dz'\right\} = \frac{1}{(2\pi)^2}\iint \frac{e^{i(k_1x+k_2y)}}{k_1+ik_2}\, dk_1 dk_2 \cdot$$

$$\cdot \int_C f' e^{-i(k_1x'+k_2y')}\, dz' =$$

$$= \int_C f(z',\bar{z}')\, dz' \frac{1}{(2\pi)^2}\iint \frac{e^{i[k_1(x-x')+k_2(y-y')]}}{k_1+ik_2}\, dk_1\, dk_2$$

The last integral in the above relation can be obtained by means of relation (2.7). Finally we obtain

$$c f(z,\bar{z}) = \frac{1}{\pi}\iint_D \frac{g(z',\bar{z}')}{z-z'}\, dx'dy' + \frac{1}{2\pi i}\int_C \frac{f(z',\bar{z}')}{z'-z}\, dz' \qquad (5.3)$$

Formula (5.3) is just the integral formula obtained by D.Pompei in 1912 /3/. For $g(z,\bar{z})=0$ the function f(z) is holomorphic in D

and the relation (5.3) reduces to Cauchy's integral formula. This formula was used in developing the CVBEM /4/.

References

/1/ Brebbia,C.A., The Boundary Element Method for Engineers, Pentech Press, London, 1978.

/2/ Jacob,C., Comptes Rendus, Paris, t.226, 1948, p.1793.

/3/ Pompei,D., Rend circolo mat. Palermo, t.33, 1912, p.108.

/4/ Hromadka II, T.V., The Complex Variable Boundary Element Method, Springer-Verlag, New York, 1904.

AN INTERACTIVE PROGRAMME FOR SOLVING MIXED BVP FOR THE 2D-LAPLACE EQUATION BY CVBEM

Dorel Homentcovschi

Polytechnic Institute of Bucharest,
Department of Mathematics,
313 Splaiul Independentei,
Bucharest, Romania

Dan Cocora

Design Institute for Typified Buildings
21, T.Arghezi,
Bucharest, Romania

Razvan Magureanu

Polytechnic Institute of Bucharest,
Department of Electrical Engineering
313 Splaiul Independentei,
Bucharest, Romania

An Interactive Programme for Solving Mixed BVP for the 2D-Laplace Equation by CVBEM

D.Homentcovschi; D.Cocora, R.Magureanu

Polytechnic Institute of Bucharest, ICPE Bucharest, Roumania

Abstract: MIXED is a programme for solving the mixed Dirichlet-Neumann Boundary-Value Problem (BVP) for the Laplace equation in plane domains. It is based on transforming the problem into a modified Volterra BVP and next, on solving this problem by means of the Complex Variable Boundary Element Method (CVBEM). The programme furnishes the complete potential function. It also incorporates an error estimating algorithm which determines the error in matching the boundary data.

The Statement of the Problem

Many physical problems are modelled by the Laplace equation. Here we mention the steady-states of the electromagnetic fields and the steady, vortex-free motions of incompressible fluids. In the last years, the Boundary Element Method (BEM) proved to be a very efficient tool for solving such problems /1/. However, in the case of the 2D problems, the complex variable theory is a very suitable method for approaching the boundary value problems for harmonic functions. A numerical treatment based on the complex variable theory, known as the Complex Variable Boundary Element Method, was developed in /2/. The method given in /3/ constitutes a numerical treatment of the complex variable approach for solving mixed BVP for the Laplace equation. The programme MIXED that we are presenting here is a numerical implementation of this method.

Let the boundary Γ of the simply-connected domain Ω be divided into 2p arcs by the points $z(I(1))$, $z(J(1))$, ..., $z(I(p))$, $z(J(p))$. We denote:

$$\Gamma_u = \bigcup_{k=1}^{p} z(I(k))\, z(J(k)), \quad \Gamma_v = \Gamma - \Gamma_u$$

The mixed Dirichlet-Neumann BVP consists in determining the function $u(x,y)$ which meets the conditions

$$\Delta u(x,y) = 0 \qquad \text{in } \Omega \qquad (1)$$

$$u(x,y) = \tilde{u}(s) \qquad \text{on } \Gamma_u \qquad (2)$$

$$\frac{\partial u}{\partial n}(x,y) = \tilde{v}_1(s) \qquad \text{on } \Gamma_v \qquad (3)$$

where s is the curvilinear abscissa on the curve, $\partial/\partial n$ is the derivative in the direction of the external normal and $\tilde{u}(s)$, $\tilde{v}_1(s)$ are two given functions.

Let $v(x,y)$ be the harmonic conjugate function of $u(x,y)$. The complex function

$$f(z) = u(x,y) + iv(x,y)$$

is a holomorphic function on the variable $z = x + iy$ inside the domain Ω. The function $v(x,y)$ as well as the function $f(z)$ have a definite physical meaning in many problems /2/, /4/. So, in this case function $u(x,y)$ is the electrostatic potential, function v is the flux function and $f(z)$ is the electrostatic complex potential function, $(-f'(z))$ is the complex conjugate of the electric field intensity). In the hydrodynamic problems, $u(x,y)$ is the potential function, $f(z)$ is the complex potential function, and $v(x,y)$ is the stream function.

Taking into account the Cauchy-Riemann conditions, equation (3) can be written as

$$\frac{\partial v}{\partial s} = v_1(s) \qquad \text{on } \Gamma_v$$

and hence

$$v(s) = v(J(r)) + \int_{s(J(r))}^{s} \tilde{v}_1(s')ds' = v(J(r)) + v^*(s) \qquad (4)$$

on the arc $z(J(r))\, z(I(r+1))$ $(r = 1, \ldots, p)$

Relation (4) includes a quadrature which should be (analytically or numerically) performed before the programme starts. The constants $v(J(r))$ are unknown. As the function $v(x,y)$ is determined up to a real constant we can put $v(J(p)) = 0$; the other constants should be determined while solving the problem. These constants also have a definite physical meaning: fluxes on the arcs $z(I(r))\, z(J(r))$ in electrical field problems, rates of flow in hydrodynamic problems, etc. That is why in many problems these constants are the main elements of interest.

In this way we have to determine the complex function $f(z)$, holomorphic inside Ω and whose real and imaginary parts comply with the boundary conditions (2) and (4) respectively. This is a modified Volterra BVP /5/.

We consider a mesh on the curve given by the set of points $z(1)$, ..., $z(N)$ which includes points $z(I(r))$, $z(J(r))$, $(r = 1, \ldots, p)$. The boundary conditions written in the mesh points are:

$$u(k) = \tilde{u}(k) \text{ for } k \in [I(r), J(r)], (r=1, \ldots, p)$$

$$v(k) = v(J(r)) + v^*(k) \text{ for } k \in [J(r), I(r+1)], r=1 \ldots, p$$

where $u(k) = u(z(k))$, $v(k) = v(z(k))$, $\tilde{u}(k) = \tilde{u}(z(k))$

$$v^*(k) = v^*(z(k)),\ I(p+1) = N+1,\ z(N+1) = z(1). \tag{5}$$

We have $v(J(p)) = 0$ and we also denoted by $[a,b]$ the integers between a and b (the extremites being included).

The programme is based on CVBEM and at the beginning it determines the unknown values of the functions u and v on the boundary, that is the values

$$v(r) \text{ for } r \in \bigcup_{k=1}^{p-1} [I(k)+1,\ J(k)] \cup [I(p+1),\ J(p)-1] \tag{6}$$

$$u(r) \text{ for } r \in \bigcup_{k=1}^{p} [J(k)+1,\ I(k+1)-1]$$

At every mesh point we have two relations, one for the real part and the other for the imaginary part of the potential function f(z). For determining the values (6) we use only a half of these relations; the other half will be considered for estimating the error in matching the boundary conditions.

We obtain the values $f(k) = u(k) + iv(k)$ of the potential function at all mesh points. Afterwards, the approximation F(z) of the function f(z) inside is given by the formula

$$F(z) = \sum_{j=1}^{n} f(j) \cdot \hat{L}_j(z) \tag{7}$$

where

$$\hat{L}_j(z) = \frac{1}{2\pi i} \left\{ \frac{z-z(j-1)}{z(j)-z(j-1)} \ln \frac{z-z(j)}{z(j)-z(j+1)} + \frac{z-z(j+1)}{z(j)-z(j+1)} \ln \frac{z-z(j+1)}{z-z(j)} \right\} \tag{8}$$

The above relations apply to all regular mesh points. At the singular points (e.g. the corner points of the curve or the points where the boundary condition changes its type) the function f(z) has the following development:

$$f(z) = f(z_k) + a_1(z-z_k)^{\mu} + a_2(z-z_k)^{2\mu} + \ldots \tag{9}$$

where the exponent μ equals π/θ_k at a corner singularity, it equals 1/2 at a point where we have a change from Dirichlet to Neumann (or conversely) boundary conditions, and equals $\pi/2\theta_k$ at a corner point where at the same time the boundary condition type changes. θ_k denotes the angle between directions $z_k z_{k+1}$, $z_k z_{k-1}$ inside the domain Ω.

In this case, the approximating functions on the boundary took into account the behaviour (9) of the function f(z) in the neighbourhood of the singularity. We considered a linear type approximation and also a quadratic one. The functions $\hat{L}_j(z)$ corresponding to singular nodes are expressed then by means of the function

$$F_{\mu}(z) = \int_0^1 \frac{t^{\mu}}{t-z}\, dt \tag{10}$$

The computations are performed for rational values of the index μ ($\mu = m/n$, where m,n are two integer numbers).

The User's Guide

The MIXED programme is written in FORTRAN-77 and it has been implemented on a PDP-11/34 minicomputer running under an RSX-11M operating system. This programme consists of approximately 700 source statements contained in a main programme and 13 subroutines (see Appendix A). The flowchart in Figure 1 denotes the relationship of the MIXED main programme with each of the subroutines. The extra-storage was not used; the programme needs only a 64K internal storage.

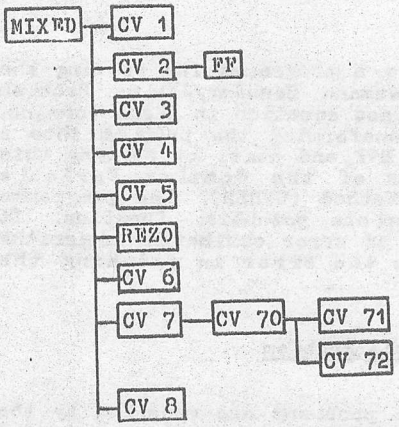

Figure 1: The Hierarchal Structure of the MIXED Programme.

When the programme has been installed on the system, the user calls the MIXED programme by the command:

>RUN MIXED.

The programme displays:

ENTER: TITLE OF THE PROBLEM

and the user must prompt the problem heading (up to 72 characters). Let Γ be the boundary of the simply-connected analysed domain which must be broken up into a series of pieces which must join together in a sequence (a boundary piece is delimited by two nodes). The numbering of the nodes is assumed to be in counter-clockwise order.

The nodes are represented in a Cartesian co-ordinate system. A non-rectangular domain can be specified: node by node, by automatic rectilinear or circular engendering. The maximal number of nodes received by the MIXED programme is 56.

This information is input in an interactive mode from the keyboard as an answer to the following option:

NODE,X,Y OR NODE,R,ALPHA,INDEX =

where:

NODE - the node number (in a sequential order, beginning by 1)

X,Y - the Cartesian co-ordinates of the nodes (the abscisae and ordinate)

R,ALPHA - the Polar co-ordinates of the nodes (the radius and the angle)

INDEX = 0 denotes the Cartesian system

>0 denotes the center index in the Polar co-ordinate system

Note: Automatic Generation: The end of the node introduction (input) is indicated by NODE=0.

If Polar co-ordinates are used, the user must indicate the Cartesian co-ordinates of all the defined cen ers (by INDEX).

The boundary conditions (BC) are given in each node if the Dirichlet or Neumann conditions are variable from node to node, or from a node I(p) to another J(p) if the Dirichlet or Neumann conditions are uniform.

The type of BC is input as IBC = 1 for uniform BC, or IBC = 2 for variable BC.

For IBC = 1, the user must prompt the following options:

NODE,Uo,Vo =

where NODE - the start I(p) or final J(p) node number for the type of boundary

Uo - the Dirichlet BC prescribed value in the NODE

Vo - the Neumann BC prescribed value in the NODE

Notes:

(a) The first node number must be 1, corresponding to the Dirichlet BC (Uo). The next node number denotes the change of Dirichlet in the Neumann BC, etc. In the last changing node we must have Vo = v(J(p)) = 0.

(b) The point where the type of BC changes must be a node of the mesh.

(c) Between two changing nodes there must be no less than two nodes of the mesh.

(d) The end of the uniform BC input is indicated by NODE=0.

For IBC = 2 the user must pr mpt, for each node of the mesh, the following options:

NODE i, KODE,Uo,Vo =

where: KODE = 1 - for given Uo and Vo (both)

= 0 - for given Uo or Vo

Uo - the Dirichlet BC prescribed value in NODE i

Vo - the Neumann BC prescribed value in NODE i

Notes (a), (b) and (c) are common for IBC = 1 and IBC = 2.

The boundary singularity can be a corner point of the curve or a collision point (where the BC changes its type). To take into account the function special behaviour in the neighbourhood of the boundary singularity points, it is necessary to indicate the interpolation type (linear or quadratic). The user must prompt the following options:

ENTER: TYPE OF INTERPOLATION (INT)

where: INT = 0 - for a linear interpolation

1 - for a quadratic interpolation

NODE,M,N (MIU = M/N) =

where: NODE - the singular node number

M,N - two integer values which represent μ=M/N [see (9)].

Notes:

(a) The singularity point must be a point of the mesh.

(b) The end of the singularity point input is indicated by NODE = 0.

At its completion, the MIXED programme executes an automatic error control. The error output listing contains only the relative error. The programme displays the option:

ENTER: ERROR CONTROL (ERC)

where: ERC = 0 - the user skips this option.

1 - the user accepts error processing.

Note: If the value of the u or v function is zero the relative error equals 1.

A brief description of the resulting output:

- All the input data are written on the output listing.

- The programme displays the values U and V for all boundary nodes - the problem solution.

- The programme displays the solutions for each internal points of the analysed domain (when the user asks this) and prompts the co-ordinates of these points - X,Y to the option:

X,Y,MX,MY,DX,DY =

where: X,Y - an iniatial Cartesian co-ordinate

MX,MY - the interval numbers (in the X and Y directions respectively)

DX,DY - the interval values

Note: The end of the internal point co-ordinate inputs is indicated by MX = 0 and MY = 0.

The problem graphically represents, on the output listing, the solutions for the internal points of the rectangular simply-connected domain. In this case, the programme displays:

GRAPHIC: NX,NY =

for an NX by NY grid to produce a plot of the domain.

Note: The maximal number of NX or NY is 100.

Engineers are often required to solve a mixed BV problem with many sets of different boundary conditions, especially for design purpose analyses. Care must be taken at this stage of the node singularities.

As an example we consider the domain shown in Figure 2, and in Appendix B the input data and the resulting output are presented.

```
C ++++++++++++++++++++++++++++++++++++++++++++++++
C +    MAIN PROGRAM: "MIXED"
C ++++++++++++++++++++++++++++++++++++++++++++++++
C
      COMPLEX Z(56)
      REAL    RM(56,56),RN(56,56),A(56,56)
      REAL    F(56),X(56)
      INTEGER IND(56),CR,MM(26),MN(26)
      DIMENSION LI(52),LJ(52),V(56),U(56)
      EQUIVALENCE (LI,MM),(LI(27),MN),(U,IND)
C
C     DEFINE STORAGE REQUIRMENTS:
      DATA NL,MP /56,52/
C     ASSIGN DATA SET NUMBERS FOR
C           INPUT (CR)  AND OUTUT (LP):
      DATA CR,LP / 2, 1/
C
      CALL CV1(LP,CR,N,NP,NL,INTER,ISC,IND,LJ
     .        ,MM,MN,V,Z,TPI)
C
      TT1=SECNDS(0.0)
      CALL CV2(LP,N,NP,NL,INTER,LJ,MM,MN,TPI,
     .        RM,RN,Z)
C
      TT2=SECNDS(0.0)
      WRITE(LP,1) 1,TT2-TT1
 50   CALL CV3(LI,LJ,U,V,N,NP,CR,LP,MP)
C
      TT3=SECNDS(0.0)
C
      CALL CV4(LI,LJ,U,V,RM,RN,F,A,N,NP,NL)
      TT4=SECNDS(0.0)
      WRITE(LP,1) 2,TT4-TT3
      IF (NP.LE.0) GO TO 50
C
      CALL CV5(LI,LJ,F,A,N,NP,NL,JS)
C
      TT5=SECNDS(0.0)
C
      CALL REZO (JS,NL,A,F,X)
C
      TT6=SECNDS(0.0)
      CALL CV6 (N,NP,LI,LJ,X,U,V)
C
      WRITE(LP,1) 3,TT6-TT5
 1    FORMAT('0TIME LOC.',I2,F13.2)
C
      CALL CV7 (N,CR,LP,Z,U,V,F,A)
C
      IF(ISC.NE.0)CALL CV8(N,LP,NL,RM,RN,U,V)
C
      GOTO 50
      END
C ++++++++++++++++++++++++++++++++++++++++++++++++
C +    THE DATA GENERATION SUBPROGRAM WHICH
C +    DEFINES THE GEOMETRY OF STRUCTURAL OUTLINE
C ++++++++++++++++++++++++++++++++++++++++++++++++
C
      SUBROUTINE CV1(LP,CR,N,NP,NL,INTER,ISC,
     .        IND,LJ,MM,MN,V,Z,TPI)
C
      COMPLEX ZA,ZZ,Z(1)
      INTEGER IND(1),CR,MM(1),MN(1)
      DIMENSION R(2),LJ(2),V(1)
      EQUIVALENCE (ZZ,R)
C
C     READ BASIC INFORMATION:
      TPI=ATAN(1.)*8.
      WRITE(CR,'12)
      READ (CR,108) (V(I),I=1,18)
      WRITE(CR,100)
      READ (CR,1) INTER
      WRITE(CR,105)
      READ (CR,1) ISC
      WRITE(LP,3) NL,(V(I),I=1,18)
      WRITE(LP,5)
C
      DO 30 I=1,NL
 30   IND(I)=-1
      WRITE (CR,7)
C
C     N = NUMBER OF COORDINATE POINTS DEFINING
C         THE STRUCTURAL OUTLINE
C     NP= THE TOTAL NUMBER OF CENTER
      K=0
      NP=0
      GOTO 32
 31   WRITE(CR,102)
 32   WRITE(CR,101)
      READ (CR,103) L,ZZ,J
      IF(L.GT.NL.OR.L.LE.0) GOTO 33
      N=L
      IF(NP.LT.J) NP=J
      IF(K.EQ.0)  N =1
      IF(J.LT.0.OR.K.GE.N) GOTO 31
      K=N
      WRITE(LP,104) N,ZZ,J
      Z(N)=ZZ
      IND(N)=J
      GOTO 32
 33   I=1
C
C     GENERATION OF NODAL COORDINATES
      DO 35 J=2,N
      IF(IND(J).LT.0) GOTO 35
      K=J-1
      IF(K.LE.1) GOTO 36
      C=K
      ZZ=Z(J)-Z(I)
      R(1)=R(1)/C
      R(2)=R(2)/C
      DO 34 K=I+1,J-1
      Z(K)=Z(K-1)+ZZ
 34   IND(K)=IND(I)
      IF((IND(J).GT.0.AND.IND(I).EQ.0).OR.
     .(IND(J).EQ.0.AND.IND(I).GT.0))
     .  WRITE(LP,106) I,J
 36   I=J
 35   CONTINUE
C
C     TRANSFORM THE POLAR COORDINATES IN
C           CARTESIAN SYSTEM
      IF(NP.LE.0) GOTO 39
      DO 38 I=1,NP
      WRITE(CR,107) I
      READ (CR,2) ZA
      DO 37 J=1,N
      IF(IND(J).NE.I) GOTO 37
      ZZ=Z(J)
      C=R(2)*TPI/360.
      D=R(1)
      R(1)=D*COS(C)
      R(2)=D*SIN(C)
      Z(J)=ZZ+ZA
 37   CONTINUE
 38   WRITE(LP,104) I,ZA
C
C     DEFINE THE SINGULARITIES NODES:
 39   WRITE(CR,6)
      K=0
 75   K=K+1
      WRITE(CR,4)
      READ (CR,1) LJ(K),MM(K),MN(K)
      IF(LJ(K).LE.0)  GOTO 76
      C=MM(K)
      D=MN(K)
      V(K)=0.
      IF (MN(K).NE.0) V(K)=C/D
      GOTO 75
 76   NP=K-1
C
C     NP= THE NUMBER OF SINGULARITIES POINTS
      IF (NP.LE.0)  INTER=0
      IF(INTER.EQ.0) WRITE(LP,109)
      IF(INTER.NE.0) WRITE(LP,111)
      IF(NP.EQ.0)  GOTO 79
      WRITE(LP,110) (LJ(J),V(J),J=1,NP)
 79   R E T U R N
  1   FORMAT(3I5)
  2   FORMAT(8F10.0)
  3   FORMAT(/'1"MIXED" - AN INTERACTIVE PROGRAM '
     .,'FOR SOLVING'/11X,'MIXED BVP FOR 2D 'APLACE'
     .,' EQUATION BY CVBEM'/'0WRITTEN BY: D.HOH'
     .,'NTCOVSCHI, D.COCORA, R.MAGUREANU'/'0DATE'
     .,': DECEMBER 1985'/'0N.MAX=',I5/'0APPLICAT'
```

```
     .,'ION : ',18A4//)
   4  FORMAT('$NODE, M, N   (MIU=M/N)  =  ')
   5  FORMAT('OINPUT DATA:'/' NODE',12X,'X/R',9X
     .,'Y/ALPHA',5X,'INDEX')
   6  FORMAT(' =>ENTER: SINGULAR NODES')
   7  FORMAT(' =>ENTER: MESCH NODES:')
 100  FORMAT(' =>ENTER: TYPE OF INTERPOLATION (I'
     .,'NT)'/8X,'0 -FOR LINEAR'/8X,'1 -FOR QUADR'
     .,'ATIC'/'$INT =')
 101  FORMAT('$NODE, X, Y  OR NODE, R, ALPHA, I'
     .,'NDEX=')
 102  FORMAT(' ERROR: NOT SEQUENTIAL NODE OR NE'
     .,'GATIVE INDEX')
 103  FORMAT(I5,2F10.0,I5)
 104  FORMAT(I5,2F15.3,I11)
 105  FORMAT(' =>ENTER: ERROR CONTROL (ERC)'/8X,
     .'0 -SKIP'/8X,'1 -ERROR PROCESSING'/'$ERC =')
 106  FORMAT(' ERROR: GENERATION FAILED DUE TO '
     .,'WRONG NODE INDEX=',2I4)
 107  FORMAT('$THE CENTER NO.',I3,'  OF COORDIN'
     .,'ATES=')
 108  FORMAT(18A4)
 109  FORMAT('OLINEAR INTERPOLATION')
 110  FORMAT('OSINGULAR NODES:'/' NODE    MIU='
     .,'M/N'/(I5,F11.3))
 111  FORMAT('OQUADRATIC INTERPOLATION')
 112  FORMAT(' =>ENTER: TITLE OF THE PROBLEM')
      END
C ++++++++++++++++++++++++++++++++++++++++++++++++
C +     COMPUTE THE M AND N MATRIX
C ++++++++++++++++++++++++++++++++++++++++++++++++
C
      S"BROUTINE CV2(LP,N,NP,NL,INTER,LJ,MM,
     .               MN,TPI,RM,RN,Z)
C
      COMPLEX ZA,ZB,ZC,ZD,ZE,ZF,ZZ,Z(NL),ZU,
     .        ZL,ZH,Z3,Z4,FF
      REAL    RM(NL,NL),RN(NL,NL),R(2)
      DIMENSION LJ(NL),MM(NL),MN(NL)
      EQUIVALENCE (ZZ,R)
C
      ZU=(1.,0.)
      DO 15 J=1,N
      L=3
      JS=1
      IF(NP.LE.0) GOTO 81
      DO 77 I=1,NP
      JS=LJ(I)
      MS=MM(I)
      NS=MN(I)
      JM1=JS-1
      IF(JM1.EQ.0) JM1=N
      JP1=JS+1
      IF(JS.EQ.N) JP1=1
      JM2=JM1-1
      IF(JM2.EQ.0) JM2=N
      JP2=JP1+1
      IF(JP1.EQ.N) JP2=1
      IF (J.EQ.JM1)  GOTO 78
      IF (J.EQ.JS )  GOTO 74
      IF (J.EQ.JP1)  GOTO 79
77    C O N T I N U E
      GOTO 81
74    L=0
      GOTO 81
78    L=1
      GOTO 81
79    L=2
81    JP=J+1
      JM=J-1
      IF (J .EQ.N) JP=1
      IF (JM.EQ.0) JM=N
      ZD=Z(J)-Z(JM)
      ZE=Z(J)-Z(JP)
      ZP=Z(JM)-Z(JP)
      DO 14 I=1,N
      C=1.
      IF (NP.LE.0)  GOTO 84
      ZH=Z(JM1)-Z(JS)
      ZL=Z(JP1)-Z(JS)
      Z3=Z(I)-Z(JS)
      Z4=Z3/ZH
      Z3=Z3/ZL
      IF (INTER.EQ.0) GOTO 68
      ZZ=CLOG(ZH/ZL)
      IF(R(2).LT.0.) R(2)=R(2)+TPI
      ZH=ZZ
      C=MS
      D=NS
      R(1)=C/D
      R(2)=0.
      ZH=CEXP(ZZ*ZH)
68    IF(L.EQ.0)  GOTO 64
      IF (L-2) 82,83,84
84    IF (I.EQ.J)  GOTO 10
      IF (I.EQ.JP) GOTO 11
      IF (I.EQ.JM) GOTO 12
      ZA=Z(I)-Z(JM)
      ZB=Z(I)-Z(J )
      ZC=Z(I)-Z(JP)
      ZZ=ZA/ZD*CLOG(ZB/ZA) + ZC/ZE*CLOG(ZC/ZB)
      GOTO 13
64    IF(INTER.NE.0)ZL=(ZU+ZH)*FF(MS,NS,Z4)-
     - (ZU+ZU/ZH)*FF(MS,NS,Z3)+FF(2*MS,NS,Z3)/
     / ZH-ZH*FF(2*MS,NS,Z4)
      ZD=Z(JM1)-Z(JP1)
      ZE=Z(JP1)-Z(JS)
      ZF=Z(JM1)-Z(JS)
      IF(I.EQ.JM1) GOTO 65
      IF (I.EQ.JS) GOTO 66
      IF (I.EQ.JP1)GOTO 67
      IF(INTER.EQ.0) ZL=FF(MS,NS,Z4)-FF(MS,NS,
     ,                   Z3)
      ZZ=ZL+CLOG((Z(I)-Z(JP1))/(Z(I)-Z(JM1)))
      GOTO 13
65    IF(INTER.EQ.0) ZL=FF(MS,NS,ZU)-FF(MS,NS,
     ,                   Z3)
      ZZ=ZL+CLOG(ZD/ZF)
      GOTO 13
66    R(1)=.5*D/C
      R(2)=0.
      ZL=(0.,.0)
      IF(INTER.NE.0) ZL=ZZ*(ZH-ZU/ZH)
      ZZ=CLOG(ZE/ZF)
      IF (R(2).LT.0.) R(2)=R(2)+TPI
      ZZ=ZZ+ZL
      GOTO 13
67    IF(INTER.EQ.0) ZL=FF(MS,NS,Z4)-FF(MS,NS,
     ,                   ZU)
      ZZ=ZL+CLOG(-ZE/ZD)
      GOTO 13
82    ZD=Z(JM2)-Z(JM1)
      ZE=Z(JM1)-Z(JS )
      IF(INTER.NE.0) ZL=ZU+(FF(MS,NS,Z3)/ZH-
     -  FF(MS,NS,Z4)+ZH*FF(2*MS,NS,Z4)-
     -  FF(2*MS,NS,Z3)/ZH)/(ZU-ZH)
      IF(I.EQ.JM2)   GOTO 61
      IF(I.EQ.JM1)   GOTO 62
      IF(I.EQ.JS )   GOTO 63
      ZA=Z(I)-Z(JM2)
      ZB=Z(I)-Z(JM1)
      IF(INTER.EQ.0) ZL=ZU-FF(MS,NS,Z4)
      ZZ=ZL-ZA/ZD*CLOG(ZD/ZA)
      GOTO 13
61    ZZ=ZU-FF(MS,NS,Z4)
      IF (INTER.NE.0) ZZ=ZL
      GOTO 13
62    ZZ=CLOG(-ZE/ZD)
      IF(R(2).LT..0) R(2)=R(2)+TPI
      IF(INTER.EQ.0) ZL=ZU-FF(MS,NS,ZU)
      ZZ=ZZ+ZL
      GOTO 13
63    ZL=ZU-FF(MS,NS,(0.,.0))
      R(1)=.5*D/C
      R(2)=0.
      IF(INTER.NE.0) ZL=(ZU-ZH)/ZH*ZZ+ZU
      ZF=Z(JM2)-Z(JS)
      ZZ=ZL+ZF/ZD*CLOG(ZE/ZF)
      GOTO 13
83    ZD=Z(JP2)-Z(JP1)
      ZE=Z(JP1)-Z(JS )
      IF(INTER.NE.0) ZL=(ZH*FF(MS,NS,Z4)-
     -  FF(MS,NS,Z3)-ZH*FF(2*MS,NS,Z4)+
     +  FF(2*MS,NS,Z3)/ZH)*ZH/(ZU-ZH)-ZU
      IF(I.EQ.JS )   GOTO 71
      IF(I.EQ.JP1)   GOTO 72
      IF(I.EQ.JP2)   GOTO 73
```

```
      ZA=Z(I)-Z(JP2)
      ZB=Z(I)-Z(JP1)
      IF(INTER.EQ.0) ZL=FF(MS,NS,Z3)-ZU
      ZZ=ZL-ZA/ZD*CLOG(ZA/ZB)
      GOTO 13
71    ZL=FF(MS,NS,(0.,.0))-ZU
      R(1)=.5*D/C
      R(2)=0.
      IF(INTER.NE.0) ZL=(ZU-ZH)*ZZ-ZU
      ZF=Z(JP2)-Z(JS)
      ZZ=ZL+ZF/ZD*CLOG(ZF/ZE)
      GOTO 13
72    ZZ=CLOG(-ZD/ZE)
      IF(R(2).LT..0) R(2)=R(2)+TPI
      IF(INTER.EQ.0) ZL=FF(MS,NS,ZU)-ZU
      ZZ=ZZ+ZL
      GOTO 13
73    ZZ=FF(MS,NS,Z3)-ZU
      IF(INTER.NE.0) ZZ=ZL
      GOTO 13
10    ZZ=CLOG(ZE/ZD)
      IF (R(2).LT.0) R(2)=R(2)+TPI
      GOTO 13
11    ZZ=-ZF/ZD*CLOG(ZE/ZF)
      GOTO 13
12    ZZ= ZF/ZE*CLOG(-ZF/ZD)
13    ZZ=(0.,-0.159155)*ZZ
      RM(I,J)=R(1)
14    RN(I,J)=R(2)
15    C O N T I N U E
      RETURN
      END
C +++++++++++++++++++++++++++++++++++++++++++++++++++
C +     DEFINE THE BOUNDARY CONDITIONS
C +++++++++++++++++++++++++++++++++++++ ++++++++++
C
      SUBROUTINE CV3(LI,LJ,U,V,N,NP,CR,LP,MP)
      DIMENSION LI(MP),LJ(MP),U(N),V(N)
      INTEGER CR
C
      WRITE(CR,110)
      READ (CR,103) IW
      IF (IW.EQ.0)          S T O P  'O.K.'
      WRITE(LP,109)
      WRITE(CR,114)
      NP=0
      J=1
      IF (IW.EQ.1) GO TO 42
      WRITE(CR,113)
      DO 30 I=1,N
      WRITE(CR,111) I
      READ (CR,103) K,U(I),V(I)
      IF (K.EQ.0)  GOTO 28
      IF (K.EQ.1)  J=-J
      IF (J.GT.0)  GOTO 27
      NP=NP+1
      IF (NP.GT.MP)          GOTO 94
      LI(NP)=I
      GOTO 29
27    LJ(NP)=I
28    IF (I.EQ.1)            GOTO 93
29    IF(K.EQ.1) WRITE(LP,112) I,U(I),V(I)
      IF(K.EQ.0.AND.J.GT.0) WRITE(LP,104) I,V(I)
      IF(K.EQ.0.AND.J.LT.0) WRITE(LP,112) I,U(I)
30    C O N T I N U E
      GOTO 50
42    WRITE(CR,108)
      READ (CR,103) L3,C,D
      J=-J
      IF (J.GT.0) GOTO 44
      NP=NP+1
      IF (NP.GT.MP)          GOTO 94
      LI(NP)=L3
      GO TO 43
44    LJ(NP)=L3
43    L1=K
      L2=N
      IF (L3.LE.0)  GOTO 45
      L2=L3-1
45    IF(L3.EQ.1) GOTO 47
      IF(L1.GT.L2)           GOTO 92
      DO 46 I=L1,L2
      U(I)=CC
46    V(I)=DD
      WRITE(LP,112) K,CC,DD
47    CC=C
      DD=D
      K=L3
      IF(L3.NE.0) GOTO 42
      NP=NP-1
50    IF (LI(1).NE.1)        GOTO 91
      LI(NP+1)=1
      IF(V(NP).NE.0.)        GOTO 95
      RETURN
91    WRITE (CR,115)
      GOTO 99
92    WRITE (CR,116)  L1,L2
      GOTO 99
93    WRITE (CR,117)
      GOTO 99
94    WRITE (CR,118)  NP,MP
      GOTO 99
95    WRITE (CR,119)
99    WRITE (LP,120)
      S T O P  'FATAL ERROR'
103   FORMAT(I5,2F10.0)
104   FORMAT(I5,F20.2)
108   FORMAT('$NODE, U0, V0   =')
109   FORMAT('0BOUNDARY CONDITIONS - PRESCRIB'
     .,'ED VALUES:'/' NODE',8X,'U0',8X,'V0')
110   FORMAT(' =>ENTER: TYPE OF BOUNDARY CONDIT'
     .,'ION (IBC)'/8X,'0 -STOP'/8X,'1 -UNIFORM '
     .,'BOUNDARY CONDITION'/8X,'2 -VARIABLE BOU'
     .,'NDARY CONDITION'/'$IBC =')
111   FORMAT('$NODE',I3,'  KODE, U0, V0 =')
112   FORMAT(I5,2F10.2)
113   FORMAT(' CONVENTION: KODE=1 FOR GIVEN U0'
     .,' AND V0'/13X,'KODE=0 FOR GIVEN  U0 OR V0'
     .)
114   FORMAT(' =>ENTER: BOUNDARY CONDITIONS VAL'
     .,'UES')
115   FORMAT(' FIRST NODE MUST BE 1')
116   FORMAT(' WRONG ORDER:',2I4)
117   FORMAT(' WRONG START')
118   FORMAT(' NO STORAGE:',2I4)
119   FORMAT(' IN THE LAST NODE; V0=0.0')
120   FORMAT('0F A T A L   E R R O R')
      END
C +++++++++++++++++++++++++++++++++++++++++++++++++++
C +     ASSEMBLE COEFFICIENT MATRIX A AND
C +                VECTOR F.
C +++++++++++++++++++++++++++++++++++++++++++++++++++
C
      SUBROUTINE CV4(LI,LJ,U,V,RM,RN,F,A,N,
     .               NP,NL)
      DIMENSION LI(NL),LJ(NL),RM(NL,NL),F(NL)
     *  ,RN(NL,NL),A(NL,NL),U(NL),V(NL)
C
      DO 70 L=1,NP
      L1=LI(L)
      L2=LJ(L)
      IF (L.EQ.NP) L2=L2-1
      IF (L1+1.GE.L2)                GOTO 90
      DO 40 K=L1,L2
      F(K)=RM(K,1)*V(1)
      DO 40 I=1,NP
      JS=LJ(I)
      DO 21 J=LI(I),JS
21    F(K)=F(K)+RN(K,J)*U(J)
      L3=LI(I+1)
      IF (I.EQ.NP) L3=N
      DO 22 J=JS+1,L3
22    F(K)=F(K) + RM(K,J)*V(J)
      DO 23 J=LI(I)+1,JS-1
      C=0.
      IF (K.EQ.J) C=1.
23    A(K,J)=C - RM(K,J)
      L3=LI(I+1)-1
      IF (I.EQ.NP) L3=N
      IF (I.EQ.NP) GOTO 25
      C=0.
      IF (K.EQ.JS) C=1.
      DO 24 J=JS,L3+1
24    C=C - RM(K,J)
      A(K,JS)=C
25    DO 26 J=JS+1,L3
```

```
 26     A(K,J)= -RN(K,J)
 40     C O N T I N U E
        L1=LI(L+1)
        C=A(L2,L2)
        D=A(L1,L2)
        F(L2)=F(L2)*C + F(L1)*D
        DO 41 J=1,N
 41     A(L2,J)=C*A(L2,J) + D*A(L1,J)
        L1=LJ(L)+1
        L2=LI(L+1)-1
        IF (L.EQ.NP) L2=N
        IF (L1.GT.L2)                    GOTO 90
        DO 60 K=L1,L2
        F(K)=-RN(K,1)*V(1)
        DO 60 I=1,NP
        JS=LJ(I)
        DO 50 J=LI(I),JS
 50     F(K)=F(K) + RM(K,J)*U(J)
        L3=LI(I+1)
        IF (I.EQ.NP) L3=N
        DO 51 J=JS+1,L3
 51     F(K)=F(K) - RN(K,J)*V(J)
        L3=LI(I+1)-1
        IF (I.EQ.NP) L3=N
        DO 52 J=LI(I)+1,JS-1
 52     A(K,J)=RN(K,J)
        IF (I.EQ.NP)  GOTO 55
        C=0.
        DO 53 J=JS,L3+1
 53     C=C + RN(K,J)
        A(K,JS)=C
 55     DO 56 J=JS+1,L3
        C=0.
        IF (K.EQ.J) C=1.
 56     A(K,J)=C - RM(K,J)
 60     C O N T I N U E
 70     C O N T I N U E
 80     RETURN
 90     NP=0
        GOTO 80
        END
C +++++++++++++++++++++++++++++++++++++++++++++++++
C +     REORDERING COEFFICIENT MATRIX A AND
C +                 VECTOR F.
C +++++++++++++++++++++++++++++++++++++++++++++++++
C
        SUBROUTINE CV5(LI,LJ,F,A,N,NP,NL,JS)
        DIMENSION LI(NL),LJ(NL),F(NL),A(NL,NL)
C
        JS=N
        DO 93 L1=1,NP
        DO 93 L2=1,2
        IF(L1.NE.1.AND.L2.EQ.1) GOTO 93
        IF (L2.EQ.1) L=LJ(NP+1-L1)
        IF (L2.EQ.2) L=LI(NP+1-L1)
        JS=JS-1
        DO 91 K=L,JS
        F(K)=F(K+1)
        DO 91 J=1,N
 91     A(K,J)=A(K+1,J)
        DO 92 K=L,JS
        DO 92 J=1,N
 92     A(J,K)=A(J,K+1)
 93     C O N T I N U E
        RETURN
        END
C +++++++++++++++++++++++++++++++++++++++++++++++++
C +     PERFORM THE COMPLITING OF THE BOUNDARY
C +                 VALUES
C +++++++++++++++++++++++++++++++++++++++++++++++++
C
        SUBROUTINE CV6 (N,NP,LI,LJ,X,U,V)
C
        DIMENSION LI(N),LJ(N),X(N),U(N),V(N)
C
        J=1
        K=1
        L=1
      1 DO 5 I=1,N
        IF (I.EQ.LI(L)) GOTO 6
        IF (I.NE.LJ(L)) GOTO 1
        C=0.
        IF (L.GE.NP)  GOTO 4
        C=X(K)
        L=L+1
        K=K+1
        GOTO 7
 6      IF(I.EQ.1) GOTO 4
 7      V(I)=V(I)+C
        GOTO 4
  1     IF (J.GT.0) GOTO 2
        V(I)=X(K)
        GOTO 3
  2     U(I)=X(K)
        V(I)=V(I)+C
  3     K=K+1
        GOTO 5
  4     J= -J
  5     CONTINUE
        RETURN
        END
C +++++++++++++++++++++++++++++++++++++++++++++++++
        SUBROUTINE CV7 (N,LT,LP,Z,U,V,BU,BV)
C
        REAL U(N),V(N)
        COMPLEX Z(N)
C
        CALL CV71(N,LT,LP,Z,U,V)
        CALL CV72(N,LT,LP,Z,U,V,BU,BV)
        RETURN
C
        END
C +++++++++++++++++++++++++++++++++++++++++++++++++
C +     RESULTS PRINTING
C +++++++++++++++++++++++++++++++++++++++++++++++++
C
        SUBROUTINE CV71 (N,LT,LP,Z,U,V)
C
        REAL U(N),V(N),W(2)
        COMPLEX Z(N),ZC,ZD
C
        EQUIVALENCE (ZD,W)
C
C       THE BOUNDARY VALUES PRINTING:
C
        WRITE(LP,1)
        WRITE(LP,2) (I,Z(I),U(I),V(I),I=1,N)
        WRITE(LP,3)
C
C       DEFINE THE INNER POINTS:
C
        WRITE (LT,5)
 4      WRITE(LT,7)
        READ (LT,8) X,Y,NX,NY,DX,DY
        IF (NX+NY.EQ.0)                  R E T U R N
        IF (DX.EQ.0.) NX=0
        IF (DY.EQ.0.) NY=0
        DO 6 MX=1,NX+1
        W(1)=X+(MX-1)*DX
        DO 6 MY=1,NY+1
        W(2)=Y+(MY-1)*DY
        CALL CV70 (N,Z,U,V,ZD,ZC)
C
C       VALUES AT INNER POINTS ARE PRINTED:
 6      WRITE(LP,9) ZD,ZC
        GOTO 4
C
 1      FORMAT('0BOUNDARY RESULTS:'/' NODE ',
     *  7X,'X',8X,'Y',18X,'U',14X,'V')
 2      FORMAT(I5,2F9.3,4X,2F15.5)
 3      FORMAT('0INTERNAL RESULTS:'/13X,'X',8X,
     *  'Y',18X,'U',14X,'V')
 5      FORMAT(' =>ENTER: INTERNAL POINTS TO',
     *  ' OBTAIN RESULTS')
 7      FORMAT('$X,Y,MX,MY,DX,DY=')
 8      FORMAT(2F10.0,2I5,2F10.0)
 9      FORMAT(5X,2F9.3,4X,2F15.5)
        END
C +++++++++++++++++++++++++++++++++++++++++++++++++
C +     GRAPHICAL REPRESENTATION WITH AN ALPHA-
C +                 NUMERIC OUTPUT DEVICE
C +++++++++++++++++++++++++++++++++++++++++++++++++
C
        SUBROUTINE CV72 (N,LT,LP,Z,U,V,BU,BV)
C
        REAL U(N),V(N),W(2)
```

```
      BYTE B(21),BU(100),BV(100,100)
      COMPLEX Z(N),ZC,ZD
C
      EQUIVALENCE (ZD,W)
      DATA NF,Q /21,1.0E+38/
      DATA B/'0',' ','1',' ','2',' ','3',' ',
     . '4',' ','5',' ','6',' ','7',' ','8',' ',
     . '9',' ','#'/
C
      WRITE(LT,1)
      READ (LT,2) NX,NY
      IF(NX*NY.EQ.0) RETURN
      IF(NX.GT.100) NX=100
      IF(NY.GT.100) NY=100
      XMA=-Q
      XMI= Q
      YMA=-Q
      YMI= Q
      UMA=-Q
      UMI= Q
      VMA=-Q
      VMI= Q
      DO 13 I=1,N
      ZD=Z(I)
      IF(W(1).GT.XMA) XMA=W(1)
      IF(W(1).LT.XMI) XMI=W(1)
      IF(W(2).GT.YMA) YMA=W(2)
      IF(W(2).LT.YMI) YMI=W(2)
      IF(U(I).GT.UMA) UMA=U(I)
      IF(U(I).LT.UMI) UMI=U(I)
      IF(V(I).GT.VMA) VMA=V(I)
      IF(V(I).LT.VMI) VMI=V(I)
 13   CONTINUE
      PASX=(XMA-XMI)/(NX+1)
      PASY=(YMA-YMI)/(NY+1)
      HU = (UMA-UMI)/(NF-1)
      HV = (VMA-VMI)/(NF-1)
C
      WRITE(LP,6)
      DO 19 J=1,NY
      DO 14 I=1,NX
      W(1)=XMI+I*PASX
      W(2)=YMA-J*PASY
      CALL CV70 (N,Z,U,V,ZD,ZC)
      ZD=ZC
      DO 15 L=1,NF-1
      IF(W(1).LE.UMI+L*HU) GOTO 16
 15   CONTINUE
      L=NF
 16   BU(I)=B(L)
      DO 17 L=1,NF-1
      IF(W(2).LE.VMI+L*HV) GOTO 18
 17   CONTINUE
      L=NF
 18   BV(I,J)=B(L)
 14   CONTINUE
 19   WRITE(LP,3) (BU(I),I=1,NX)
      WRITE(LP,7)
      DO 20 J=1,NY
 20   WRITE(LP,3)(BV(I,J),I=1,NX)
      WRITE(LP,8)
      XMA=UMI
      YMA=VMI
      DO 21 I=1,NF-1
      XMI=UMI+I*HU
      YMI=VMI+I*HV
      WRITE(LP,4) I,XMA,XMI,YMA,YMI,B(I)
      XMA=XMI
 21   YMA=YMI
      WRITE(LP,9) B(NF)
      RETURN
C
 1    FORMAT('$GRAPHIC:  NX,NY= ')
 2    FORMAT(2I5)
 3    FORMAT(2X,100A1)
 4    FORMAT(I5,2F10.4,5X,2F10.4,5X,A1)
 6    FORMAT(//2X,'-- U(X,Y) ',90('-'))
 7    FORMAT(//2X,'-- V(X,Y) ',90('-'))
 8    FORMAT(//2X,100('-')/'0 NR.',7X,'UL1 -'
     *  ,'UL2',17X,'VL1 -VL2',5X,'SYMBOL')
 9    FORMAT(7X,'POINTS WHERE THE FUNCTION IS'
     *  ,' NOT DEFINED',8X,A1)
      END
```

```
C +++++++++++++++++++++++++++++++++++++++++++++++++
C +   COMPUTING RELATIVE ERRORS
C +++++++++++++++++++++++++++++++++++++++++++++++++
C
      SUBROUTINE C"8 (N,L" NL,RM,RN,U,V)
      REAL RM(NL,NL),RN(NL,NL),U(NL),V(NL)
C
      WRITE(LP,40)
C
      DO 20 K=1,N
      S1=0.
      S2=0.
      S3=0.
      S4=0.
      DO 10 J=1,N
      UJ=U(J)
      VJ=V(J)
      A=RM(K,J)
      S1=S1+A*UJ
      S2=S2+A*VJ
      A=RN(K,J)
      S3=S3+A*UJ
 10   S4=S4+A*VJ
      UJ=S1-S4
      VJ=S2+S3
      UE=0.
      VE=0.
      IF(UJ.NE.0.) UE=(UJ-U(K))/UJ
      IF(VJ.NE.0.) VE=(VJ-V(K))/VJ
 20   WRITE(LP,30) K,UJ,VJ,UE,VE
      RETURN
 30   FORMAT (I5,2F12.5,2(4X,F8.5))
 40   FORMAT (//2X,51('=')/'0TEST FOR MATCHIN'
     .,'G THE REMAINING BOUNDARY EQUATIONS'/
     .' NODE',11X,'U',11X,'V',8X,'RELATIVE ERRO'
     .,'R')
      END
C +++++++++++++++++++++++++++++++++++++++++++++++++
C +   FOR SOLVING SYSTEMS OF LINEAR EQUATIONS:
C +            A.X=B
C +++++++++++++++++++++++++++++++++++++++++++++++++
C
      SUBROUTINE REZO (N,NL,A,B,X)
C
      DIMENSION   A(NL,NL),B(NL),X(NL)
C
      NB=N-1
      DO 20 J=1,NB
      L=J+1
      DO 20 JJ=L,N
      XM=A(JJ,J)/A(J,J)
      DO 10 I=J,N
 10   A(JJ,I)=A(JJ,I)-A(J,I)*XM
 20   B(JJ)=B(JJ)-B(J)*XM
      X(N)=B(N)/A(N,N)
      DO 40 J=1,NB
      JJ=N-J
      L=JJ+1
      SUM=0.
      DO 30 I=L,N
 30   SUM=SUM+A(JJ,I)*X(I)
 40   X(JJ)=(B(JJ)-SUM)/A(JJ,JJ)
      RETURN
      END
C +++++++++++++++++++++++++++++++++++++++++++++++++
C +   THE FUNCTION DEFINED BY EQS. (10)
C +++++++++++++++++++++++++++++++++++++++++++++++++
C
      COMPLEX FUNCTION FF(M,N,Z)
      COMPLEX Z,ZU,ZO,ZR,ZM,ZC,ZA,ZQ,ZP,ZE,ZS
      REAL R(2)
      EQUIVALENCE (ZE,R)
      ZU=(1.,0.0)
      ZO=(0.,0.0)
      H=M
      H=N/H
      IF (Z.EQ.ZO) GOTO  3
      ZQ=ZO
      ZP=ZU
      Q=8.*ATAN(1.)
      K=M
      IF(M-N) 1,2,3
      FF=ZU
```

```
      IF(Z.NE.ZU) FF=CLOG((Z-ZU)/Z)*ZE+ ZU
      GOTO 9
8     FF=ZQ+ZP*ZE
9     R E T U R N
1     IF(Z.EQ.ZU)     GOTO 4
      R(1)=1./N
      R(2)=0.
      ZR=CEXP(CLOG(Z)*ZE)
      R(1)=R(1)*K
      ZM=CEXP(CLOG(Z)*ZE)
      R(1)=0.
      ZC=Z0
      DO 5 J=1,N
      R(2)=Q*(J-1)*K/N
      ZA=CEXP(ZE)
      R(2)=Q*(J-1)/N
      ZS=CEXP(ZE)
5     ZC=ZC+ZA*CLOG((ZR*ZS-ZU)/(ZR*ZS))
      R(1)=N
      R(1)=R(1)/K
      R(2)=0.
      ZF=ZE+ZC*ZM
      GOTO 8
4     A=0.
      I=(N+1)/2
      IF(I.LE.1) GOTO 7
      DO 6 J=1,I-1
6     A=A+COS(Q*J*K/N)*ALOG(SIN(Q*J/N/2.))
7     T=Q*K/N/2.
      R(1)=2.*A-ALOG(2.*N)-Q/4.*COS(T)/SIN(T)+H
      R(2)=0.
      GOTO 8
3     R(1)=N
      R(1)=R(1)/M
      R(2)=0.
      ZQ=ZE
      FF=ZE
      IF (Z.EQ.Z0)  GOTO  9
      ZP= Z
      K=M-N
      GOTO 1
      E N D
```

"MIXED" - AN INTERACTIVE PROGRAM FOR SOLVING
MIXED BVP FOR 2D LAPLACE EQUATION BY CVBEM

WRITTEN BY: D.HOMENTCOVSCHI, D.COCORA, R.MAGUREANU

N.MAX= 56

APPLICATION : TEST

INPUT DATA:

NODE	X/R	Y/ALPHA	INDEX
1	0,000	10,000	0
6	0,000	0,000	0
9	2,250	0,000	0
13	4,750	0,000	0
15	5,250	0,000	0
19	6,750	0,000	0
21	7,750	0,000	0
25	9,250	0,000	0
28	11,750	0,000	0
32	13,250	0,000	0
34	15,000	0,000	0
37	15,000	5,250	0
41	15,000	6,750	0
44	15,000	10,000	0
50	4,750	10,000	0
54	2,750	10,000	0
56	1,000	10,000	0

QUADRATIC INTERPOLATION

SINGULAR NODES:

NODE	MIU=M/N
11	0,500
17	0,500
23	0,500
30	0,500
39	0,500
52	0,500

BOUNDARY CONDITIONS - PRESCRIBED VALUES:

NODE	U0	V0
1	20,00	0,00
6	20,00	0,00
11	100,00	0,00
17	100,00	0,00
23	50,00	0,00
30	50,00	0,00
34	0,00	0,00
39	0,00	0,00
44	80,00	0,00
52	80,00	0,00

BOUNDARY RESULTS:

NODE	X	Y	U	V
1	0,000	10,000	20,00000	0,00000
2	0,000	8,000	20,00000	-21,54075
3	0,000	6,000	20,00000	-40,62680
4	0,000	4,000	20,00000	-59,36860
5	0,000	2,000	20,00000	-81,30775
6	0,000	0,000	20,00000	-108,29551
7	0,750	0,000	30,74912	-108,29551
8	1,500	0,000	41,94586	-108,29551
9	2,250	0,000	54,68169	-108,29551
10	2,875	0,000	68,22363	-108,29551
11	3,500	0,000	100,00000	-108,29551
12	4,125	0,000	100,00000	-75,60375
13	4,750	0,000	100,00000	-61,22192
14	5,000	0,000	100,00000	-55,99691
15	5,250	0,000	100,00000	-50,69382
16	5,625	0,000	100,00000	-41,82255
17	6,000	0,000	100,00000	-22,46557
18	6,375	0,000	82,11998	-22,46557
19	6,750	0,000	75,01465	-22,46557
20	7,250	0,000	68,23475	-22,46557
21	7,750	0,000	62,61707	-22,46557
22	8,125	0,000	58,56362	-22,46557
23	8,500	0,000	50,00000	-22,46557
24	8,875	0,000	50,00000	-28,16075
25	9,250	0,000	50,00000	-30,16264
26	10,083	0,000	50,00000	-31,04287
27	10,917	0,000	50,00000	-28,87630
28	11,750	0,000	50,00000	-22,90913
29	12,125	0,000	50,00000	-17,69605
30	12,500	0,000	50,00000	-3,45516
31	12,875	0,000	33,88088	-3,45516
32	13,250	0,000	26,59847	-3,45516
33	14,125	0,000	12,67505	-3,45516
34	15,000	0,000	0,00000	-3,45516
35	15,000	1,750	0,00000	-27,97679
36	15,000	3,500	0,00000	-51,19223
37	15,000	5,250	0,00000	-80,00158
38	15,000	5,625	0,00000	-89,76748
39	15,000	6,000	0,00000	-113,20849
40	15,000	6,375	23,70253	-113,20849
41	15,000	6,750	33,34259	-113,20849
42	15,000	7,833	52,27738	-113,20849
43	15,000	8,917	66,82402	-113,20849
44	15,000	10,000	80,00000	-113,20849
45	13,292	10,000	80,00000	-93,28308
46	11,583	10,000	80,00000	-76,46927
47	9,875	10,000	80,00000	-63,20080
48	8,167	10,000	80,00000	-52,18712
49	6,458	10,000	80,00000	-41,31853
50	4,750	10,000	80,00000	-26,38626
51	4,250	10,000	80,00000	-19,22114
52	3,750	10,000	80,00000	0,00000
53	3,250	10,000	61,29425	0,00000
54	2,750	10,000	52,72536	0,00000
55	1,875	10,000	41,03665	0,00000
56	1,000	10,000	30,84263	0,00000

INTERNAL RESULTS:

X	Y	U	V
2.000	2.000	44.60169	-78.36338
2.000	4.000	39.05726	-57.89440
2.000	6.000	37.78184	-40.94693
2.000	8.000	40.02124	-22.92820
2.000	10.000	42.57481	-0.03137
2.000	12.000	-0.07540	-0.23211
4.000	2.000	65.16951	-64.87601
4.000	4.000	53.75972	-53.15664
4.000	6.000	52.14421	-42.28172
4.000	8.000	58.00362	-29.75783
4.000	10.000	81.18230	-12.42527
4.000	12.000	0.03750	-0.38390
6.000	2.000	68.65618	-46.56705
6.000	4.000	59.77675	-47.97459
6.000	6.000	59.77428	-45.16266
6.000	8.000	66.96272	-40.69780
6.000	10.000	80.67895	-37.80207
6.000	12.000	0.25118	-0.29965
8.000	2.000	59.16332	-38.30350
8.000	4.000	57.46618	-46.13588
8.000	6.000	60.48023	-49.82924
8.000	8.000	68.72451	-51.05667
8.000	10.000	80.46605	-51.23130
8.000	12.000	0.29321	-0.14531

NR.	UL1	-UL2	VL1	-VL2	SYMBOL
1	0.0000	5.0000	-113.2085	-107.5481	0
2	5.0000	10.0000	-107.5481	-101.8876	
3	10.0000	15.0000	-101.8876	-96.2272	1
4	15.0000	20.0000	-96.2272	-90.5668	
5	20.0000	25.0000	-90.5668	-84.9064	2
6	25.0000	30.0000	-84.9064	-79.2459	
7	30.0000	35.0000	-79.2459	-73.5855	3
8	35.0000	40.0000	-73.5855	-67.9251	
9	40.0000	45.0000	-67.9251	-62.2647	4
10	45.0000	50.0000	-62.2647	-56.6042	
11	50.0000	55.0000	-56.6042	-50.9438	5
12	55.0000	60.0000	-50.9438	-45.2834	
13	60.0000	65.0000	-45.2834	-39.6230	6
14	65.0000	70.0000	-39.6230	-33.9625	
15	70.0000	75.0000	-33.9625	-28.3021	7
16	75.0000	80.0000	-28.3021	-22.6417	
17	80.0000	85.0000	-22.6417	-16.9813	8
18	85.0000	90.0000	-16.9813	-11.3209	
19	90.0000	95.0000	-11.3209	-5.6604	9
20	95.0000	100.0000	-5.6604	0.0000	

POINTS WHERE THE FUNCTION IS NOT DEFINED #

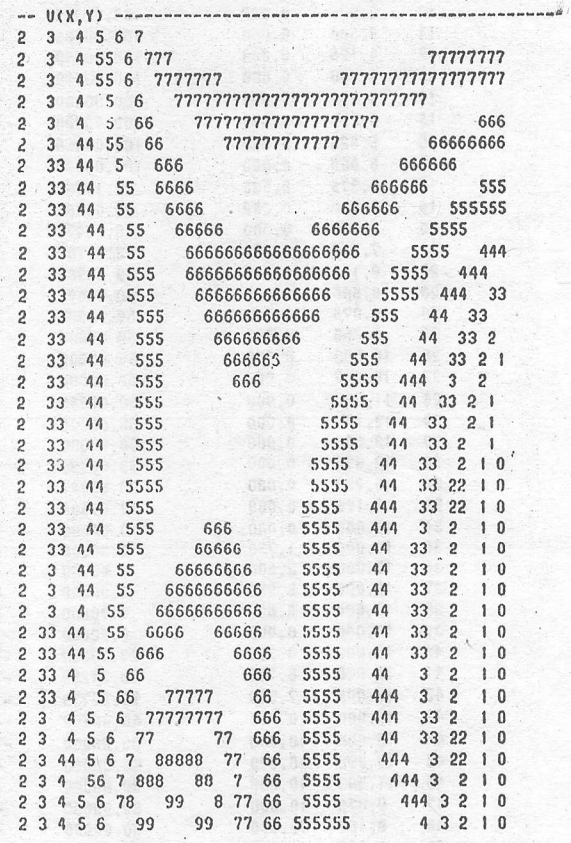

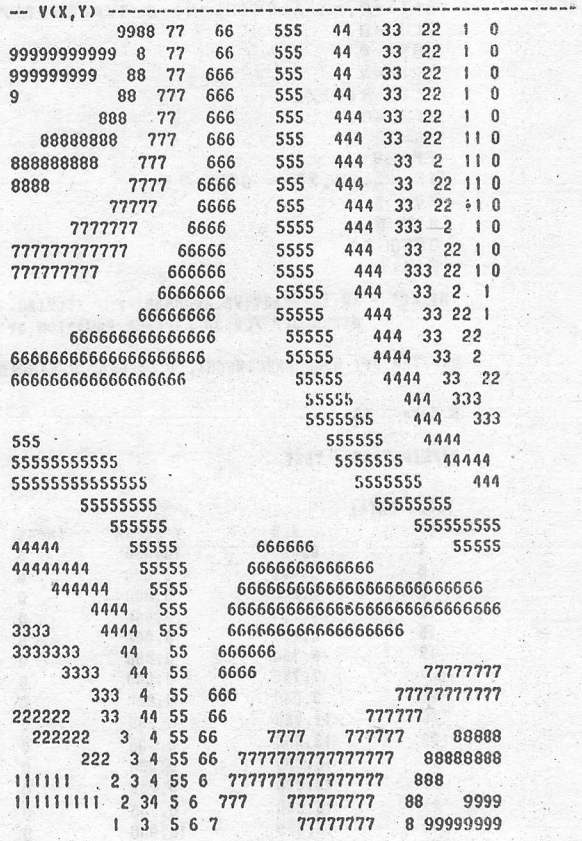

TEST FOR MATCHING THE REMAINING BOUNDARY EQUATIONS

NODE	U	V	RELATIVE ERROR	
1	19.91744	-0.17839	-0.00414	1.00000
2	19.79447	-21.54074	-0.01038	0.00000
3	19.71333	-40.62680	-0.01454	0.00000
4	19.73254	-59.36860	-0.01355	0.00000
5	19.95609	-81.30778	-0.00220	0.00000
6	20.10583	-108.29549	0.00526	0.00000
7	30.74912	-108.34933	0.00000	0.00050
8	41.94585	-108.33145	0.00000	0.00033
9	54.68169	-108.29391	0.00000	-0.00001
10	68.22363	-107.95898	0.00000	-0.00312
11	100.10712	-108.19942	0.00107	-0.00089
12	99.94548	-75.60375	-0.00055	0.00000
13	100.16474	-61.22193	0.00164	0.00000
14	100.10675	-55.99691	0.00107	0.00000
15	100.11144	-50.69381	0.00111	0.00000
16	99.96812	-41.82256	-0.00032	0.00000
17	100.02148	-22.46556	0.00021	0.00000
18	82.11997	-22.60648	0.00000	0.00623
19	75.01466	-22.39296	0.00000	-0.00324
20	68.23475	-22.32936	0.00000	-0.00610
21	62.61707	-22.29892	0.00000	-0.00747
22	58.56362	-22.10642	0.00000	-0.01258
23	50.25490	-22.22918	0.00507	-0.01063
24	50.41075	-20.16074	0.00815	0.00000
25	50.24052	-30.16264	0.00479	0.00000
26	50.08611	-31.04286	0.00172	0.00000
27	50.08867	-20.87631	0.00177	0.00000
28	49.87086	-22.90913	-0.00259	0.00000
29	49.77334	-17.69605	-0.00455	0.00000
30	49.94025	-3.45517	-0.00120	0.00000
31	33.88088	-3.51014	0.00000	0.01566
32	26.59847	-3.50095	0.00000	0.01300
33	12.67505	-3.40053	0.00000	-0.01607
34	0.00330	-3.44918	1.00000	-0.00173
35	-0.20382	-27.97679	1.00000	0.00000
36	-0.47590	-51.19223	1.00000	0.00000
37	0.47211	-80.00157	1.00000	0.00000
38	0.41476	-89.76748	1.00000	0.00000
39	0.15594	-113.20850	1.00000	0.00000
40	23.70254	-113.00134	0.00000	-0.00183
41	33.34259	-112.98363	0.00000	-0.00199
42	52.27738	-113.35757	0.00000	0.00132
43	66.82401	-113.28958	0.00000	0.00072
44	79.97597	-113.21834	-0.00030	0.00009
45	80.00208	-93.28308	0.00003	0.00000
46	80.14967	-76.46927	0.00187	0.00000
47	80.25003	-63.20081	0.00312	0.00000
48	80.32708	-52.18712	0.00408	0.00000
49	80.43244	-41.31854	0.00538	0.00000
50	80.00861	-26.38627	0.00011	0.00000
51	80.16319	-19.22121	0.00204	0.00000
52	80.29654	-0.37432	0.00369	1.00000
53	61.29425	-0.54380	0.00000	1.00000
54	52.72537	-0.28890	0.00000	1.00000
55	41.03665	-0.16027	0.00000	1.00000
56	30.84263	-0.18571	0.00000	1.00000

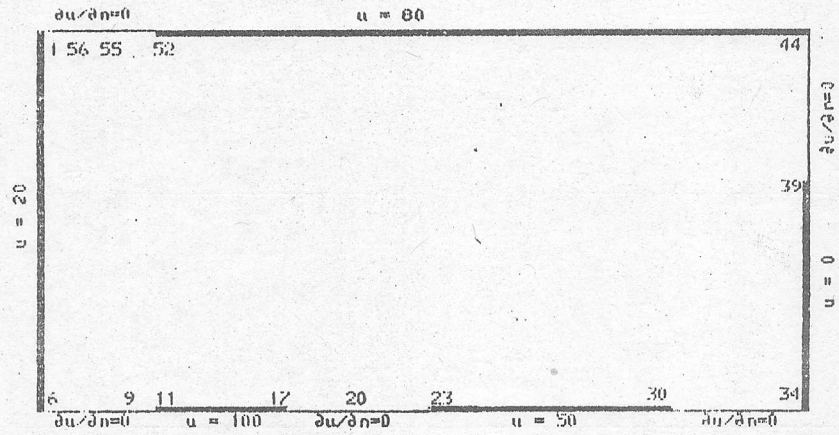

Figure 2

References

/1/ Brebbia,C.A., Telles,J.C.F. and Wrobel,L.C., - Boundary Element Techniques, Springer-Verlag, Berlin, 1984.

/2/ Hromadka II,T.,V.,- The complex variable boundary element method, Springer-Verlag, Berlin, 1984.

/3/ Homentcovschi,D., Cocora,D., Magureanu,R., - Some developments of the CVBEM. An application to the mixed boundary-value problem for the Laplace equation, Engineering Analysis, t4,1987 15-20.

/4/ Homentcovschi,D., - Complex function theory with applications in science and engineering, Ed.Tehnica, Bucharest, 1986.

/5/ Homentcovschi,D., - On the mixed boundary-value problem for harmonic functions in plane domains, ZAMP, t.31, 1980, pp. 352-366.

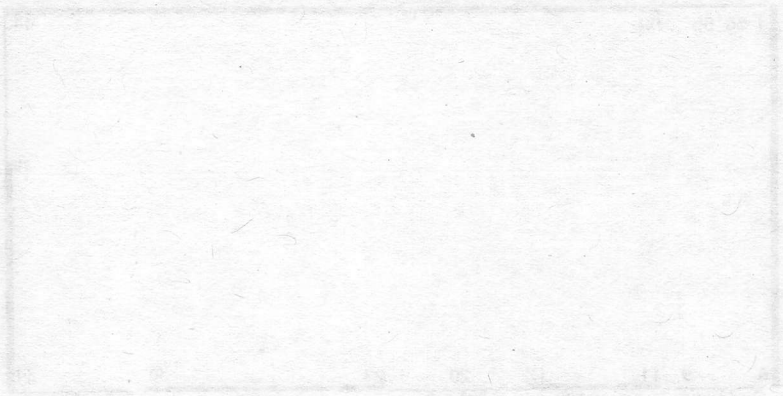

COMPLEX VARIABLE SPLINE BOUNDARY ELEMENT METHOD

Dorel Homentcovschi

Polytechnic Institute of Bucharest,
Department of Mathematics,
313 Splaiul Independentei,
Bucharest, Romania

Liviu Kreindler

Polytechnic Institute of Bucharest,
Department of Electrical Engineering,
313 Splaiul Independentei,
Bucharest, Romania

Abstract

The CVSBEM combines the complex variable cubic splines with the boundary element method.This new procedure enjoys the same advantages as the CVBEM; moreover the good convergence of the approximate potential function to the complex potential as well as of the derivative of the approximate complex potential function to the complex velocity (or complex intensity function) may be proved for CVSBEM.

1.Introduction

Of late the boundary element method (BEM) has proved to be a very efficient tool for solving boundary value problems involved in the engineering analysis. It has been applied to various engineering areas and represents the object of numerous developments [1].

Recently a complex variable variant of the BEM (referred to as CVBEM) was given in [2] and extended in [3], [4], [5], [6]; this method is applicable to two-dimensional harmonic functions, or, equivalently, to analytic complex functions. It is based on the Cauchy integral formula and uses some piecewise polynomial

type approximations for the boundary values of the unknown analytic function f(z). An approximation for the function f(z) in the domain Ω in terms of some elementary functions is obtained. This approximation involves a number of complex constants which are next obtained by collocation .

In this paper we suggest a method for solving boundary-value problems for harmonic functions which combines the complex cubic splines theory with the boundary element method. The complex variable cubic splines were introduced in [7]; they are obtained by approximating the boundary values of the function $f(\zeta)$ in Cauchy's integral formula by means of a cubic spline in variable ζ . The new method can be considered as a variant of the CVBEM. However, it has a remarkable convergence order stated by the theorem on section 2 and by the numerical results as well. That is why in what follows we shall refer to it as CVSBEM.

In section 2 we determined the complex cubic spline in the domain Ω in a form suitable to solve boundary-value problems. A convergence theorem is also enunciated. In section 3 it is shown how the CVSBEM works for the Dirichlet boundary-value problem with special reference to the conformal mapping problem. In the next section we give some examples emphasising the advantages of the new method versus other boundary element methods.

As known, the main advantages of the CVBEM against other BEM procedures consist in giving a straightforward approximation to the complete complex potential function and also the possibility to estimate the error involved in matching the boundary conditions and hence to provide an error reduction algorithm. The

method does not require any approximation of the domain or any numerical quadrature. Apart from these advantages of the CVSBEM there is a convergence theorem. This theorem provides a good convergence order of the approximating potential and its derivative to the complex potential function and to its derivative respectively (as the finesses of the mesh approaches zero). Consequently, the CVSBEM yields good approximations for the complex potential function and also for the complex velocity (or complex intensity function).

2. Complex - variable cubic splines

Let Γ be a rectifiable Jordan curve in the complex z-plane, Ω - the region interior to Γ, and let $z_1, z_2, \ldots, z_n$ be nodal points on Γ, ordered counterclockwise, separating the curve into boundary elements $\Gamma_j (j=1,2,\ldots,n)$ where Γ_j is the arc from z_{j-1} to z_j, ($z_0 \equiv z_n$), (fig.1).

FIG.1

Assume that the function $f(z) = u(x,y) + iv(x,y)$ is analytic on the domain Ω and continuous in $\bar{\Omega} = \Omega \cup \Gamma$. In order to approximate this function inside Ω we shall use the Cauchy integral formula:

$$f(z) = \frac{1}{2\pi i} \int_{\Gamma} \frac{f(\zeta)}{\zeta - z} d\zeta \qquad (1)$$

The values $f(\zeta)$ of the function on the curve Γ are unknown. In the case of the Dirichlet problem the only values we know are those of the real part of $f(\zeta)$; for other boundary-value problems usually a combination of the real and imaginary part of $f(\zeta)$ is

given.

Apart from this, once the values of the function $f(\zeta)$ are determined we need also a numerical procedure to estimate the complex integral in relation (1).

To overcome all these difficulties we shall approximate the boundary values $f(\zeta)$ by means of a cubic spline $F(\zeta)$, i.e. a function which is a cubic polynom on every element Γ_j and which has continuous derivatives up to the second order on the curve Γ. Let us start with the Hermite interpolation formula:

$$F(\zeta) = \sum_{j=1}^{n} f_j H_j^0(\zeta) + \sum_{j=1}^{n} m_j H_j^1(\zeta) \qquad (2)$$

where $f_j=f(z_j)$, $m_j=f'(z_j)$ and denote $h_j=z_j-z_{j-1}$. Then, we have the following expressions for the functions of the base:

$$H_j^0(\zeta)=\begin{cases} \dfrac{(\zeta-z_{j-1})^2}{h_j^3}\cdot 2(z_j-\zeta)+h_j, & \text{for } \zeta\in\Gamma_j \\ \dfrac{(z_{j+1}-\zeta)^2}{h_{j+1}^3}\,2(\zeta-z_j)+h_{j+1}, & \text{for } \zeta\in\Gamma_{j+1} \\ 0, & \text{otherwise} \end{cases} \qquad (3)$$

$$H_j^1(\zeta)=\begin{cases} \dfrac{(\zeta-z_{j-1})^2(\zeta-z_j)}{h_j^2}, & \text{for } \zeta\in\Gamma_j \\ \dfrac{(\zeta-z_j)(\zeta-z_{j+1})^2}{h_{j+1}^2}, & \text{for } \zeta\in\Gamma_{j+1} \\ 0, & \text{otherwise} \end{cases} \qquad (4)$$

$$(j=1,\ldots,n)$$

By substituting expresion (2) into Cauchy integral formula we get the approximating function (complex cubic spline) inside

the domain

$$F(z) = \sum_{j=1}^{n} f_j \hat{H}_j^{\,0}(z) + \sum_{j=1}^{n} m_j \hat{H}_j^{\,1}(z) \tag{5}$$

where

$$\hat{H}_j^{\,0}(z) = \frac{1}{\tilde{\pi} i}\left\{\frac{z-z_{j-1}}{h_j} + \frac{z-z_{j+1}}{h_{j+1}} - \left(\frac{z-z_{j-1}}{h_j}\right)^2 + \left(\frac{z-z_{j+1}}{h_{j+1}}\right)^2\right\} +$$

$$+ \hat{H}_j^{\,0*}(z) \tag{6}$$

$$\hat{H}_j^{\,1}(z) = \frac{1}{2\tilde{\pi} i}\left\{-\frac{2}{3}(h_j+h_{j+1}) + \frac{(z-z_{j-1})^2}{h_j} + \frac{(z-z_{j+1})^2}{h_{j+1}}\right\} + \hat{H}_j^{\,1*}(z)$$

$$\hat{H}_j^{\,0*}(z) = \frac{1}{2\tilde{\pi} i}\left\{\left(\frac{z-z_{j-1}}{h_j}\right)^2 \cdot \left(3-2\cdot\frac{z-z_{j-1}}{h_j}\right) \cdot \ln\frac{z-z_j}{z-z_{j-1}}\right.$$

$$\left. + \left(\frac{z-z_{j+1}}{h_{j+1}}\right)^2 \cdot \left(3-2\cdot\frac{z_{j+1}-z}{h_{j+1}}\right) \cdot \ln\frac{z-z_{j+1}}{z-z_j}\right\} \tag{7}$$

$$\hat{H}_j^{\,1*}(z) = \frac{1}{2\tilde{\pi} i}\left\{\frac{(z-z_{j-1})^2}{h_j} \cdot \frac{z-z_j}{h_j} \cdot \ln\frac{z-z_j}{z-z_{j-1}} + \right.$$

$$\left. + \frac{(z-z_{j+1})^2}{h_{j+1}} \cdot \frac{z-z_j}{h_{j+1}} \cdot \ln\frac{z-z_{j+1}}{z-z_j}\right\}$$

In formulae (7) we chose the logarithm determination

$$\ln\frac{z-z_j}{z-z_{j-1}} = \ln\left|\frac{z-z_j}{z-z_{j-1}}\right| + i\hat{\gamma}_j \tag{8}$$

defined in the complex z-plane with the cut Γ_j and the value $\hat{\gamma}_j$ given in figure 1.

For the time being we suppose the values f_j as being known, and we shall consider the condition that the second derivative of the function $F(\zeta)$ is continuous at all nodal points. There follows the linear system

$$\lambda_j m_{j-1} + 2m_j + (1-\lambda_j)m_{j+1} = \hat{d}_j \quad , \quad (j = 1,\ldots,n) \qquad (9)$$

where

$$\lambda_j = \frac{h_{j+1}}{h_j+h_{j+1}}$$

$$\hat{d}_j = 3\lambda_j \cdot \frac{f_j - f_{j-1}}{h_j} + 3\cdot(1-\lambda_j)\cdot \frac{f_{j+1} - f_j}{h_{j+1}} \qquad (10)$$

The system (9) determines the quantities m_j. To solve such systems a very efficient algorithm is available [8]. We shall write the solution in the form

$$\vec{m} = D\cdot\vec{f} \qquad (11)$$

By substituting the values m_j into relation (5) we obtain the complex cubic spline for the function f(z) (at the points of the given mesh) in the form

$$\hat{F}(z) = \sum_{j=1}^{n} f_j \left\{ \hat{H}_j{}^{0*}(z) + \sum_{p=1}^{n} d_{pj} \hat{H}_p{}^{1*}(z) \right\} \qquad (12)$$

Let us now determine the nodal values of the function F(z). We obtain:

$$F_k = \sum_{j=1}^{n} H_{kj} f_j \ , \qquad (13)$$

where

$$F_k = \hat{F}(z_k) \qquad (14)$$

$$H_{kj} = \hat{H}_j{}^{0*}(z_k) + \sum_{p=1}^{n} \hat{H}_p{}^{1*}(z_k)\cdot d_{pj} \ , \ (k,j = 1,\ldots,n)$$

By using the matrix notation, the last relation can be written as:

$$\mathbb{H} = \mathbb{H}^{0*} + \mathbb{H}^{1*}\cdot\mathbb{D} \qquad (14')$$

In obtaining the matrix $\mathbb{H}$ we have to compute the function of the base at all nodal points. The logarithm function in relations (7) can give us some troubles; that is why we shall explicitate it in the form

$$\hat{H}_j^{0*}(z_{j-1}) = \frac{1}{2\tilde{\pi}i}\cdot\left(1+\frac{h_j}{h_{j+1}}\right)^2\cdot\left(1-2\cdot\frac{h_j}{h_{j+1}}\right)\cdot\ln\frac{z_{j-1}-z_{j+1}}{z_{j-1}-z_j}$$

$$\hat{H}_j^{0*}(z_j) = \frac{1}{2\tilde{\pi}i}\cdot\ln^*\frac{z_j-z_{j+1}}{z_j-z_{j-1}}$$

$$\hat{H}_j^{0*}(z_{j+1}) = \frac{1}{2\tilde{\pi}i}\cdot\left(1+\frac{h_{j+1}}{h_j}\right)^2\cdot\left(1-2\cdot\frac{h_{j+1}}{h_j}\right)\cdot\ln\frac{z_{j+1}-z_j}{z_{j+1}-z_{j-1}} \qquad (15)$$

$$\hat{H}_j^{1*}(z_{j-1}) = -\frac{1}{2\tilde{\pi}i}\cdot\left(1+\frac{h_j}{h_{j+1}}\right)^2\cdot h_j\cdot\ln\frac{z_{j-1}-z_{j+1}}{z_{j-1}-z_j}$$

$$\hat{H}_j^{1*}(z_j) = 0$$

$$\hat{H}_j^{1*}(z_{j+1}) = \frac{1}{2\tilde{\pi}i}\cdot\left(1+\frac{h_{j+1}}{h_j}\right)^2\cdot h_{j+1}\cdot\ln\frac{z_{j+1}-z_j}{z_{j+1}-z_{j-1}}$$

The star in the second relation above indicates that we must take that logarithm branch whose imaginary part lies in the interval $[0,2\tilde{\pi})$; all the other logarithm determinations are the principal ones.

We can explicitate the real and the imaginary part of the introduced quantities as

$$H_{kj} = M_{kj}^* + i\cdot N_{kj}^*$$

$$F_k = U_k + i\cdot V_k \qquad (16)$$

$$f_k = u_k + i\cdot v_k$$

Formula (13) gives

$$U_k = \sum_{j=1}^{n} M_{kj}^*\cdot u_j - \sum_{j=1}^{n} N_{kj}^*\cdot v_j$$

$$V_k = \sum_{j=1}^{n} M_{kj}^{*} \cdot v_j + \sum_{j=1}^{n} N_{kj}^{*} \cdot u_j \quad , \quad (k = 1,\ldots,n) \qquad (17)$$

Let us now take $f(z)\equiv 1$. We have $F(z)\equiv 1$ and hence relations (17) give

$$\sum_{j=1}^{n} M_{kj}^{*} = 1 \ , \ \sum_{j=1}^{n} N_{kj}^{*} = 0 \quad , \quad (k = 1,\ldots,n) \qquad (18)$$

Consequently, relations (17) give

$$U_k = \sum_{j=1}^{n} M_{kj}^{*} \cdot u_j - \sum_{j=2}^{n} N_{kj}^{*} \cdot (v_j - v_1) \qquad (19)$$

$$V_k - v_1 = \sum_{j=2}^{n} M_{kj}^{*} \cdot (v_j - v_1) + \sum_{j=1}^{n} N_{kj}^{*} \cdot u_j \quad , \quad (k = 1,\ldots,n)$$

Note that, generally, $F_k \neq f_k$ ($k = 1,\ldots,n$) so that, in fact, the function $F(z)$ does not interpolate the given function $f(z)$. However, $F(z)$ is a good approximation for the analytical function $f(z)$ (as the fineness of the underlying mesh approaches zero) as stated by the convergence theorem proved in [7].

We consider a sequence of meshes on Γ

$\Delta^{(m)} = \{ z_0^{(m)}, z_1^{(m)}, \ldots, z_n^{(m)} \}$ and denote

$h_j^{(m)} = z_j^{(m)} - z_{j-1}^{(m)}$, $h^{(m)} = \max_j \left| h_j^{(m)} \right|$

We shall also write $F_\Delta(z)$ for the complex spline function corresponding to the mesh Δ and function $f(z)$.

Theorem Let $f(z)$ be analytic on Ω and of $C^{(3)}$ class on and let $^{(m)}$ be a sequence of meshes on Γ (a smooth curve), where $h^{(m)}$ approaches zero as $m \longrightarrow \infty$ and

$$\max_j \frac{h^{(m)}}{\left| h_j^{(m)} \right|} \leqslant c_1 \leqslant \infty$$

If $f'''(z)$ satisfies a Hölder condition of the order β on

Γ , $0<\beta<1$, then for $z \in \bar{\Omega}$ and for any β', $0 < \beta' < \beta$ we have:

$$F^{(p)}_{\Delta(m)}(z) - f^{(p)}(z) = O\left[(h^{(m)})^{3+\beta'-p} \right], (p=0,1,2) \quad (20)$$

On any closed subset of Ω we have

$$F^{(p)}_{\Delta(m)}(z) - f^{(p)}(z) = O\left[(h^{(m)})^{3+\beta'} \right], (p=0,1,2,3) \quad (20')$$

The theorem states that we have a high convergence order of the complex spline approximation to the function f(z); beside this, the derivatives of the function f(z) are uniformly approximated by derivatives of the complex cubic spline.

3. Solution of the Dirichlet problem by CVSBEM. Application to the conformal mapping problem.

Let u(x,y) be a harmonic function in the domain Ω

$$\Delta u(x,y)=0 \text{ in } \Omega \quad (21)$$

and let

$$u(x,y)\Big|_{(x,y)\in\Gamma} = \tilde{u}(s) \quad (22)$$

be the Dirichlet-type boundary condition. By $\tilde{u}(s)$ we have denoted a given function. Let also v(x,y) be the harmonic conjugate function of u(x,y); the function

$$f(z)=u(x,y)+iv(x,y)$$

is a holomorphic function with respect to the complex variable $z = x+iy$ in the domain Ω. We shall approximate the function f(z) by means of the complex cubic spline F(z) of the type (12). In this formula the values f_j are unknown; in fact we known only the real part u_j as follows from the boundary condition (22).

In order to obtain a system of equations to determine the values v_k we can use the first or the second set of relations (19) where U_k and V_k will be replaced by u_k and v_k respectively. The second set of relations (19) has the advantage of giving a

better conditioned system of linear equations; that is why next we shall consider the system of linear equations

$$v_k - v_1 - \sum_{j=2}^{n} M_{kj}^{*}\cdot(v_j - v_1) = \sum_{j=1}^{n} N_{kj}^{*}\cdot u_j \quad , (\ k = 2,\ldots,n\ ) \qquad (23)$$

for obtaining the values $v_k - v_1$ $(k = 2,\ldots,n)$. The imaginary part of the function $v(x,y)$ is determined up to a real constant so that the value v_1 can be taken as arbitrary. Hence, system (23) provides all the unknown values, and relation (12) gives the complex spline $F(z)$ whose real part approximates the solution of the given Dirichlet boundary-value problem.

As a by-product we can obtain also an error estimate. This is given by the first set of relations (19)

$$\varepsilon_k \equiv u_k - U_k = u_k - \sum_{j=1}^{n} M_{kj}^{*}\cdot u_j + \sum_{j=2}^{n} N_{kj}^{*}\cdot(v_j - v_1) \quad , \qquad (24)$$
$$(\ k = 1,\ldots,n\ )$$

These relations can be used to develop an error reduction algorithm by adding new points to the boundary part where the error is large.

Now, as an application we consider the problem of determining the function $w = w(z)$ which conformingly maps the bounded simply-connected domain Ω on to the unit disc $|w|<1$ in the w - plane in such a way that the particular point $z_0 \in \Omega$ corresponds to the center, $w=0$, of the disc. We can write

$$w = (z - z_0)\cdot g(z) \qquad (25)$$

where the complex function $g(z)$ has to be determined. We have

$$\ln w = \ln(z - z_0) + \ln g(z)$$

Taking into account this relation on the boundary curve we obtain a Dirichlet-type boundary condition

$$\ln|g(z)| = -\ln|\zeta - z_0| \quad , \zeta \in \Gamma \tag{26}$$

for determining the analytic function $f(z)=\ln g(z)$.

By solving this boundary-value problem by CSBEM the approximating conformal maping has the form

$$w = (z-z_0)\cdot \exp\{F(z)+iv_1\}$$

Now, the arbitrary constant v_1 represents the rotation angle around z_0 induced by the conformal mapping function.

Note that the mapping function obtained above can be directly estimated at any complex point of $\bar{\Omega}$; it does not require any additional numerical quadratures as is the case with other numerical conformal mapping methods based on the boundary element technique.

4. Numerical results

We have applied the CVSBEM to solve some Dirichlet-type boundary-value problems. The first two examples concern some conformal mapping test problems considered earlier in the literature. The third problem is an application to compute the magnetic field in a brushless d.c. motor with ceramic permanent magnets.

Example 1. Let the curve Γ be the ellipse

$$\frac{x^2}{a^2} + y^2 = 1$$

The nodal points of Γ are

$$z_j = a\cos\frac{2\pi}{N}j + i\cdot\sin\frac{2\pi}{N}j \quad , \quad (j = 1,\ldots,N)$$

By EM we also denote an estimate of the maximum error of the modulus of our mapping function

$$EM = \max_j \left| \left| w(z_{j+\frac{1}{2}}) \right| - 1 \right|$$

The intermediate points $z_{j+\frac{1}{2}}$ are

$$z_{j+\frac{1}{2}} = a \cdot \cos \frac{2\pi}{N}(j + \frac{1}{2}) + i \cdot \sin \frac{2\pi}{N}(j + \frac{1}{2}) \ , \ (j = 1, \ldots, N)$$

Let also EA be an estimate of the maximum error of the argument of the determined mapping function defined as $\max |v(x,y)|$ at the mesh points which lie on the symmetry axis of Ω. We take $z_0=0$, $v_1=0$. The results for N=32 and for various values of a are given in table 1.

a	Symm [9]		CVSBEM	
	EM	EA	EM	EA
1.25	6.E-4	5.1E-3	5.4E-6	5.7E-7
2.5	6.5E-3	1.1E-3	4.3E-4	3.3E-4
5.	5.E-2	9.E-4	1.E-3	5.1E-4
10.	.2116	5.E-3	6.1E-2	1.9E-2
20.	.4878	1.6E-2	.31	.36

TABLE 1.

For comparation, the results obtained for the same problem by Symm [9] by the integral equation method are included in table 1. Generally, the results given by CVSBEM are better by an order of magnitude; we get that the same result is valid for other number N of nodal points and also for other tested domains.

Example 2. We consider the domain Ω as being the rectangle $-1<x<1$, $-a<y<a$. In this case we applied the error reduction algorithm, starting with 8 nodal points (the vertices of the rectangle and the points of symmetry of Γ) and adding new nodal

points to the part of Γ where the values of ε_k are larger. In table 2 we give the obtained results (N is the final number of mesh points and EM is defined by taking the intermediate points $z_{j+\frac{1}{2}}$ as midpoints between the nodes). We increased the number of nodes until we reached the precision of the results obtained by Symm [9] by using 128 nodal points.

a	Symm [9]		CVSBEM	
	N	EM	N	EM
.1	128	1.6E-2	28	1.5E-2
.2	128	2.4E-3	28	1.5E-3
.4	128	4.E-4	28	4.E-4
.8	128	1.E-4	36	1.E-4
1.	128	1.E-4	32	1.E-4
2.	128	3.E-4	28	2.7E-4

TABLE 2.

The obtained results indicate a sharp reduction of the number of nodes (and correspondingly of the computation time) to obtain a prescribed precision.

Example 3. As the last example we consider the computation of the magnetic field of a brushless d.c. motor with ceramic permanent magnets. The domains are shown in fig. 2 . The scalar

FIG.2

magnetic potential u satisfies Laplace's equation inside domain D (the air-gap of the machine) and the following Dirichlet-type boundary conditions

$$u(r) = \frac{r - r_B}{r_A - r_B} U_0 \qquad \text{for } r_B \leqslant r \leqslant r_A,$$

over AB portion,

$$u = U_0 \quad \text{(constant)},$$

over the arcs BCDEF,

$$u(\theta) = \frac{\frac{\pi}{2p} - \theta}{\frac{\pi}{2p} - \frac{\theta_p}{2}} \cdot U_0 \qquad \text{for } \frac{\theta_p}{2} \leqslant \theta \leqslant \frac{\pi}{2p}$$

over the FG line, and

$$u = 0 \quad \text{over GHA.}$$

Here r and θ are polar coordinates with respect to the machine axis. The parameters of interest are : the flux of the magnetic field between two points $\Phi_{pq}=V(p)-V(q)$, and the intensity of the magnetic field

$$H(z) = - \frac{df(z)}{dz}, \qquad z = x+iy \ , \ f = u+iv.$$

The results for the magnetic induction in the air-gap of the machine (along the dotted line in fig. 2), by using a 48-nodal-point mesh are given in fig. 3. (points 49 to 73).

FIG. 3

The obtained results compare favorably with those given in [10] (by using the classical BEM) as concerns the accuracy and also the computation time.

5. Conclusion

The advantages of the CVSBEM against other BEM procedures are:

1.Being a CVBEM procedure, the CVSBEM yields an approximation for the complete complex potential function in terms of some easily computable functions. Beside this, CVSBEM enables us to compute the derivatives of the complex potential, i.e. the complex field function, with high accuracy. The values $m_j = f'(z_j)$ are given by relation (11) and the derivative $f'(z)$ in other points is approximated by $F'(z)$.

2.The method does not require any approximation of the boundary curve or any numerical quadrature.

3.There is a convergence theoreme which states that the method has a high convergence order.

4.It is possible to obtain an error estimation ε_k at all mesh points and hence to develop an error reduction algorithm by adding new points in the neighbourhood of the nodes where the error is large.

The main shortcoming of the method consists in the fact that it can be applied only to the harmonic functions of two independent variables (respectively to the complex analytic funtions).

References

1. Brebbia,C.A.(ed.). Boundary Element Techniques in Computer-Aided Engineering, Martinus Nijhoff Publishers,

Dordecht / Boston /, Lancaster , 1984

2. Hromadka II,T.V. The Complex Variable Boundary Element Method, Springer - Verlag, Berlin, 1984.

3. Hromadka II,T.V., Yen,C.C., Guyman,G.L.. The Complex Variable Boundary Element Method: Applications. Int.J.Numer.Methods Eng., t21 (1985) pp. 1013-1025

4. Hromadka II.,T.V. , Durbin,I.D., Modelling steady-state, advective contaminant transport by the complex variable boundary element method, Engineering Analysis t3 (1986), pp.9-14.

5. Hromadka II, T.V., Best approximation of two-dimensional potential problems using the CVBEM, Engineering Analysis, t3 (1986), pp.118-122.

6. Homentcovschi, D., Cocora ,D., Magureanu ,R. Some Developments of the CVBEM - Application to the Mixed Boundary Value Problem for the Laplace Equation. Engineering Analysis, t3 (1986) nr.4.

7. Ahlberg,J.H., Nilson,E.N., Walsh,J.L. Complex Cubic Splines, Transactions of the American Mathematical Society, t.129 , nr.3(1967), pp. 391-413.

8. Ahlberg,J.H., Nilson,E.N., Walsh,J.L. The Theory of Splines and their Applications, Academic Press, New York and London,1967.

9. Symm,G.T. An Integral Equation Method in Conformal Mapping. Numer. Math. t.9, pp. 250-258 (1966).

10. Magureanu,R., Vasile,N., Tiba,M. Calculation of the Magnetic Field and Parameters of Synchronous Motors with Ceramic

Permanent Magnets Using the Boundary Element Method, Engineering Analysis, t.4, nr.1 (1987).

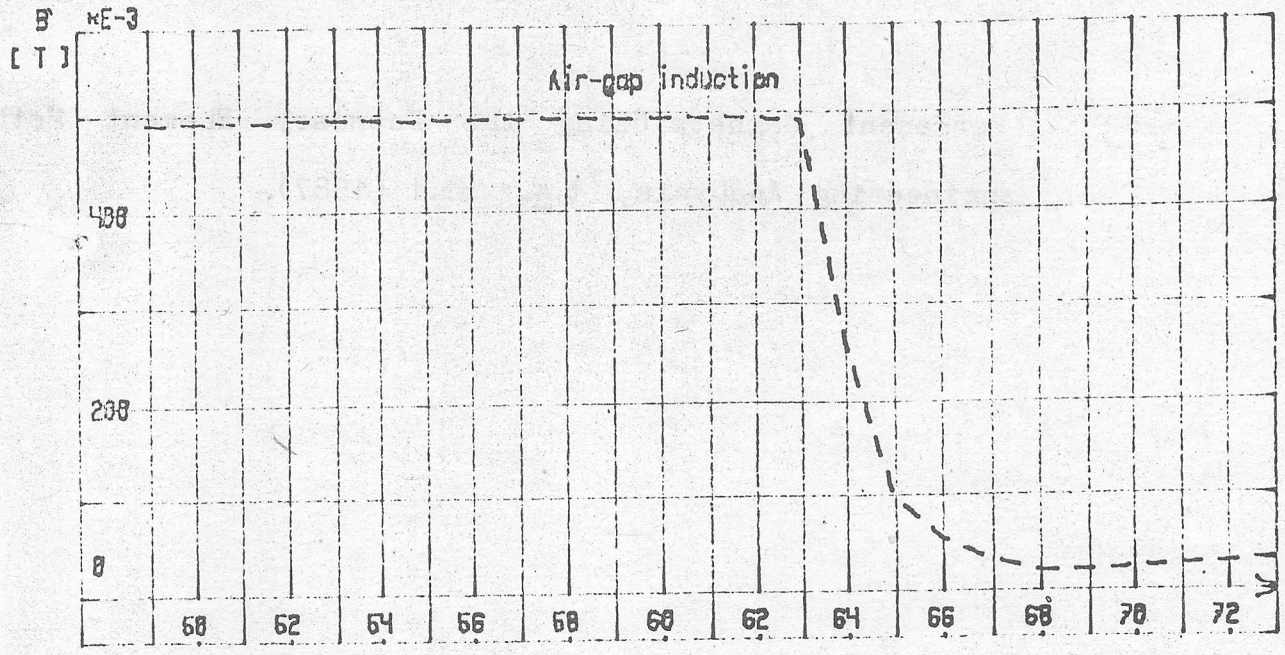

Fig. 3

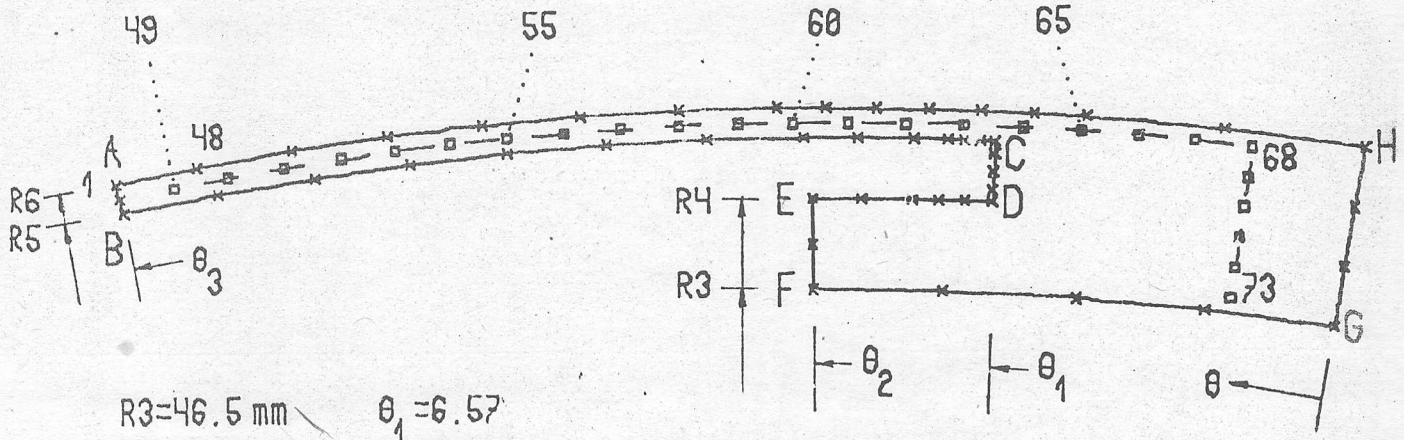

R3=46.5 mm
R4=48.0 mm
R5=49.0 mm
R6=49.5 mm

θ_1=6.57
θ_2=9.85
θ_3=22.5

Fig. 2

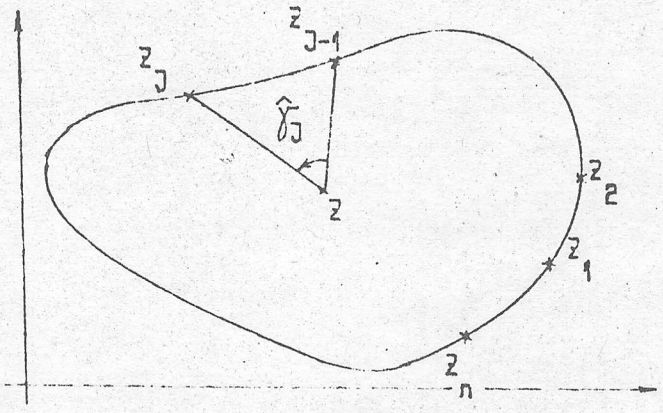

Fig. 1

AN ANALYTIC SOLUTION TO THE POISSON EQUATION IN SOME PLANE DOMAINS

Dorel Homentcovschi

Polytechnic Institute of Bucharest,

Department of Mathematics,

313 Splaiul Independentei,

Bucharest,

Romania.

AN ANALYTIC SOLUTION TO THE POISSON EQUATION IN SOME PLANE DOMAINS

An Analytic Solution to the Poisson Equation in Some Plane Domains

The paper proposes a particular analytical solution to the Poisson equation in case the density function $f(x,y)$ is analytic in its variables in the polygonal region D_1, and vanishes in $D-\bar{D}_1$. By means of this solution the numerical evaluation of the domain integrals in BEM can be avoided.

Introduction

As it is well-known, the source-term in the right-hand side of the Poisson equation gives us some trouble due to the domain integrals involved in Green's formula used in BEM. The numerical evaluation of the domain integrals needs a discretisation of the whole domain into finite elements (cells), which somehow affects the simplicity of the boundary element methods.

In case the source term is a harmonic function, the domain integral in Green's formula can be turned into a boundary integral, the domain discretisation being no longer necessary /1/. The second case in which the occurrence of the domain integrals can be avoided is the case when we know a particular solution to the Poisson equation.

In this paper we are giving a particular analytical solution to the Poisson equation in case we have an analytical distribution of sources inside polygonal regions included in the domain D where we must solve the boundary-value problem.

The Basic Formula

Let D_1 be a polygonal region inside the domain D, and z_1, z_2, ..., z_n the vertices of the polygon, numbered counterclockwise with respect to the region D_1. We use the complex variables

$$z = x + iy, \quad \bar{z} = x - iy$$

The equation of the $z_{k-1}z_k$ side of the polygon can be written in a complex form as

$$\bar{z} = m_k z + n_k \tag{1}$$

where

$$m_k = \frac{\bar{z}_k - \bar{z}_{k-1}}{z_k - z_{k-1}},$$

$$n_k = \frac{\bar{z}_{k-1}z_k - z_{k-1}\bar{z}_k}{z_k - z_{k-1}} \tag{2}$$

$(k = 1, \ldots, n)$

Fig.1

We have also denoted $z_{n+1} = z_1$, $z_0 = z_n$.

We consider the complex differential operators /2/

$$\frac{\partial}{\partial z} = \frac{1}{2}\left(\frac{\partial}{\partial x} - i\frac{\partial}{\partial y}\right), \quad \frac{\partial}{\partial \bar{z}} = \frac{1}{2}\left(\frac{\partial}{\partial x} + i\frac{\partial}{\partial y}\right)$$

We have

$$\frac{\partial}{\partial z}\frac{\partial}{\partial \bar{z}}V = \frac{1}{4}\left(\frac{\partial^2 V}{\partial x^2} + \frac{\partial^2 V}{\partial y^2}\right)$$

and hence the Poisson equation can be written as

$$\frac{\partial^2 V}{\partial z \partial \bar{z}} = \frac{1}{4} f(z, \bar{z}) \tag{3}$$

where

$$f(x,y) = f\left(\frac{z+\bar{z}}{2}, \frac{z-\bar{z}}{2i}\right) = f(z,\bar{z})$$

is the source density. We suppose the function $f(z,\bar{z})$ to be analytic in its variables inside region D.

Let us also denote by

$$d_z^{-1} f = \int f(z,\bar{z})\, dz \quad , \quad d_{\bar{z}}^{-1} f = \int f(z,\bar{z})\, d\bar{z}$$

$$g_k(\bar{z}) = (d_z^{-1} f)(\bar{w}_k \bar{z} + \bar{n}_k, \bar{z})$$
$$G_k(\bar{z}) = d_{\bar{z}}^{-1} g_k(\bar{z}) \qquad (4)$$
$$F(z,\bar{z}) = d_{\bar{z}}^{-1} d_z^{-1} f(z,\bar{z})$$

the antiderivatives (indefinite integrals) of the corresponding functions.

Theorem. The function

$$V(z,\bar{z}) = \frac{\delta}{4} F(z,\bar{z}) - \frac{1}{8\pi i} \sum_{j=1}^{\infty} F(z, m_j z + n_j) \ln \frac{z - z_j}{z - z_{j-1}} +$$

$$+ \frac{1}{8\pi i} \sum_{j=1}^{\infty} \left\{ G_j(\bar{z}) \ln \frac{\bar{z} - \bar{z}_j}{\bar{z} - \bar{z}_{j-1}} + G_j(m_j z + n_j) \ln \frac{z - z_j}{z - z_{j-1}} \right\} \qquad (5)$$

$$+ \frac{1}{8\pi i} \sum_{j=1}^{\infty} \left\{ G_{j+1}(\bar{z}_j) - G_j(\bar{z}_j) \right\} \ln \left[(z - z_j)(\bar{z} - \bar{z}_j) \right]$$

is a particular solution of the Poisson equation

$$\frac{1}{4} \Delta V \equiv \frac{\partial^2 V}{\partial z \partial \bar{z}} = \frac{\delta}{4} f(z,\bar{z}) \qquad (6)$$

where

$$\delta = \begin{cases} 1 & \text{for } z \in D_1 \\ 0 & \text{for } z \in D - \bar{D}_1 \end{cases}$$

The determinations of the complex logarithms in relation (5) are the main ones.

Proof. The function $V(z,\bar{z})$ defined by the relation (5) is continuous and differentiable outside the polygonal line, and hence in the domains D_1 and $D-\bar{D}_1$.

We have

$$\ln\frac{z-z_k}{z-z_{k-1}} = \ln\left|\frac{z-z_k}{z-z_{k-1}}\right| + i\hat{\gamma}_k$$

the angle $\hat{\gamma}_k \in (-\pi, \pi]$ being outlined in Fig.1 and therefore this function is continuous in all complex plane but the side $[z_{k-1}, z_k]$. Let the point $z^* \in (z_{k-1}, z_k)$.

We have

$$\lim_{\substack{z\to z^*\\ z\in D_1}}\left\{\frac{\delta}{4}F(z,\bar{z}) - \frac{1}{8\pi i}\sum_{j=1}^{n} F(z, m_j z+n_j)\ln\frac{z-z_j}{z-z_{j-1}}\right\} = \frac{1}{4}F(z^*,\bar{z}^*) -$$

$$-\frac{1}{8\pi i}\sum_{\substack{j=1\\ j\neq k}}^{n} F(z^*, m_j z^*+n_j)\ln\frac{z^*-z_j}{z^*-z_{j-1}} - \frac{1}{8\pi i}F(z^*,\bar{z}^*)\left\{\ln\left|\frac{z^*-z_k}{z^*-z_{k-1}}\right| + i\pi\right\}$$

$$\lim_{\substack{z\to z^*\\ z\in D-\bar{D}_1}}\left\{\frac{\delta}{4}F(z,\bar{z}) - \frac{1}{8\pi i}\sum_{j=1}^{n} F(z, m_j z+n_j)\ln\frac{z-z_j}{z-z_{j-1}}\right\} =$$

$$= -\frac{1}{8\pi i}\sum_{\substack{j=1\\ j\neq k}}^{n} F(z^*, m_j z^*+n_j)\ln\frac{z^*-z_j}{z^*-z_{j-1}} -$$

$$-\frac{1}{8\pi i}F(z^*,\bar{z}^*)\left\{\ln\left|\frac{z^*-z_k}{z^*-z_{k-1}}\right| - i\pi\right\}$$

Similarly, we have

$$\lim_{\substack{z\to z^*\\ z\in D_1}}\sum_{j=1}^{n}\left\{G_j(\bar{z})\ln\frac{\bar{z}-\bar{z}_j}{\bar{z}-\bar{z}_{j-1}} + G_j(m_j z+n_j)\ln\frac{z-z_j}{z-z_{j-1}}\right\} =$$

$$= \lim_{\substack{z\to z^* \\ z\in D-\bar{D}_1}} \sum_{j=1}^{m} \left\{ G_j(\bar{z}) \ln \frac{\bar{z}-\bar{z}_j}{\bar{z}-\bar{z}_{j-1}} + G_j(m_j z+n_j) \ln \frac{z-z_j}{z-z_{j-1}} \right\}$$

The relations above prove the continuity of the function $V(z,\bar{z})$ in the whole complex plane.

We equally have

$$\frac{\partial V}{\partial \bar{z}} = \frac{\delta}{4} \partial_z^{-1} f(z,\bar{z}) + \frac{1}{8\pi i} \sum_{j=1}^{m} q_j(\bar{z}) \ln \frac{\bar{z}-\bar{z}_j}{\bar{z}-\bar{z}_{j-1}} +$$

$$+ \frac{1}{8\pi i} \sum_{j=1}^{m} \left\{ \frac{G_j(\bar{z}) - G_j(\bar{z}_j)}{\bar{z}-\bar{z}_j} - \frac{G_j(\bar{z}) - G_j(\bar{z}_{j-1})}{\bar{z}-\bar{z}_{j-1}} \right\}$$

Again, this function is continuous in the complex plane. (The functions in the last sum have eliminable singularities at the $\bar{z}_j$ points.) By taking the derivative with respect to z we obtain the relation (6).

Formula (5) can be used to compute the values of the function $V(z,\bar{z})$ at all complex points but the vertices of the polygon. At point z_k ($k = 1, \ldots, n$) we shall use the formula

$$V(z_k,\bar{z}_k) = -\frac{1}{8\pi i} \sum_{\substack{j=1 \\ j\neq k,k+1}}^{m} F(z_k, m_j z_k + n_j) \ln \frac{z_k - z_j}{z_k - z_{j-1}} +$$

$$+ \frac{1}{8\pi i} \sum_{\substack{j=1 \\ j\neq k,k+1}}^{m} \left\{ G_j(\bar{z}_k) \ln \frac{\bar{z}_k - \bar{z}_j}{\bar{z}_k - \bar{z}_{j-1}} + G_j(m_j z_k + n_j) \ln \frac{z_k - z_j}{z_k - z_{j-1}} \right\} +$$

$$+ \frac{1}{8\pi i} \sum_{\substack{j=1 \\ j\neq k}}^{m} \left\{ G_{j+1}(\bar{z}_j) - G_j(\bar{z}_j) \right\} \ln\left[(z_k - z_j)(\bar{z}_k - \bar{z}_j) \right] - \qquad (5')$$

$$- \frac{1}{8\pi i} F(z_k,\bar{z}_k) \ln^* \frac{z_k - z_{k+1}}{z_k - z_{k-1}} + \frac{1}{8\pi i} \left\{ G_{k+1}(\bar{z}_k) \ln\left[(z_k - z_{k+1})(\bar{z}_k - \bar{z}_{k+1}) \right] - \right.$$

$$\left. - G_k(\bar{z}_k) \ln\left[(z_k - z_{k-1})(\bar{z}_k - \bar{z}_{k-1}) \right] \right.$$

We denoted

$$\ln^* z = \ln|z| + i\theta \quad , \quad -2\pi < \theta \leq 0$$

An Illustrative Example

As an application of the above theorem we consider the domain D_1 as being the square with vertices $z_1 = 1 + i$, $z_2 = -1 + i$, $z_3 = -1 - i$, $z_4 = 1 - i$ (Fig.2), and we take $f(z,\bar{z}) = 1$. Therefore we have a uniform source term in the region D_1 and the function V is harmonic in $D-\bar{D}_1$.

The relations (4) give

$$\alpha_z^{-1} f(z,\bar{z}) = z, \quad \alpha_{\bar{z}}^{-1} f(z,\bar{z}) = \bar{z}$$

$$g_k(\bar{z}) = \bar{m}_k \bar{z} + \bar{n}_k$$

$$G_k(\bar{z}) = \bar{m}_k \frac{\bar{z}^2}{2} + \bar{n}_k \bar{z}$$

$$F(z,\bar{z}) = z\bar{z}$$

Fig.2

We computed the values of the function $V(x,y)$ in a grid of 0.25 width. The results for the bottom right-hand-side corner of the square rounded by the dashed line in Fig.2 are given in Table 1. To check the accuracy of these results we computed ΔV using the five-point formula

$$\Delta V(i,j) = \frac{V(i,j+1) + V(i+1,j) + V(i,j-1) + V(i-1,j) - 4V(i,j)}{h^2} \qquad (7)$$

The results are given in Table 2.

Table 1

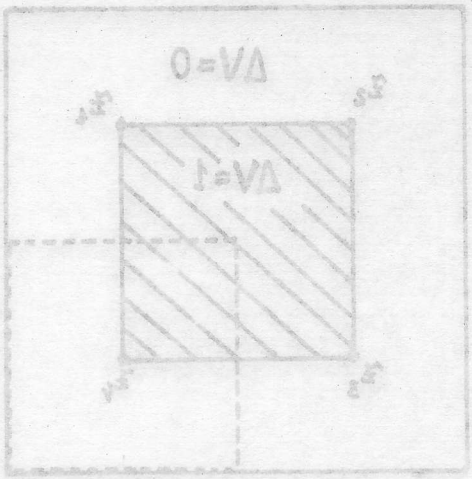

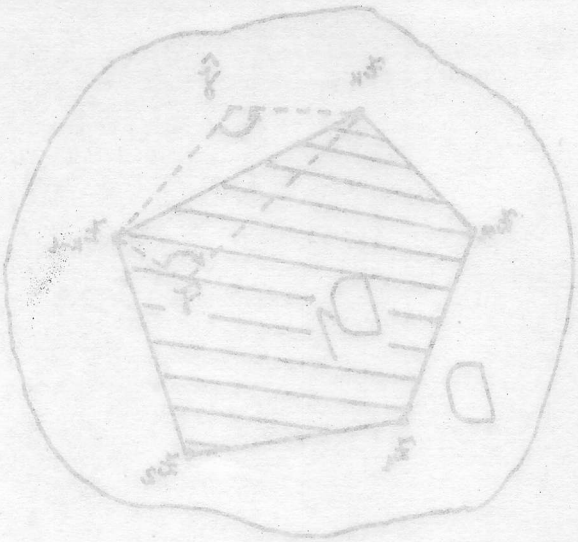

Table 2

It is to be noticed that the errors are within the limits of the truncation error in formula (7).

Conclusions. The particular solution to the Poisson equation given in this paper can be used to reduce the solving of a Poisson-type problem to a Laplace equation. Thus we can avoid the numerical evaluation of the domain integrals in BEM, preserving the reduced dimensionality characteristic to the boundary element methods.

The method is useful when thee functions $F(z,\bar{z})$, $G(\bar{z})$ can be effectively computed. This is the case for example with the polynomial, exponential, trigonometric density functions.

Due to its linearity, the method can be used to obtain a particular solution to the Poisson equation in case the density function is piecewise analytical.

References

/1/ Brebbia,C.A., Telles,L.C. and Wrobel,L.C., Boundary Element Techniques, Springer Verlag, 1984.

/2/ Homentcovschi,D., Complex Functions with Applications in Science and Engineering, (in Romanian), Ed. Tehnica, Bucharest, 1986.

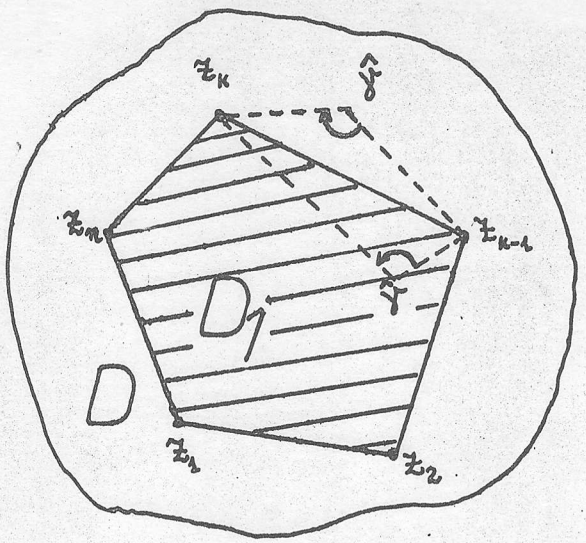

fig.1

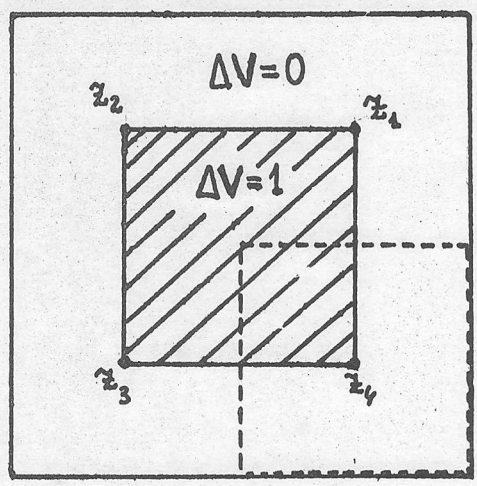

fig.2

0.721	0.736	0.784	0.865	0.984	1.111	1.221	1.315	1.399
0.736	0.752	0.798	0.878	0.995	1.120	1.228	1.321	1.403
0.784	0.798	0.842	0.918	1.028	1.147	1.249	1.338	1.417
0.865	0.878	0.918	0.985	1.083	1.191	1.283	1.365	1.438
0.984	0.995	1.028	1.083	1.162	1.248	1.327	1.400	1.467
1.111	1.120	1.147	1.191	1.248	1.313	1.378	1.441	1.500
1.221	1.228	1.249	1.283	1.327	1.378	1.432	1.485	1.537
1.315	1.321	1.338	1.365	1.400	1.441	1.485	1.531	1.576
1.399	1.403	1.417	1.438	1.467	1.500	1.537	1.576	1.616

Table 1.

1.003	1.003	1.003	1.002	0.501	-0.001	-0.002	0.000	0.000
1.003	1.003	1.003	1.003	0.501	-0.002	-0.002	0.000	0.000
1.003	1.003	1.004	1.005	0.500	-0.004	-0.003	0.000	0.000
1.002	1.003	1.005	1.014	0.500	-0.013	-0.004	0.000	0.000
0.501	0.501	0.500	0.500	0.250	0.000	0.000	0.000	0.000
-0.001	-0.002	-0.004	-0.013	0.000	0.013	0.004	0.000	0.000
-0.002	-0.002	-0.003	-0.004	-0.000	0.004	0.003	0.000	0.000
0.000	0.000	0.000	0.000	0.000	0.000	0.000	0.000	0.000
0.000	0.000	0.000	0.000	0.000	0.000	0.000	0.000	0.000

Table 2.

AN ANALYTICAL SOLUTION FOR THE COUPLED STRIPLINE-LIKE MICROSTRIP LINES PROBLEM

Dorel Homentcovschi
Polytechnic Institute of Bucharest,
Department of Mathematics,
313 Splaiul Independentei,
Bucharest, Romania

Anton Manolescu
Polytechnic Institute of Bucharest,
Department of Electronics,
313 Splaiul Independentei,
Bucharest, Romania

Anca Manuela Manolescu
Polytechnic Institute of Bucharest,
Department of Electronics
313 Splaiul Independentei,
Bucharest, Romania

Liviu Kreindler
Polytechnic Institute of Bucharest,
Department of Electrical Engineering,
313 Splaiul Independentei,
Bucharest, Romania

AN ANALYTICAL SOLUTION FOR THE COUPLED STRIPLINE-LIKE MICROSTRIP LINES PROBLEM

Dorel Homentcovschi
Polytechnic Institute of Bucharest,
Department of Mathematics,
313 Splaiul Independenței,
Bucharest, Romania

Anton Manoleescu
Polytechnic Institute of Bucharest,
Department of Electronics,
313 Splaiul Independenței,
Bucharest, Romania

Anca Manuela Manoleescu
Polytechnic Institute of Bucharest,
Department of Electronics
313 Splaiul Independenței,
Bucharest, Romania

Liviu Kreindler
Polytechnic Institute of Bucharest,
Department of Electrical Engineering,
313 Splaiul Independenței,
Bucharest, Romania

AN ANALYTICAL SOLUTION FOR THE COUPLED STRIPLINE-LIKE MICROSTRIP LINES PROBLEM

by Dorel Homentcovschi, Anton Manolescu, Anca Manuela Manolescu and Liviu Kreindler

Abstract - An analytical method for determining the Maxwell's capacitance matrix of multiconductor coupled stripline-like microstrip lines in an unhomogeneous medium is presented. The method is based on conformal mapping and on the theory of singular integral equations. The paper contains some applications.

I. INTRODUCTION

In the last few years the study of multiconductor coupled stripline-like microstrip lines has been of great interest due to the good high frequency properties of these lines, useful for developing some new microwave integrated circuits such as directional couplers, parallel coupled filters and so on. In contrast with the so-called "microstripline" classical half-shielded structure, the full-shielded structure named "stripline-like microstrip" /1/, offers the same phase velocities for both odd and even modes and, as a consequence, a very good coupling directivity and a well defined electrical behaviour.

For multiconductor coupled structures with very tight performances (interdigitated directional couplers, high order parallel coupled line filters) an accurate calculation method is required in order to estimate the influence of all the conducting

strips. A multitude of methods to perform this analysis are currently used; all of them are meant to solve the Laplace equation for the bidimensional electrostatic equivalent problem for low-order, quasi-TEM modes. One can mention several commonly used methods such as: conformal mapping technique for simple symmetrical cases /2/, numerical methods based on lattice approximations /3/, variational methods /4/, methods based on solving the integral equations derived from Green functions /5/-/7/ and so on. Although some of the numerical methods are quite general, none of the above mentioned methods could be thought as suitable for analysis and especially for synthesis of all the high performance structures.

The present paper presents a new analytical method of determining Maxwell's capacitance matrix of multiconductor stripline-like microstrips with coupled conductors with arbitrary widths and spacings and unhomogeneous media.

II. BASIC CONFIGURATION

The analysed multiconductor system consists of n zero-thickness conducting strips A_kB_k, with arbitrary widths and spacings, located on a dielectric substrate with thickness h. The system is fully shielded by ground planes on all sides, as shown in fig.1, and subject to the constraint that the shield spacing l equals the substrate thickness h. However, the relative dielectric constants ε_1 and ε_2 corresponding to the upper and lower dielectric media may be different.

Fig.1 Full-shielded multiconductor coupled striplines

The electrostatic field $\bar{E}(E_x, E_y)$ in the two dielectric media, inside the shielded box, can be written by means of the electrostatic potentials as

$$E_x^{(j)}(x,y) = -\partial\psi^{(j)}/\partial x \ ,$$
$$E_y^{(j)}(x,y) = -\partial\psi^{(j)}/\partial y \ , \quad j=1,2 \tag{1}$$

As $\psi^{(j)}(x,y)$ are harmonic functions we can introduce the harmonic conjugate functions $\varphi^{(j)}(x,y)$ - the field functions. Therefore, the complex potential functions

$$f^{(j)}(z) = \varphi^{(j)}(x,y) + i\cdot\psi^{(j)}(x,y) \ , \quad j=1,2 \tag{2}$$

are holomorphic of the complex variable $z=x+i\cdot y$ inside the two dielectric media.

On the shielded box the potential functions must vanish i.e.

$$\psi^{(1)}(x,y) = 0 \text{ for } y>0$$
$$\psi^{(2)}(x,y) = 0 \text{ for } y<0 \ , \text{ on the box .} \tag{3}$$

On the other hand on the symmetry axis we must have the physical conditions

$$D_y(x,+0) - D_y(x,-0) = \sigma(x)$$
$$E_x(x,+0) - E_x(x,-0) = 0 \ , \tag{4}$$

where $\sigma(x)$ is the surface density of the electrical charges and $\bar{D}(D_x, D_y)$ the electrical induction. This induction can be expressed by means of the potential and field functions

$$D_y(x,+0) = -\varepsilon_1 \frac{\partial\psi^{(1)}(x,0)}{\partial y} = -\varepsilon_1 \frac{\partial\varphi^{(1)}(x,0)}{\partial x}$$

$$D_y(x,-0) = -\varepsilon_2 \frac{\partial\psi^{(2)}(x,0)}{\partial y} = -\varepsilon_2 \frac{\partial\varphi^{(2)}(x,0)}{\partial x} \tag{5}$$

and therefore relations (4) become

$$-\varepsilon_1 \frac{\partial \varphi^{(1)}(x,0)}{\partial x} + \varepsilon_2 \frac{\partial \varphi^{(2)}(x,0)}{\partial x} = \rho(x) \qquad (6a)$$

$$\frac{\partial \psi^{(1)}(x,0)}{\partial x} = \frac{\partial \psi^{(1)}(x,0)}{\partial x} \qquad (6b)$$

On the insulating segments $B_k A_{k+1}$ we must have $\rho(x) = 0$; by integrating the relation (6a) we obtain

$$-\varepsilon_1 \cdot \varphi^{(1)}(x,0) + \varepsilon_2 \cdot \varphi^{(2)}(x,0) = -q_k \ , \quad x \in B_k A_{k+1} \ , \qquad (7)$$
$$k = 1, \ldots, n$$

where q_k are unknown constants. Relation(6b) gives

$$\psi^{(1)}(x,0) = \psi^{(2)}(x,0) \qquad (8)$$

On the conducting strip $A_k B_k$ we must have

$$\psi^{(1)}(x,0) = \psi^{(2)}(x,0) = V_k \ , \ k = 1, \ldots, n \ , \ x \in A_k B_k \qquad (9)$$

where V_k is the potential of the k-th electrode. Relation (6a) determines in this case the function $\rho(x)$. The total charge Q_k on the strip $A_k B_k$ is given by

$$Q_k = \int_{A_k}^{B_k} \rho(x)\, dx = -q_{k+1} + q_k$$

Hence

$$q_k = Q_k + q_{k+1} = \sum_{j=k}^{n} Q_j + q_{n+1} \quad ;(\ k=1, \ldots, n\ ) \qquad (10)$$

Finally, relations(7) and (8) are the boundary conditions on the insulating lines and relations (9) are the boundary conditions on the conducting strips.

III. DETERMINATION OF THE MAXWELL'S CAPACITANCE MATRIX

In order to solve the above settled boundary value problem

we conformally transform the domain filled by the two dielectric materials into a canonic domain. The upper region may be conformally mapped on the upper complex half-plane $\mathrm{Im}\{Z\} > 0$. (If the studied domain is actually a rectangular one, as in fig.1, the mapping function $z = w^{-1}(Z)$ is given by the Schwarz-Cristoffel formula and will be expressed by the first kind incomplete elliptical functions). Let $(-\infty, b_0) \cup (a_{n+1}, \infty)$ be the image of the upper side of the shielded box and the segment (a_k, b_k) the image of the strip $A_k B_k$ $(k=1,2,\ldots n)$. By symmetry reasons the lower region of the domain in fig.1 will be conformally mapped on the lower half-plane, fig.2.

Fig.2. The canonic domain obtained by conformal mapping of the domain in fig.1.

Thus the method can be used for more general geometries of the two dielectric media. The only restriction is the symmetry of the two dielectric domains with respect to the electrode line. In the sequel the actual shape of the shielded boundary is involved only through the abscissae a_k, b_k on the real axis $Y=0$ in the Z - plane, corresponding to the points A_k, B_k.

By conformal mapping the complex potentials $f^{(1)}(z)$, $f^{(2)}(z)$ become two holomorphic functions in the upper and respectively in the lower half-planes $F^{(1)}(Z)$, $F^{(2)}(Z)$.

We can write

$$F^{(1)}(Z) = \frac{1}{\pi i}\int_{-\infty}^{+\infty} \frac{\mu(t)}{t-Z}\,dt\,, \quad F^{(2)}(Z) = -\frac{1}{\pi i}\int_{-\infty}^{+\infty} \frac{\mu(t)}{t-Z}\,dt \qquad (11)$$

where the real function $\mu(t)$ must be determined by taking into account the boundary conditions.

$$\psi^{(1)}(x,0) = \psi^{(2)}(x,0) = \begin{cases} 0 & \text{for } x \in (-\infty, b_0) \cup (a_{n+1}, \infty) \\ V_k & \text{for } x \in (a_k, b_k), (k=1,\ldots,n) \end{cases} \quad (12)$$

and

$$\varepsilon_1 \phi^{(1)}(x,0) - \varepsilon_2 \phi^{(2)}(x,0) = q_k \quad \text{for } x \in (b_k, a_{k+1}) \quad (13)$$
$$\psi^{(1)}(x,0) = \psi^{(2)}(x,0) \qquad k = 0,1,\ldots,n$$

The values of functions $F^{(1)}(Z)$ and $F^{(2)}(Z)$ on the real axis can be obtained by using the Plemelj relations /8/.

$$F^{(1)}(x) = \phi^{(1)}(x,0) + i\psi^{(1)}(x,0) = i\mu(x) + \frac{1}{\pi} \int_{-\infty}^{+\infty}{}' \frac{\mu(t)}{t-x} dt \quad (14)$$

$$F^{(2)}(x) = \phi^{(2)}(x,0) + i\psi^{(2)}(x,0) = i\mu(x) - \frac{1}{\pi} \int_{-\infty}^{+\infty}{}' \frac{\mu(t)}{t-x} dt$$

where $\int'$ stands for the Cauchy principal value of the integral.

Relations (11) - (13) give

$$\mu(x) = 0 \quad \text{for } x \in (-\infty, b_0) \cup (a_{n+1}, \infty)$$

$$\mu(x) = V_k \quad \text{for } x \in (a_k, b_k), \quad k = 1,\ldots,n$$

$$\frac{\varepsilon_1+\varepsilon_2}{\pi} \int_{-\infty}^{+\infty} \frac{\mu(t)}{t-x} dt = q_k \quad \text{for } x \in (b_k, a_{k+1}), \; k=0,1,\ldots,n \quad (15)$$

The first two relations (15) determine the values of the function $\mu(x)$ on the electrodes; the last relation (15) gives the equation of the problem

$$\sum_{j=0}^{n} \frac{1}{\pi} \int_{b_j}^{a_{j+1}} \frac{\mu(t)}{t-x} \cdot dt = \frac{q_k}{\varepsilon_1+\varepsilon_2} - \sum_{j=1}^{n} \frac{1}{\pi} \int_{a_j}^{b_j} \frac{V_j}{t-x} dt$$

$$x \in (b_k, a_{k+1}) \;, \; k = 0,1,\ldots,n \quad (16)$$

This is a singular integral equation. Its solution is given in Appendix. The existence of a bounded solution of the integral equation is conditioned by compatibility conditions (A.6). In the case of equation (16) these conditions become

$$\sum_{k=0}^{n} \frac{q_k}{\varepsilon_1+\varepsilon_2} \int_{b_k}^{a_{k+1}} \frac{t^{l-1}}{\sqrt{P(t)}} \cdot dt - \sum_{j=1}^{n} V_j \int_{a_j}^{b_j} dt' \sum_{k=0}^{n} \frac{1}{\pi}\!\!\!\!\!\!\int_{b_k}^{a_{k+1}} \frac{t^{l-1}}{(t'-t)\sqrt{P(t)}} \cdot dt = 0$$

$$l = 1,2,\ldots,n \qquad (17)$$

where

$$P(Z) = \prod_{j=1}^{n+1} (Z-a_j)\cdot(Z-b_j)$$

By using relations

$$\sum_{k=0}^{n} \frac{1}{\pi}\!\!\!\!\!\!\int_{b_k}^{a_{k+1}} \frac{t^{l-1}}{(t'-t)\sqrt{P(t)}} \cdot dt = -i \frac{(t')^{l-1}}{\sqrt{P(t')}}$$

$$\sum_{k=0}^{n} \int_{b_k}^{a_{k+1}} \frac{t^{l-1}}{\sqrt{P(t)}}\, dt = 0$$

formula (17) becomes

$$\sum_{k=0}^{n} \frac{q_k}{\varepsilon_1+\varepsilon_2} \int_{b_k}^{a_{k+1}} \frac{t^{l-1}}{\sqrt{P(t)}}\, dt + i \sum_{k=1}^{n} V_k \int_{a_k}^{b_k} \frac{t^{l-1}}{\sqrt{P(t)}}\, dt = 0 \,,$$

$$l = 1,2,\ldots,n \qquad (18)$$

If we substitute q_k given by relation (10) in formula (18) we obtain

$$\frac{1}{\varepsilon_1+\varepsilon_2} \sum_{k=1}^{n} Q_k \sum_{j=0}^{k-1} \int_{b_j}^{a_{j+1}} \frac{t^{l-1}}{\sqrt{P(t)}}\, dt + i \sum_{k=1}^{n} V_k \int_{a_k}^{b_k} \frac{t^{l-1}}{\sqrt{P(t)}}\, dt = 0 \qquad (19)$$

Finally the conditions for the existence of bounded solutions of eqn. (16) become:

$$\sum_{k=1}^{n} N_{lk} \cdot Q_k = (\varepsilon_1+\varepsilon_2) \sum_{k=1}^{n} M_{lk} \cdot V_k \ , \quad l = 1,\ldots,n \tag{20}$$

where we denoted

$$A_{lk} = (-1)^k \int_{a_k}^{b_k} \frac{t^{l-1}}{\sqrt{|P(t)|}}\, dt \tag{21}$$

$$B_{lk} = (-1)^{k+1} \int_{b_k}^{a_{k+1}} \frac{t^{l-1}}{\sqrt{P(t)}}\, dt \tag{22}$$

and

$$M_{lk} = A_{lk} \ ; \ N_{lk} = \sum_{j=0}^{k-1} B_{lj} \quad , \quad l = 1,\ldots,n \tag{23}$$

Relation (20) gives the Maxwell's capacitance matrix $\mathbf{C}$

$$\mathbf{C} = (\varepsilon_1+\varepsilon_2) \cdot \mathbf{N}^{-1} \cdot \mathbf{M}, \tag{24}$$

where the matrices $\mathbf{M}$, $\mathbf{N}$ are defined by relations (21) - (23).

Let us denote now by $\mathbf{C}_{hom}$ the Maxwell capacitance matrix corresponding to the homogeneous dielectric medium ($\varepsilon_1=\varepsilon_2=\varepsilon_0$). Relations (24) give

$$\mathbf{C} = \frac{\varepsilon_1+\varepsilon_2}{2\varepsilon_0} \mathbf{C}_{hom} \tag{24'}$$

Therefore, in order to obtain the Maxwell capacitance matrix of a multiconductor system in a stratified dielectric (as represented in fig.1) it is necessary to know only the Maxwell capacitance matrix $\mathbf{C}_{hom}$ of the same multiconductor structure in free space.

In this way we obtained an analytical solution for the

Maxwell's capacitance matrix of the considered structure in terms of some hyperelliptic integrals depending on the structure geometry only by means of constants $a_1,\dots,a_{n+1}$ and $b_1,\dots,b_{n+1}$. These relations are similar to those characterising the impedance matrix of a resistive distributed structure /9/.

IV. APPLICATIONS

Let us now apply the above developed method to some concrete structures. We consider two kinds of problems. The first one consists of simple structures with one or two coupled striplines; in this case relations (24) give analytical formulae for the capacitances in terms of elliptical functions. The other type of applications concern the general case of multiconductor coupled structures for which simple analytical expressions are no longer available; accordingly the determination of the capacitance matrix requires the use of the general formulae (24).

In most applications the domains of interest are the rectangular box and the domain between two parallel ground planes. If the dielectric media fill the rectangle $B_{n+1} < x < A_{n+1}$, $-h < y < h$, the conformal mapping function is obtained by means of elliptical functions. The abscissae a_k, b_k of the points on the X axis corresponding to the electrode extremities are obtained in terms of the Iacobi's sn function

$$X = sn\,(x \cdot K/L, k), \tag{25}$$

where the modulus k is the solution of the equation

$$\frac{K(k)}{K(k')} = \frac{L}{h}, \quad k' = \sqrt{1-k^2} \tag{26}$$

Here K(k) is the complete elliptical integral of the first kind.

As the lateral sides of the rectangle are approaching the infinity ($L \to \infty$) the domain will tend to the strip $-h < y < h$ and the abscissae a_k, b_k will be given by formula

$$X = \tanh\left(\frac{\pi x}{2h}\right)$$

in terms of coordinates x of the corresponding points in the physical plane.

1. Single stripline in a shielded box

In this case the conformal mapping provides four points on the real axis (fig.3),

Fig.3. The geometry of the single stripline (a) and the image in the Z plane (b).

the abscissae a_1, b_1, a_2, b_2 being determined by relations (25) in terms of L, h, w and d. Relation (24) gives

$$\frac{C}{\varepsilon_1+\varepsilon_2} = \frac{M_{11}}{N_{11}} \qquad (28)$$

where C stands for the total capacitance of the microstrip and M_{11}, N_{11} are the integrals given by relations (25) - (27). In the case of a single stripline these integrals can be expressed in terms of complete elliptical integrals of the first kind

$$\frac{C}{\varepsilon_1+\varepsilon_2} = \frac{K(s)}{K(s')} \qquad (29)$$

Here the modulus s is related to the above mentioned abscissae by

relation

$$s = \sqrt{\frac{(b_1-a_1)(a_2-b_0)}{(b_1-b_0)(a_2-a_1)}} \qquad , \; s' = \sqrt{1-s^2} \tag{30}$$

The result given in relations (29),(30) holds for any stripline-like structure shielded in a box.

2. Single stripline between two parallel ground planes

If the length L of the shielding box in fig.3a becomes infinite, relation (27) will be appropriate and will give

$$b_1 = -a_1 = \tanh\left(\frac{\tilde{\pi}}{4}\cdot\frac{w}{h}\right) \tag{31}$$

$$a_2 = -b_0 = 1$$

Relation (30) becomes now

$$s = \frac{2\sqrt{\tanh(\tilde{\pi}w/(4h))}}{1+\tanh(\tilde{\pi}w/(4h))} \tag{32}$$

By using some relationships between the complete elliptical integrals of the first kind /10/, formula (29) can be written as

$$\frac{C}{\varepsilon_1+\varepsilon_2} = 2\,\frac{K(k)}{K(k')} \tag{33}$$

where the modulus k is given by relation

$$k = \tanh\left(\frac{\tilde{\pi}w}{4h}\right) \tag{34}$$

Formula (33) was given previously by Cohn /11/. It is used in applications in the form

$$Z_0 = \frac{Z_{0v}}{\sqrt{\varepsilon_{eff}}}\cdot\frac{K(k')}{K(k)}$$

where $Z_{ov}=\sqrt{\mu_0/\varepsilon_0} = 376{,}7\,\Omega$ is the characteristic impedance of

the free space and $\varepsilon_{eff} = (\varepsilon_1+\varepsilon_2)/2$ is the effective relative dielectric constant.

3. Two symmetrical, coupled striplines inside a shielded box

If the configuration is symmetrical with respect to a vertical axis (fig.4) the capacitances of the system can also be expressed by means of the complete elliptical integrals. By symmetry reasons the abscissae of the six points of interest are $\pm a$, $\pm b$, $\pm c$ where the constants a,b,c, are obtained by using the geometrical dimensions L,h,w,d in relations (25),(26).

Fig.4. The geometry of the shielded couple-strip (a) and the image in the Z plane (b).

Relations (20) give now

$$N_{11}(Q_1-Q_2) = (\varepsilon_1+\varepsilon_2)M_{11}(V_1 - V_2)$$
$$N_{21}(Q_1+Q_2) = (\varepsilon_1+\varepsilon_2)M_{21}(V_1 + V_2) \qquad (35)$$

Consider two particular propagation modes: even ($V_1=V_2=V$) and odd ($V_1=-V_2=V$). The capacitances corresponding to these two modes are given by relation (35)

$$\frac{C_{ev}}{\varepsilon_1+\varepsilon_2} = \frac{M_{21}}{N_{21}}$$

and

$$\frac{C_{odd}}{\varepsilon_1+\varepsilon_2} = \frac{M_{11}}{N_{11}} \qquad (36)$$

The integrals $M_{11},\ldots,N_{21}$ can be again expressed as complete elliptical integrals of the first kind.

We obtain

$$\frac{C_{ev}}{\varepsilon_1+\varepsilon_2} = \frac{K(p)}{K(p')} \tag{38}$$

where

$$p = \sqrt{\frac{b^2-a^2}{c^2-a^2}} \quad , \quad p' = \sqrt{1 - p^2} \tag{39}$$

and

$$\frac{C_{odd}}{\varepsilon_1+\varepsilon_2} = \frac{K(s)}{K(s')} \tag{40}$$

The modulus s is now given by formula

$$s = \sqrt{\frac{c^2(b^2-a^2)}{b^2(c^2-a^2)}} \quad , \quad s' = \sqrt{1 - s^2} \tag{41}$$

The two relations (38),(40) give the capacitance of the symmetrical two-conductor complete shielded coupler.

4. Two symmetrical coupled striplines between two parallel ground planes.

When the shielding box has no lateral walls ($L \longrightarrow \infty$) formula (27) gives

$$a = \tanh\left(\frac{\pi d}{4h}\right) , \quad b = \tanh\left(\frac{\pi}{2}\,\frac{d+2w}{2h}\right) , \quad c = 1 \tag{42}$$

and therefore relations (38),(39) become

$$\frac{C_{ev}}{\varepsilon_1+\varepsilon_2} = 2\,\frac{K(k_e)}{K(k_e')} \quad , \quad k_e' = \sqrt{1 - k_e^2} \tag{43}$$

where the modulus k_e is

$$k_e = \tanh\left(\frac{\pi w}{4h}\right)\cdot\tanh\left(\frac{\pi}{4}\left(\frac{w+d}{h}\right)\right) \tag{44}$$

We have also

$$\frac{C_{odd}}{\varepsilon_1+\varepsilon_2} = 2\cdot\frac{K(k_0)}{K(k_0')} \quad , \quad k_0' = \sqrt{1-k_0^2} \tag{45}$$

$$k_0 = \left(\tanh\left(\frac{\tilde{\pi}w}{4h}\right)\right) / \left(\tanh\left(\frac{\tilde{\pi}}{4}\cdot\frac{w+d}{h}\right)\right) \tag{46}$$

Relations (43) - (46) were also obtained by another method by Cohn /12/. They are used in practice for the even and odd characteristic impedances

$$Z_{0ev} = \frac{Z_{ov}}{\sqrt{\varepsilon_{eff}}}\cdot\frac{K(k_e')}{4K(k_e)} \tag{47}$$

and

$$Z_{0odd} = \frac{Z_{ov}}{\sqrt{\varepsilon_{eff}}}\cdot\frac{K(k_0')}{4K(k_0)} \tag{47}$$

where Z_{ov} and ε_{eff} are the same as above.

5. Two coupled striplines in a shielded box

If the symmetry of the two coupled striplines is given up no analytical formulae in terms of elliptical functions are available. However, the capacitance matrix can still be expressed by means of the hyperelliptical integrals (21), (22). These can be computed by using numerical methods. To check the formulae (24) we computed the solution for $W_1/W_2=1,\ldots,10$ and $d/h=1,\ldots,10$ (fig.5).

Fig.5. The nonsymmetrically coupled transmission lines.

In the case $\varepsilon_1 = \varepsilon_2$ the obtained values agree with those

obtained by Linner /13/ by a method working only for homogeneous dielectric media. Some of the results thus obtained were communicated in /14/.

6. Multiconductor structures in a shielded box.

This is a general case which can be solved by the developed method. The abscissae a_k, b_k are determined by relations (25),(26) (in the case of the coupled striplines between ground planes we shall use relation (27)). The Maxwellian capacitance matrix is expressed by formulae (24) providing an analytical (exact) solution of the problem. Further on, the estimation of integrals can be given only by numerical methods.

In order to estimate the accuracy of the method we considered the case of a multistrip structure with a homogeneous dielectric medium between two parallel ground planes, fig.6. This case was studied by Kammler /5/. In fig.6 we also give the abscissae a_k, b_k and the numerical results obtained for Maxwell's capacitance matrix.

Fig.6. The geometry of the multiconductor stripline considered in § 6 and numerical results.

Notice that the results thus obtained are identical within the first five digits with numerical results given in /5/.

V. CONCLUSIONS

The new method, offered by this paper, is based on the conformal mapping and on the singular integral equations theory.

The use of the conformal mapping enables its application to lines having the two dielectric media only if the media have equal heights.

This method provides an analytical expression for the Maxwell's capacitance matrix in terms of some hyperelliptic integrals. The influence of the structure geometry on these formulae is expressed only by means of the images of the ends of the conducting strips by conformal mapping.

The method is general. It applies to structures with an arbitrary number of conducting strips, with arbitrary widths and spacing, placed in an unhomogeneous dielectric medium. Moreover, relation (24') expresses the capacitance of the multistrip system in a stratified dielectric by means of the Maxwell's capacitance matrix of the same system placed in free space.

APPENDIX

In this appendix we solve the singular integral equation

$$\sum_{j=0}^{n} \frac{1}{\pi} \int_{b_j}^{a_{j+1}} \frac{\mu(t)}{t-X} \cdot dt = f(X) \quad , \; X \in A \tag{A1}$$

where we denoted by A the reunion of intervals (b_j, a_{j+1}), $(j=0,1,\ldots,n)$.

Let us consider the complex variable function

$$F(Z) = \Phi(X,Y) + i\cdot\Psi(X,Y) = \sum_{j=0}^{n} \frac{1}{i\pi} \int_{b_j}^{a_{j+1}} \frac{\mu(t)}{t-Z} \cdot dt \tag{A2}$$

This is a holomorphic function in the upper half-plane. (In fact it is holomorphic in the whole complex plane C except on segments $[b_j, a_{j+1}]$, $(j=0,1,\ldots,n)$).

On the boundary we have

$$F(X+i0) = \sum_{j=0}^{n} \frac{1}{i\pi} \int_{b_j}^{a_{j+1}} \frac{\mu(t)}{t-X} \, dt \qquad \text{for } X \in \mathbb{R} - \bar{A}$$

$$F(X+i0) = \mu(X) + \sum_{j=0}^{n} \frac{1}{i\pi} \int_{b_j}^{a_{j+1}} \frac{\mu(t)}{t-X} \cdot dt \quad \text{for } X \in A \tag{A3}$$

Hence we can write

$$\Phi(X,0) = 0 \qquad , \text{ for } X \in \mathbb{R} - \bar{A}$$

$$\Psi(X,0) = -f(X) \quad , \text{ for } X \in A \tag{A4}$$

Thus, the function F(Z) is the solution of a Volterra boundary-value problem. The solution can be written in the form /8/,/9/,/14/:

$$F(Z) = \frac{1}{\tilde{\Pi}} \sqrt{P(Z)} \sum_{j=0}^{n} \int_{b_j}^{a_{j+1}} \frac{f(t)}{\sqrt{P(t)}} \cdot \frac{dt}{t-Z} \qquad (A5)$$

where

$$P(Z) = \prod_{j=0}^{n} (Z-a_j)\cdot(Z-b_j) \quad , \quad (a_0 = a_{n+1}) \qquad (A6)$$

The square root in relation (A5) has a (n+1)th order pole at the infinity. In order that the function F(Z) be holomorphic at the infinity the sum in relation (A5) must have a (n+1)th-zero at this point. But in the neighbourhood of the infinity we have

$$\int_{b_j}^{a_{j+1}} \frac{f(t)}{\sqrt{P(t)}} \cdot \frac{dt}{Z-t} = \frac{1}{Z} \int_{b_j}^{a_{j+1}} \frac{f(t)}{\sqrt{P(t)}} \cdot \frac{dt}{1-t/Z} =$$

$$= \frac{1}{Z} \int_{b_j}^{a_{j+1}} \frac{f(t)}{\sqrt{P(t)}} \cdot \left(1 + \frac{t}{Z} + \frac{t^2}{Z^2} + \ldots \right) \cdot dt \qquad (A7)$$

Hence, the condition for the holomorphy of the function F(Z) at the infinity gives the relations

$$\sum_{j=0}^{n} \int_{b_j}^{a_{j+1}} \frac{f(t)\cdot t^{l-1}}{\sqrt{P(t)}} \cdot dt = 0 \quad (l=1,\ldots,n) \qquad (A8)$$

In these relations we have

CALCULATION OF THE MAGNETIC FIELD AND PARAMETERS OF SYNCHRONOUS MOTORS WITH CERAMIC PERMANENT MAGNETS USING THE BOUNDARY ELEMENT METHOD

Razvan Magureanu
Polytechnic Institute of Bucharest,
Department of Electrical Engineering
313 Splaiul Independentei,
Bucharest, Romania

Nicolae Vasile
I.C.P.E. Bucharest,
45-47 B-dul T.Vladimirescu
Bucharest, Romania

Marinela Tiba
I.C.P.E. Bucharest,
45-47 B-dul T.Vladimirescu
Bucharest, Romania

CALCULATION OF THE MAGNETIC FIELD AND PARAMETERS OF SYNCHRONOUS MOTORS WITH CERAMIC PERMANENT MAGNETS USING THE BOUNDARY ELEMENT METHOD

Razvan Magureanu
Polytechnic Institute of Bucharest,
Department of Electrical Engineering
313 Splaiul Independentei,
Bucharest, Romania

Nicolae Vasile
I.C.P.E. Bucharest,
45-47 B-dul Tudor Vladimirescu
Bucharest, Romania

Martinela Tiba
I.C.P.E. Bucharest,
45-47 B-dul Tudor Vladimirescu
Bucharest, Romania

CALCULATION OF THE MAGNETIC FIELD AND PARAMETERS OF SYNCHRONOUS MOTORS WITH CERAMIC PERMANENT MAGNETS USING THE BOUNDARY ELEMENT METHOD

Razvan Magureanu
Nicolae Vasile
Marinela Tiba
Polytechnic Institute of Bucharest
ICPE- Bucharest- Romania

1.Introduction

In the last few years permanent magnet synchronous motors have been paid special attention both by their designers and their users.This type of motor enjoys a number of advantages such as simplicity of construction, high reliability, high power-weight ratio, and the absence of sliding contacts.

Some of the most important questions which arise in connection with these motors are how to calculate the excitation magnetic field and the leakage flux, and how to estimate the influence of the de-magnetization m.m.f.upon the excitation field.

The geometric configuration of the rotor may be widely varied,according to the type of magnet used.Thus ceramic magnets require a short axial length and a large surface , while metallic magnet requirements are quite the opposite, thus results from the magnetic characteristics of these materials.

Computing the field and parameters of these machines is not an easy task due to their complicated geometry, the nonlinearity of magnetic materials and the winding distributions.

In this paper a linear model has been used because on the one hand ceramic magnet excitation does not allow the air-gap flux density to exceed 0.5-0.6 T and on the other ,the maximum

flux density in the machine teeth is under 1.0-1.2 T in order to keep down iron losses which occur at high operating frequencies as high as 200 - 400 Hz and above.This makes it possible to consider the iron magnetic permeability to be equal to infinity.To simplify matters the relative permeability of the ceramic magnet μ_R is taken to be equal to the air permeability 1.0 .On this assumption the magnetic field density which derives from a scalar magnetic potential satisfying the Laplace equation is computed for a two dimensional domain since, the machine length is much greater than its diameter .The Laplace equation is integrated numerically using the boundary element method.In this way the excitation magnetic field, the rotor leakage flux and the steady state parameters are calculated.

2.Calculation of the excitation magnetic field

2.1. The integration domain and boudary conditions

A rotor configuration widely used with ceramic permanent magnet (PM) synchronous motors, is the one presented in Fig.1.The magnets are placed along the rotor radi, and the ferromagnetic laminations are mounted on a non-magnetic sleeve.

Fig.1

In choosing the integration domain, two requirements are to be met at the same time.First the geometrical configuration should be as simple as possible and secondly it should contain known boundary conditions.The problem is simplified if conditions of symetry are provided.Thus,in the case presented in this paper, a domain covering one half of a pole- pitch has been chosen for integration.Its boundary is the ABCDEFGHIJA-line (see Fig.2).

Fig.2

The boundary conditions are stated using the following simplying hypotheses:

- $\mu_{Fe} = \infty$;
- the air-gap segment AJ of the polar-axis is a flux line.

Thus referring to fig.2 ,the boundary conditions may be written as follows:

$$U_{AB} = 0, \qquad (1)$$

$$U_{BC} = U_{CD} = U_{DE} = 0. \qquad (2)$$

Condition (1) states that the scalar magnetic potential of the stator is zero; condition (2) is provided by the symmetry of the rotor.

Considering a linear variation for the scalar magnetic potential on segments EF and JA , and a constant scalar potential U_o on the ferromagnetic armature, it follows that:

$$U_{EF} = \frac{(\frac{\tilde{\pi}}{2p} - \vartheta)}{(\frac{\tilde{\pi}}{2p} - \frac{\vartheta_p}{2})} U_o \; ; \; \vartheta_p/2 \leq \vartheta \leq \tilde{\pi}/2p \; ; \qquad (3)$$

$$U_{FG} = U_{GH} = U_{HI} = U_{IJ} = U_o \; ; \qquad (4)$$

$$U_{JA} = \frac{R - R_6}{R_5 - R_6} U_o \; ; \; R_5 \leq R \leq R_6 \qquad (5)$$

U_o will be calculated using the magnetic flux law, which is applied to a surface including the pole piece yielding:

$$B_g \cdot S_p \cdot \sigma = B_m \cdot S_m \; , \qquad (6)$$

and the magnetic circuit law :

$$2H_g \cdot k_c \cdot k_s = H_m \cdot h_m \; , \qquad (7)$$

where: S_p = the pole piece face,

S_m = the magnet face area,

k_c = the Carter-factor,

k_s = the saturation-factor,

h_m = the magnet height,

σ = the leakage factor, unknown.

Assuming that a linear approximation for the demagnetization curve can be used for ferrite magnets then:

$$B_m = \frac{B_r}{H_c} (H_c - H_m), \qquad (8)$$

then using:

$$B_g = \mu_o \cdot H_g \; ; \quad U_o = H_g \cdot g = \frac{B_g}{\mu_o} \cdot g \qquad (9)$$

together with equations (6), (7) and (8) results in:

$$\sigma = \frac{B_r \left(H_c - 2k_c \cdot k_s \cdot \frac{U_o}{h_m} \right)}{\mu_o \frac{S_p}{S_m} \cdot \frac{U_o}{g} \cdot H_c} . \qquad (10)$$

It will be noticed that the leakage factor is proportional to the air-gap length, and decreases when S_p / S_m ratio increases.

The leakage factor σ can also be calculated using its definition:

$$\sigma = \frac{\Phi_u + \Phi_\sigma}{\Phi_u} = \frac{\Phi_{r_{AB}} + \Phi_{t_{BE}}}{\Phi_{r_{AB}}} , \qquad (11)$$

where:

$$\Phi_{r_{AB}} = l \cdot \int_0^{\vartheta_t/2} B_r(\vartheta) \, R_4 \, d\vartheta , \qquad (12)$$

$\Phi_{r_{AB}}$ = useful flux,

$$\Phi_{t_{BE}} = 1 \cdot \int_{R_1}^{R_4} B_t(R)\, d\,R, \qquad (13)$$

$\Phi_{t_{BE}}$ = leakage flux.

The integrals (12) and (13) are calculated after integrating the Laplace equation in polar coordinates on the ABCDEFGHIJA domain. Thus, in every point of the domain, two values of the magnetic flux density are found: one radial and one tangential.

From (10) and (11), two $\sigma = \sigma(U)$ curves are obtained. At their cross-point, σ_c and U_{oc}, can be found and these are used in the calculation of the magnetic flux distribution throughout the domain.

2.2. The boundary-element method: presentation

Let $$\Delta U = 0 \qquad (14)$$

be the Laplace equation on domain D, and

$$U = \bar{U} \text{ on } C_1; \quad q = \frac{\partial U}{\partial n} = \bar{q} \text{ on } C_2, \qquad (15)$$

its boundary conditions, where $C = C_1 \cup C_2$ is the boundary of domain D (see Fig.3.).

Fig. 3

Let C_i be a discretization of boundary C ($i = 1,2,3,\ldots,N$) N_1 points are on C_1, N_2 points are on C_2, $N = N_1 + N_2$.

Let D_i be a discretization of domain D (D_i = set of points inside D) and $M_i \in (D_i \cup C_i)$.

The boundary-element method is based on the numerical

calculation of the following relationships:

$$c(M_i)\, U(M_i) + \int_{C_1} Uq^*\, ds + \int_{C_2} Uq^*\, ds = \int_{C_1} q\, U^*\, ds + \int_{C_2} q\, U^*\, ds \qquad (16)$$

where: $c(M_i) = 1$, if $M_i \in D_i$,

$c(M_i) = 1/2$, if $M_i \in C_i$,

U^* is the fundamental solution of equation (14) associated with point M_i,

$$q^* = \frac{\partial U^*}{\partial n}.$$

$$\Delta U^* + \delta(M_i) = 0, \qquad (17)$$

where $\delta(M_i)$ is the Dirac distribution in point M_i.

For bidimensional domains,

$$U^*(M_i) = \frac{1}{2\pi} \ln \frac{1}{r}, \qquad (18)$$

where is r = the distance from point M_i to the current point on the boundary.

In equation (16), U and q are considered constant on each element. U and q are the values in the mid-points of each element. Based on these conditions equation (16), can be written as follows:

$$c(M_i)\, U(M_i) + \sum_{j=1}^{N_1} \bar{U}_j \cdot \int_{C_{1j}} q^*\, ds + \sum_{j=N+1} U_j \cdot \int_{C_{2j}} q^*\, ds =$$

$$= \sum_{j=1}^{N_1} q_j \cdot \int_{C_{1j}} U^*\, ds + \sum_{j=N_1+1}^{N} \bar{q}_j \cdot \int_{C_{2j}} U^*\, ds \qquad (19)$$

After writing an equation like (19) for each point $M_i \in C_i$ $(i = 1,2,\ldots,N)$, a system of N algebric linear equations is obtained. The unknown quantities are q_j

$(j=1,2,.....,N_1)$ and U_j $(j = N_1+1,\ N_1+2,...,N)$. Integrals $\int U^* ds$ and $\int q^* ds$ are calculated either analytically or numerically.

When U_j, $\bar{U}_j$, q_j and $\bar{q}_j$ are all known, (19) is applied again to calculate the magnetic potential at every point $M_i \in D_i$ The boundary-element method results in the use of less computer memory than in the case of the finite element method.This is because points inside the domain do not need to be included in the computation; only the boundary is discretized..

2.3. Calculation of the excitation magnetic field and of the leakage flux

For the integration of the Laplace-equation applied to the domain in Fig.2, the discretization in Fig.4 has been chosen.

Fig. 4

Considering the polar coordinates,

$$\int_{C_j} q^* ds = \int_{C_j} \frac{\partial U^*}{\partial n}\, ds = \frac{1}{2\pi} \cdot \int_{C_j} -\frac{\partial (\ln (1/r))}{\partial n}\, ds, \qquad (20)$$

$$\int_{C_j} U^* ds = \frac{1}{2\pi} \cdot \int_{C_j} \ln \left(\frac{1}{r}\right) ds ,$$

where: C_j =circle arcs (see Fig. 5.a) or radius segments (see Fig.5.b), r is calculated as:

$$r = \sqrt{R^2 + R_p^2 - 2 \cdot R \cdot R_p \cdot \cos (\vartheta - \vartheta_p)} \quad . \qquad (21)$$

The integrals in (20) are calculated numerically. For the boundary elements which contain singularities the integrals were done analitically. This eliminates a too fine discretisation necessary for other computational methods when applied to

configurations with very narrow air gaps.

Fig. 5

The air gap and interpolar flux distribution are presented in Fig.6.

Fig. 6

The tests have shown good agreement with the computer results. For example, for one model, the average flux density for one pole, obtained by measuring the no-load E.M.F. was 0.407 T, while the calculated value was 0.415 T.

The maximum air-gap magnetic induction B_{gmax}, the average air-gap magnetic induction B_{gmed}, and leakage coefficient have been calculated for different rotor configurations. The results are given in Fig. 7, 8, 9, 10, 11.

Fig. 7 Strontium ferrite, having B_r=0.35 T and H_c=250 kA/m,

Fig. 8 has been used in order to develop at I.C.P.E. Bucharest

Fig. 9 permanent magnet synchronous motors with rotor geo-

Fig. 10 metrical configuration given in fig. 2.

Fig. 11

3. Calculation of the steady-state parameters

The analysis of the motor and of its performance starts with the calculation of its steady-state parameters, such as: magnetization reactances, leakage reactances, phase-resistance etc.

Here, the magnetization reactances along the two axes d and q are calculated as functions of the rotor geometry for a non-saturated magnetic circuit.Thus,

$$X_{ad} = \frac{K_w}{R_d} \frac{k_{ad}}{k_{sd}}, \qquad (22)$$

$$X_{aq} = \frac{K_w}{R_q} \frac{k_{ad}}{k_{sq}},$$

where: K_w = the winding factor, which depends on the number of phases, number of poles and number of coils in the stator winding;

k_{sd}, k_{sq} = saturation factors on axes d and q ($k_{sd} = k_{sq} = 1.$, when the magnetic circuit is not saturated)

k_{ad}, k_{aq} = form factors of the air-gap flux density on the two axes, considering only the stator field sources;

R_d, R_q = reluctances on the d and q axes, respectively

R_d and R_q will be calculated using the stator magnetic field distribution, for a symmetrical current-system 3-phase stator.

3.1. Calculation of the parameters on axis d

Fig.12. Consider the configuration in Fig. 12. The integration of the Laplace-equation is done on domain ABCDEFGHIJKLMA, with the following boundary conditions :

$$U_{AB} = U_{sd} \cos\theta;$$

$$U_{BC} = U_{CD} = U_{DE} = U_{EF} = 0; \qquad (23)$$

$$U_{FG} = \frac{R - R_1}{R_2 - R_1} U_o ;$$

$$U_{GH} = U_{HI} = U_{IJ} = U_{JK} = U_{KL} = U_{LM} = U_o ;$$

$$U_{MA} = \frac{R - R_5}{R_6 - R_5} (U_{sd} - U_o) + U_o .$$

The maximum air-gap M.M.F. is:

$$V = \frac{B_g}{\mu_o} . \qquad (24)$$

the M.M.F. on axis d is:

$$V_d = V \cos \beta , \qquad (25)$$

where β is the internal angle of the machine, chosen 45^o , B_g is arbitrary 0.45 T .

The scalar magnetic potential at point A is

$$U_{sd} = U_o + V_d . \qquad (26)$$

U_o is calculated using the magnetic flux law, applied to a surface defined by the curve GHIJKLMNOPRSG :

$$\phi_1 = \phi_{LMN} = 2 \cdot \phi_{LM} = K_{11} \cdot U_0 + k_{12} = \phi_2 , \qquad (27)$$

$$\phi_2 = \phi_{NOPRSGHIJKL} = 2 \cdot \phi_{GHIJKL} = k_{21} \cdot U_0 . \qquad (28)$$

Considering two values for U_0 (U_{01} and U_{02}) and using (27) and (28), it follows that:

$$\phi_{11} = \phi_1 \Big|_{U_0 = U_{01}} , \qquad \phi_{21} = \phi_2 \Big|_{U_0 = U_{01}} ,$$

$$\phi_{12} = \phi_1 \Big|_{U_0 = U_{02}} , \qquad \phi_{22} = \phi_2 \Big|_{U_0 = U_{02}} .$$

The value of U_o on axis d is to be found at the intersection point of the two lines obtained by following four points: (ϕ_{11} , U_{01}), (ϕ_{12} , U_{02}) and (ϕ_{21} , U_{01}), (ϕ_{22} , U_{02}).

Thus,

$$U_{od} = \frac{(\phi_{21} - \phi_{11}) \cdot (U_{02} - U_{01})}{(\phi_{12} - \phi_{11}) - (\phi_{22} - \phi_{21})} + U_{01} \quad (29)$$

U_{od} given by (29) is used as in previous case in calculating the field distribution in the domain which was considered (see fig 13).

Fig. 13. The amplitude of the fundamental harmonic of the air-gap magnetic flux distribution is calculated using the Fourier-coefficients:

$$B_{gd1} = \frac{4}{\tilde{\tilde{\Pi}}} \cdot \int_0^{\frac{\tilde{\tilde{\Pi}}}{2}} b_{gdr}(\vartheta) \cos\vartheta \, d\vartheta, \quad (30)$$

where:

$$b_{gqr}(\vartheta) = -\mu_0 \cdot \left. \frac{\partial U(r,\vartheta)}{\partial r} \right|_{r = R_5}.$$

The form factor of the air gap flux distribution (mentioned above) is defined as

$$k_{ad} = \frac{B_{gd1}}{B_{gdc}}, \quad (31)$$

where for: B_{gd1} is defined by equation (30) and

$B_{gdc} = B_g \cdot \cos\beta$ = the amplitude of the fundamental harmonic of the air gap magnetic flux distribution for the ideal cylinder rotor;

β = the internal angle of the machine.

The magnetic circuit reluctance on axis d is made up of the reluctance corresponding to the air-gap for a polar pitch R_{gd} and of the reluctance R_{dpa} of the interpolar gap, occupied in

part by the magnet.

The air-gap reluctance R_{gd} defined for the first harmonic of the magnetomotive force and of the magnetic flux density is the resultant of the reluctance of the elementary flux tubes spanning the whole lenght of the machine corresponding to the discretization of arc AB.

$$R_{gd} = \frac{1}{\sum_i \left(\frac{1}{R_{gdi}}\right)} = \frac{p \cdot \Delta U_{gd1}}{\tilde{\Pi} \cdot B_{gd1} \cdot R_6 \cdot l} \qquad (32)$$

where ΔU_{gd1} is the amplitude of the fundamental of the magnetomotive force in the air-gap for d axis .

The reluctance R_{dpa} between face LKIHG of U_o potential and the face BEF of zero potential is directly yielded by the ratio of the magnetic potential difference between the two faces U_{od} to the corresponding magnetic flux ϕ_d .

$$R_{dpa} = \frac{U_{od}}{\phi_d} \qquad (32')$$

Taking into acount the manner in which the magnetic lines of force close for a 2p pole machine, the overall reluctance on axis d is found from:

$$R_d = 2 \cdot R_{gd} + \frac{2p - 1}{p} \cdot R_{dpa} \qquad (33)$$

3.2. Calculation of the parameters on axis q

Fig. 14

Consider the configuration shown in Fig. 14. the integration domain for the Laplace equation is ABCDEFGHIJKLMA, with boundary conditions as follows:

$$U_{AB} = U_{sq} \sin\vartheta ;$$

$$U_{BC} = U_{CD} = U_{DE} = U_{EF} = 0 ;$$

$$U_{FG} = \frac{R - R_1}{R_2 - R_1} U_0 ; \qquad (34)$$

$$U_{GH} = U_{HI} = U_{IJ} = U_{JK} = U_{KL} = U_{LM} = U_0 ;$$

$$U_{MA} = \frac{R - R_5}{R_6 - R_5} (U_{sq} - U_0) + U_0 .$$

When applied to the polar armature, the flux law gives $U_{oq} = 0$. The scalar magnetic potential in point A is

$$U_{sq} = V_q = V \sin\beta . \qquad (35)$$

Fig.15 — For these conditions the flux distribution is calculated. (see fig.15).

As in the case of axis d, the amplitude of first harmonic of the flux distribution in the air gap is:

$$B_{gq1} = \frac{4}{\pi} \cdot \int_0^{\frac{\pi}{2}} b_{gqr}(\vartheta) \sin\vartheta \, d\vartheta , \qquad (36)$$

where

$$b_{gqr} = -\mu_0 \cdot \frac{\partial U(r,\vartheta)}{\partial r} \Bigg|_{r = R_5} .$$

The flux distribution form factor of the air gap k_{aq}, is defined in the same way as k_{ad},

$$k_{aq} = \frac{B_{gq1}}{B_{gqc}} , \qquad (37)$$

where $B_{gqc} = B_g \sin\beta$.

The magnetic circuit reluctance on axis q, R_q consists of the reluctance corresponding to the air gap for a polar pitch

R_{gq} and the reluctance R_{qpa} of the interpolar gap in which lies the magnet.

The air gap reluctance R_{gq} defined for the first harmonic of the magnetomotive force and of the magnetic flux density is the resultant of the reluctance of the elementary flux tubes spanning the whole length of the machine corresponding to the discretization of arc AB.

$$R_{gq} = \frac{1}{\sum_i \left(\frac{1}{R_{gqi}}\right)} = \frac{p \cdot \Delta U_{gq1}}{\tilde{\pi} \cdot B_{gq1} \cdot R_6 \cdot l}, \qquad (38)$$

where ΔU_{gqi} is the amplitude of the fundamental of the magnetomotive force in the air-gap for q axis.

The reluctance R_{qpa} between the face LKIHG of linear potential varying from U_{oq} to zero and the face BEF is computed as the ratio of the average magnetic potential defference of the two faces of the corresponding magnetic flux ϕ_q.

$$R_{qpa} = \frac{U_{sq}}{2 \cdot \phi_q} \cdot \qquad (38')$$

Taking into consideration the manner in which the magnetic lines of force close for a 2p pole machine, the overall reluctance of axis d is given:

$$R_q = \frac{2 \cdot p - 1}{p} \cdot \frac{2 \cdot R_{gq} \cdot R_{qpa}}{2 \cdot R_{gq} + R_{qpa}} \cdot$$

Fig. 16 Fig. 16,17, and 18 show the variation of k_{ad},

Fig. 17 k_{aq}, R_{gd}, R_{dpa}, R_{gq}, R_{qpa}

Fig. 18 function of the polar cover-factor, where $R_{gz} = g/\mu_o \cdot \tau \cdot l$, τ is pole pitch and l is active length of the motor.

4. Conclusions

The magnetic field and parameters of synchronous motor with ceramic permanent magnets was computed numerically using the boundary element method . This offers important advantages as compared to the finite difference and finite element methods. First ,there is a significant reduction of the number of equations to be solved and hence a reduction in computer storage necessary .Secondly, unlike the other methods flux distribution on boudaries , defined as the derivatives of magnetic potential with respect to the normal to the boundary is obtained automatically in the process of integration without other additional computations.

On the basis of the computation carried out for this configuration for ferrite synchronous motors it was found that the reluctance on axis d is higher than on axis q and hence the synchronous reactance on axis d is lower than the synchronous reactance on axis q.This is entirely due to the presence of the permanent magnet of low permeability in the magnetic circuit of axis d.

5. Acknowledgement

This paper is part of a research program sponsored by the Romanian Academy of Science and I.C.P.E.-Bucharest on the one hand , and by the Royal Society of London and Computational Mechanics Institute-Southampton on the other . The authors are very much obliged to these institutions for all moral and material support.

REFERENCES

1. BREBBIA, C.A. The boundary element method for engineers. Pentech Press, London, Plymouth, 1985.

2. BREBBIA, C.A., TELLES, J.C., WROBEL, C. Boundary element techniques. Springer-Verlag, Berlin, 1984.

3. FRANSUA, Al., MAGUREANU, R. Electrical machines and drive systems. Technical Press, Oxford, 1984.

4. MAGUREANU, R., VASILE, N. Permanent magnet and variable reluctance synchronous motors. Editura Tehnica, Bucharest, 1983.

5. MAGUREANU, R. Special electrical machines for control systems. Editura Tehnica, Bucharest, 1981.

6. MAGUREANU, R., VASILE, N. Special electrical machines, design manual. Permanent magnet synchronous motors. I.P.B. Press, Bucharest, 1980.

7. VASILE, N. Magnetic field computation of ceramic permanent synchronous motors using the boundary element method. Electrotehnica, vol. 33, no 3. 1985, pag. 72-79.

8. FRANSUA, Al., VASILE, N., TIBA, M., MAGUREANU, R. Permanent magnet synchronous motors magnetic field computation by boundary element method. Proceedings of the International symposium on electromagnetic fields in electrical engineering. Warsaw, Poland. September 26-28, 1985, pag. 171-174.

9. LEAN, M.H., WEXLER, A. Accurate field computation with the boundary element method. I.E.E.E. Trans. on Magnetics, vol. MAG-18, No. 2, March 1982, P. 331-335.

10. ARMSTRONG, A.G.A.M., FAN, M.W., SIMKIN, J. Automated optimization of magnet design using the boundary integral method. I.E.E.E. Trans. Magnetics, vol MAG-18, No. 2, March 1982, p. 620-623.

11. FOUAD, F.A., NEHL, T.W., Magnetic field modeling of permanent magnet type electronicaly operated synchronous machines using finite element, I.E.E.E. Trans. on PAS, vol PAS-100 Sept. 1981.

LIST OF FIGURES

Fig. 13. Magnetic flux distribution in the air-gap on the d-axis produced by the stator winding for $\alpha_p=0.79$.

Fig. 14. The integration domain for the calculation of the parameters on axis q.

Fig. 15. Magnetic flux distribution in the air gap, on the q-axis, produced by the stator winding for $\alpha_p=0.79$.

Fig. 16. The variation of k_{ad} and k_{aq}, as function of the polar cover-factor.

Fig. 17. Variation of R_{gd}/R_{gz} and R_{dpa}/R_{gz} ratio as function of the polar cover-factor.

Fig. 18. Variation of R_{gq}/R_{gz} and R_{qpa}/R_{gz} ratio as function of the polar cover-factor.

$$\sqrt{P(X)} = \begin{cases} \sqrt{|P(X)|} & , \text{ for } X\in(-\infty, b_0) \\ (-1)^{k+1}\cdot i\cdot\sqrt{|P(X)|} & , \text{ for } X\in(b_k, a_{k+1}) \\ (-1)^{k}\sqrt{|P(X)|} & , \text{ for } X\in(a_k, b_k) \\ (-1)^{n+1}\sqrt{|P(X)|} & , \text{ for } X\in(a_{n+1}, \infty) \end{cases}$$

Finally, the bounded solution of the integral equation (A1) follows from the relations (A3) and (A5)

$$\mu(X) = -\frac{1}{\pi}\sqrt{P(X)}\cdot\sum_{j=0}^{n}\int_{b_j}^{a_{j+1}}\frac{f(t)}{\sqrt{P(t)}}\cdot\frac{dt}{X-t}\,, \quad X\in A$$

REFERENCES

/1/ Ramesh Garg "Stripline-like Microstrip Configuration", Microwave Journal, vol.22, No.4, April 1979, pp.103-104.

/2/ F.Oberhettinger and W.Magnus "Adwendung der Elliptischen Funktionen in Physik und Technik", Berlin, Germany, Springer 1949.

/3/ H.E.Green "The Numerical Solution of Some Important Transmission-Line Problems", IEEE Trans.Microwave Theory and Tech., vol.MTT-13, pp.676-692, Sept.1965.

/4/ E.Yamashita "Variational Method for the Analysis of Microstrip-like Transmission Lines", IEEE Trans.Microwave Theory Tech. vol.MTT-16, No.8, pp.529-535, Aug.1968.

/5/ D.W.Kammler "Calculation of Characteristic Admittances and Coupling Coefficients for Strip Transmission Lines", IEEE Trans.Microwave Theory Tech., vol.MTT-16, pp.925-937, Nov.1968.

/6/ T.G.Bryant and J.A.Weiss "Parametres of Microstrip Transmission lines and of Coupled Pairs of Microstrip Lines", IEEE Trans.Microwave Theory Tech., vol.MTT-16, pp.1021-1027, Dec.1968.

/7/ G.M.L.Gladwell and S.Coen "A Chebyshev Approximation Method for Mocrostrip Problems", IEEE Trans.Microwave Theory Tech., vol.MTT-23, pp.865-870, Nov.1975.

/8/ D.Homentcovschi "Complex Variable Functions and Applications in Science and Technique" (in romanian), Bucharest, 1986.

/9/ D.Homentcovschi, A.Manolescu, A.M.Manolescu, C.Burileanu

"A General Approach to Analysis of Distributed Resistive Structures",IEEE Trans.Electron Devices,vol.ED-25,pp.787-794,July 1978.

/10/I.M.Ryshik and I.S.Gradstein "Tables of Series,Products and Integrals",Berlin,Germany,VEB Deutscher Verlag 1957.

/11/S.B.Cohn "Characteristic Impedance of the Shielded-Strip Transmission Line",IRE Trans.Microwave Theory Tech.,vol.MTT-2 pp.52-57,July 1954.

/12/S.B.Cohn "Shielded Coupled-Strip Transmission Line", IRE Trans.Microwave Theory Tech.,vol.MTT-3,pp.29-38,Oct.1955.

/13/L.J.P.Linner "A Method for the Computation of the Characteristic Immitance Matrix of Multiconductor Striplines with Arbitrary Widths",IEEE Trans. Microwave Theory Tech., vol.MTT-22,pp.930-937,Nov.1974.

/14/D.Homentcovschi, A.M.Manolescu, A.Manolescu "Analysis of Multiterminal structures for Very High Frequencies" (in rom.) Microelectronica vol.15,Ed.Acad.RSR,1987.

/15/C.Jacob "Introduction mathematique a la mechanique des fluides",Bucarest - Paris 1959.

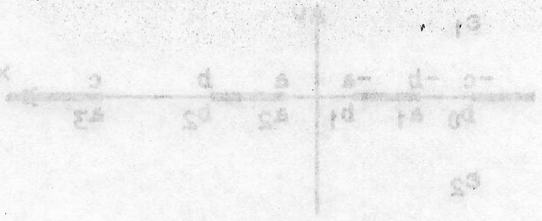

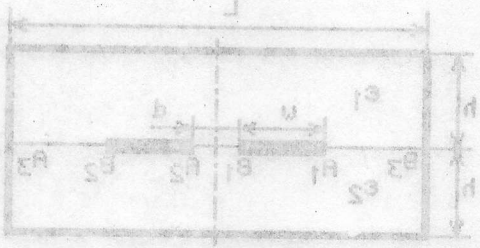

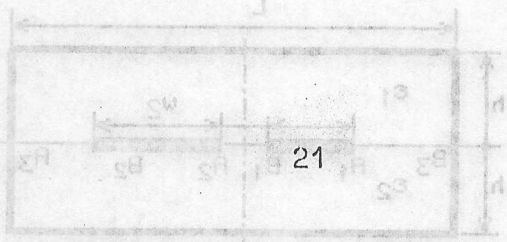

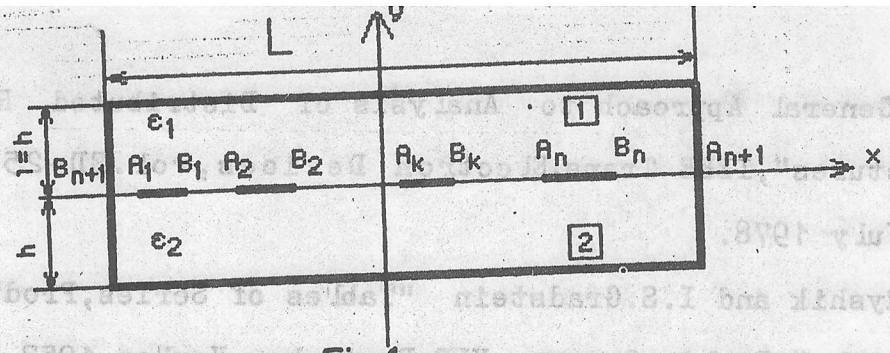

Fig. 1

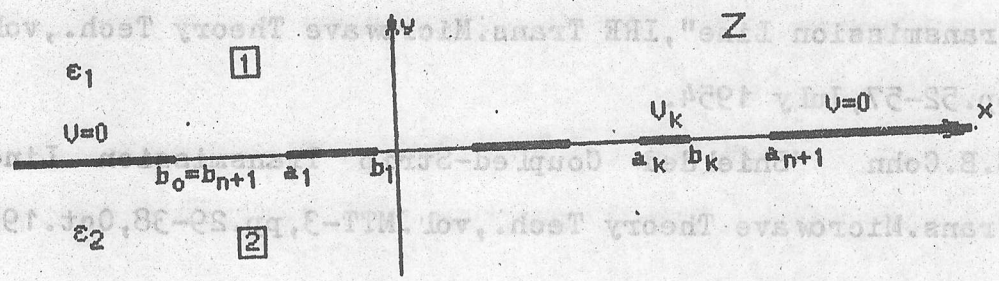

Fig. 2

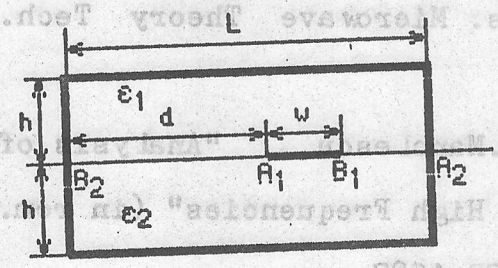

Fig. 3a

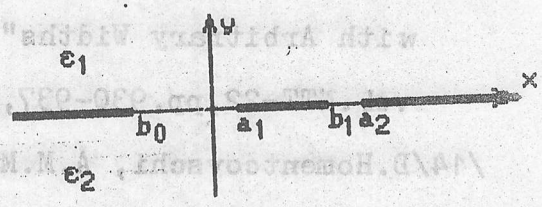

Fig. 3b

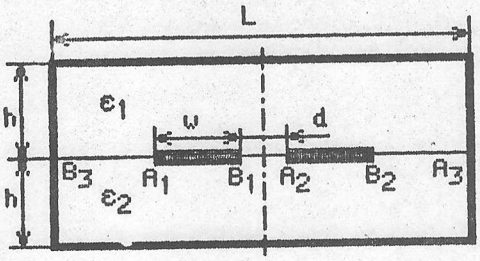

Fig. 4a

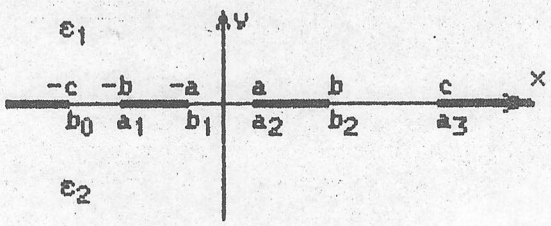

Fig. 4b

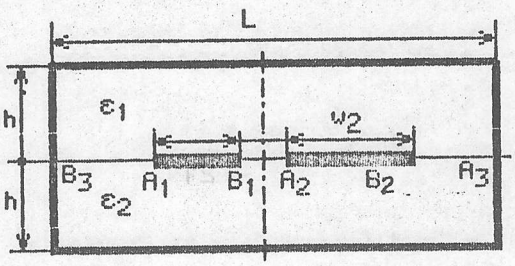

Fig. 5

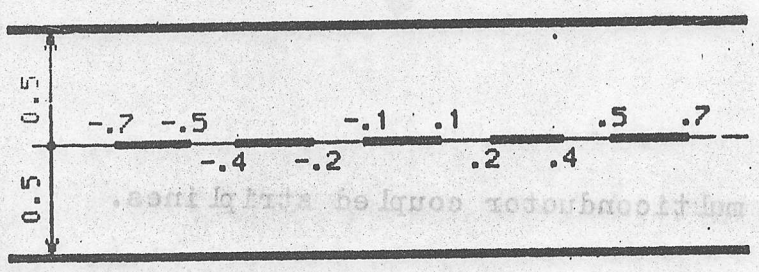

$a_6 = -b_0 = 1.$ $b_5 = -a_1 = 0.975701$ $a_5 = -b_1 = 0.917152$

$b_4 = -a_2 = 0.850134$ $a_4 = -b_2 = 0.556893$ $b_3 = -a_3 = 0.304216$

$C_{11}/\varepsilon = C_{55}/\varepsilon = 2.89143$ $C_{22}/\varepsilon = C_{44}/\varepsilon = 3.29387$

$C_{33}/\varepsilon = 3.29609$ $C_{12}/\varepsilon = C_{45}/\varepsilon = -1.00608$

$C_{23}/\varepsilon = C_{34}/\varepsilon = -0.97638$ $C_{13}/\varepsilon = C_{35}/\varepsilon = -0.07942$

$C_{14}/\varepsilon = C_{25}/\varepsilon = -0.01174$ $C_{24}/\varepsilon = -0.07512$

$C_{15}/\varepsilon = -0.00197$ $C_{ij} = C_{ji}$

Fig. 6

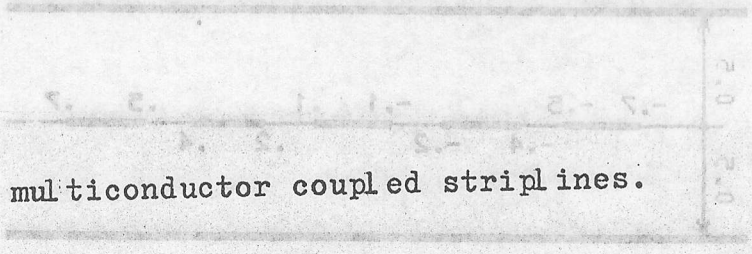

Fig.1 Full-shielded multiconductor coupled striplines.

Fig.2 The canonic domain obtained by conformal mapping of the domain in fig.1.

Fig.3 The geometry of the single stripline (a) and the image in the Z plane (b).

Fig.4 The geometry of the shielded couple-strip (a) and the image in the Z plane (b).

Fig.5 The nonsymmetrycally coupled transmission lines.

Fig.6 The geometry of the multiconductor stripline considered in 6 and numerical results.

The authors are with the Polytechnic Institute of Bucharest, Bucharest, Romania .

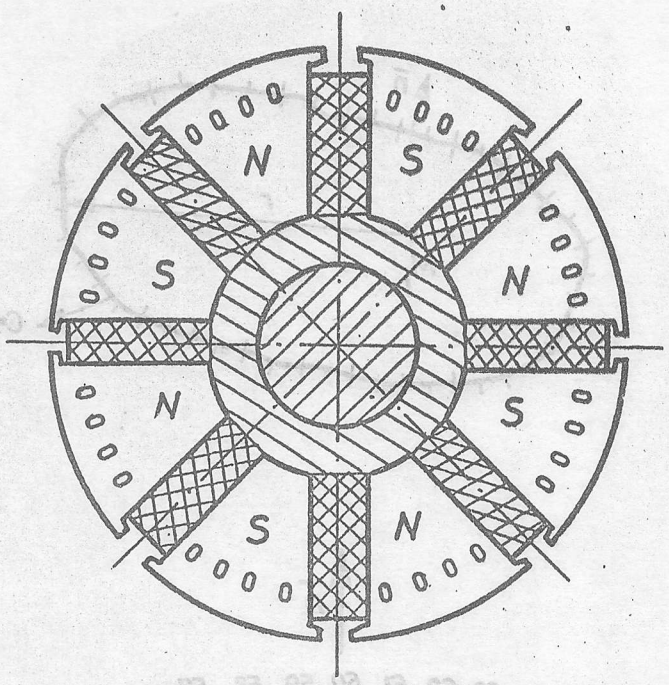

Fig.1

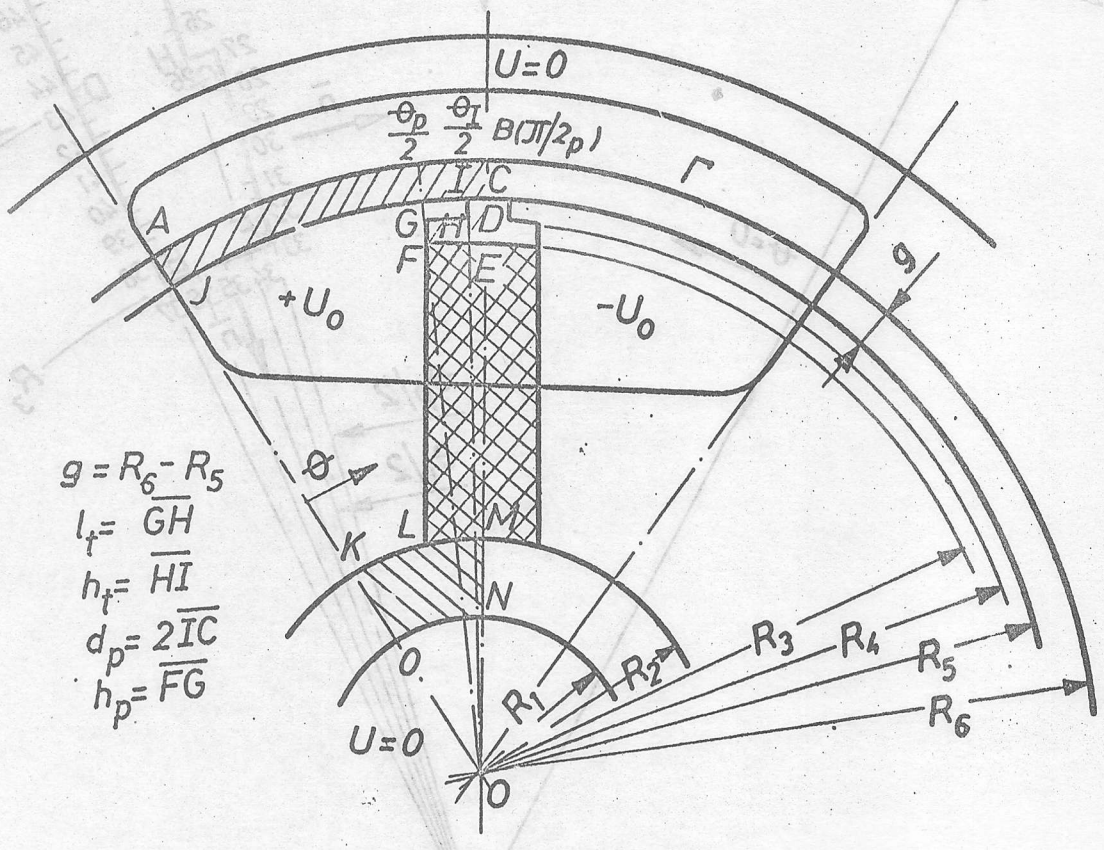

$g = R_6 - R_5$

$l_t = \overline{GH}$

$h_t = \overline{HI}$

$d_p = 2\overline{IC}$

$h_p = \overline{FG}$

Fig. 2

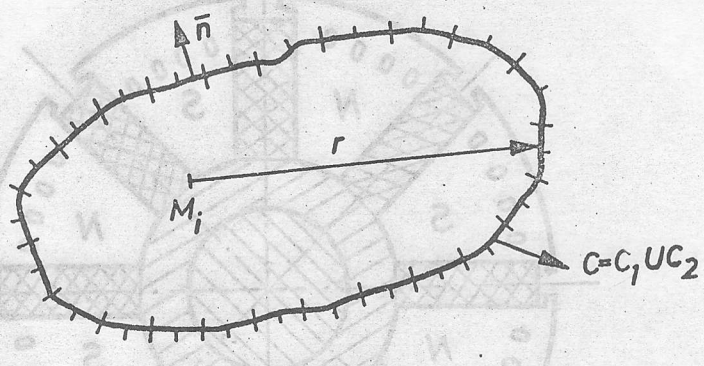
n
r
M_i
$C=C_1 \cup C_2$

Fig. 3

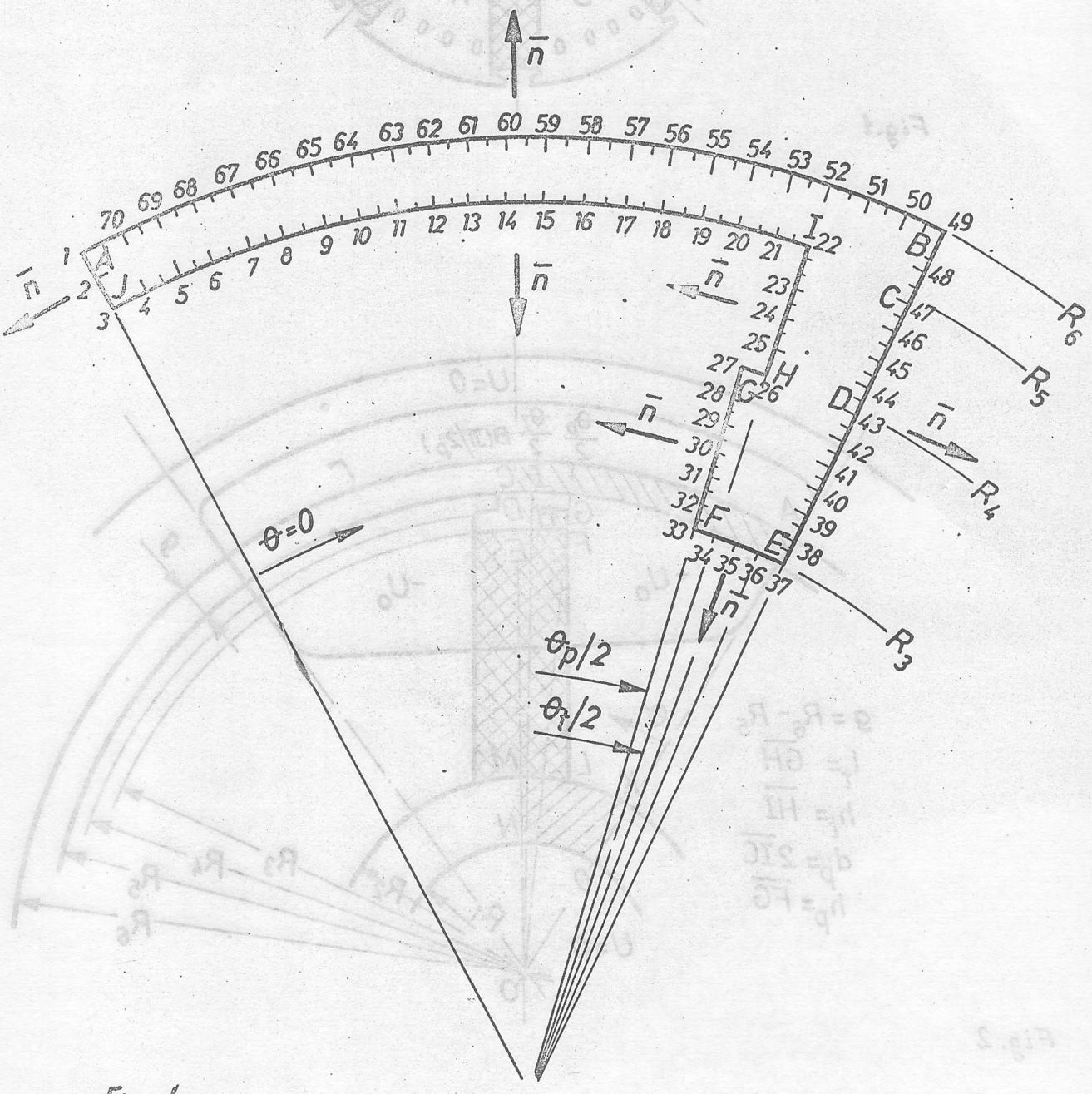
n
1 2 3 4 5 6 7 8 9 10 11 12 13 14 15 16 17 18 19 20 21 22 23 24 25 26 27 28 29 30 31 32 33 34 35 36 37 38 39 40 41 42 43 44 45 46 47 48 49 50 51 52 53 54 55 56 57 58 59 60 61 62 63 64 65 66 67 68 69 70
A
B
C
D
E
F
G
H
I
J
R_3
R_4
R_5
R_6
$\theta=0$
$\theta_p/2$
$\theta_t/2$

Fig. 4

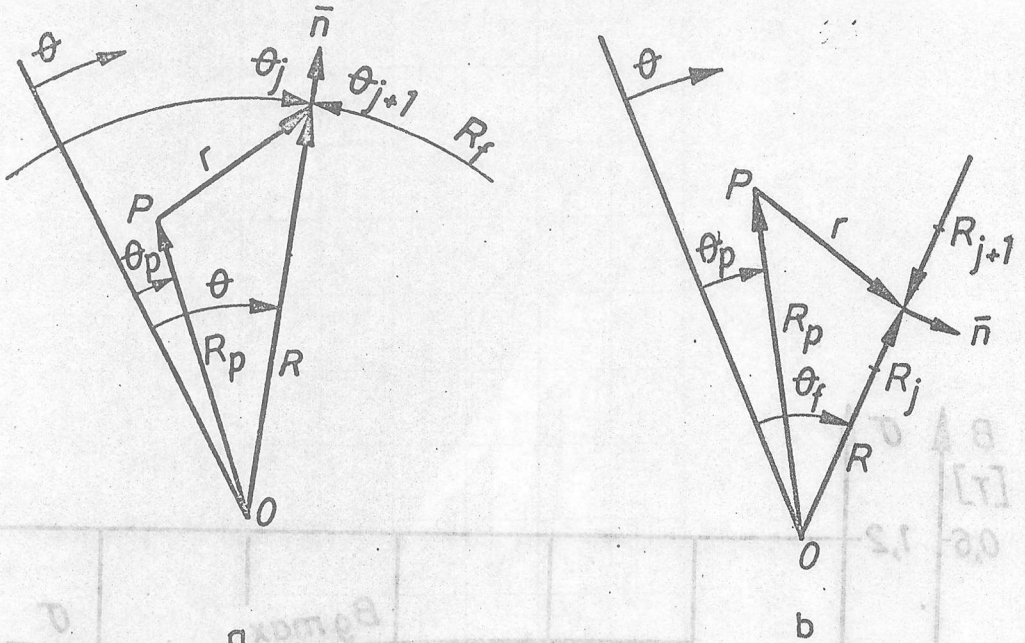

Fig. 5

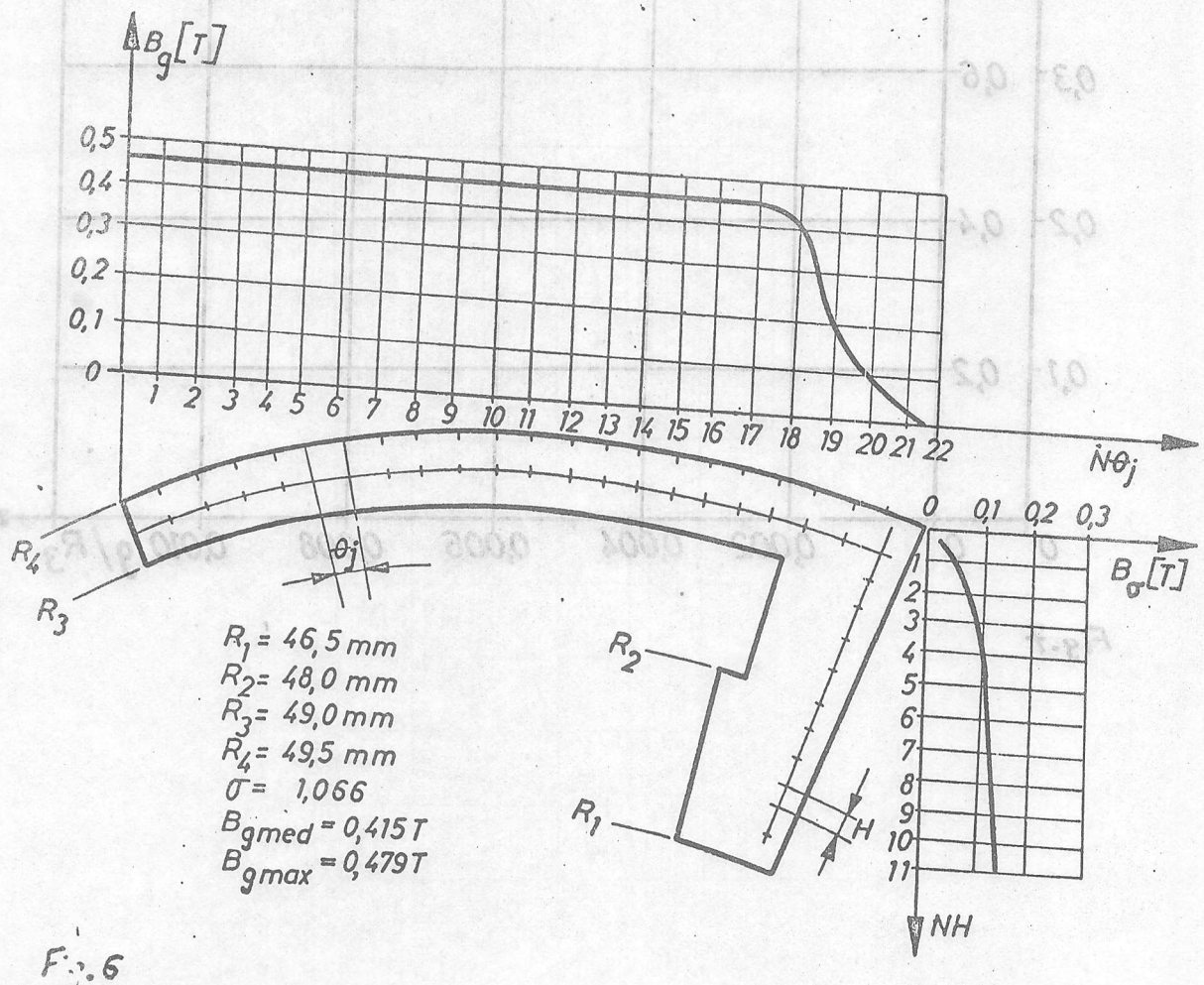

$R_1 = 46,5\ mm$
$R_2 = 48,0\ mm$
$R_3 = 49,0\ mm$
$R_4 = 49,5\ mm$
$\sigma = 1,066$
$B_{gmed} = 0,415\ T$
$B_{gmax} = 0,479\ T$

Fig. 6

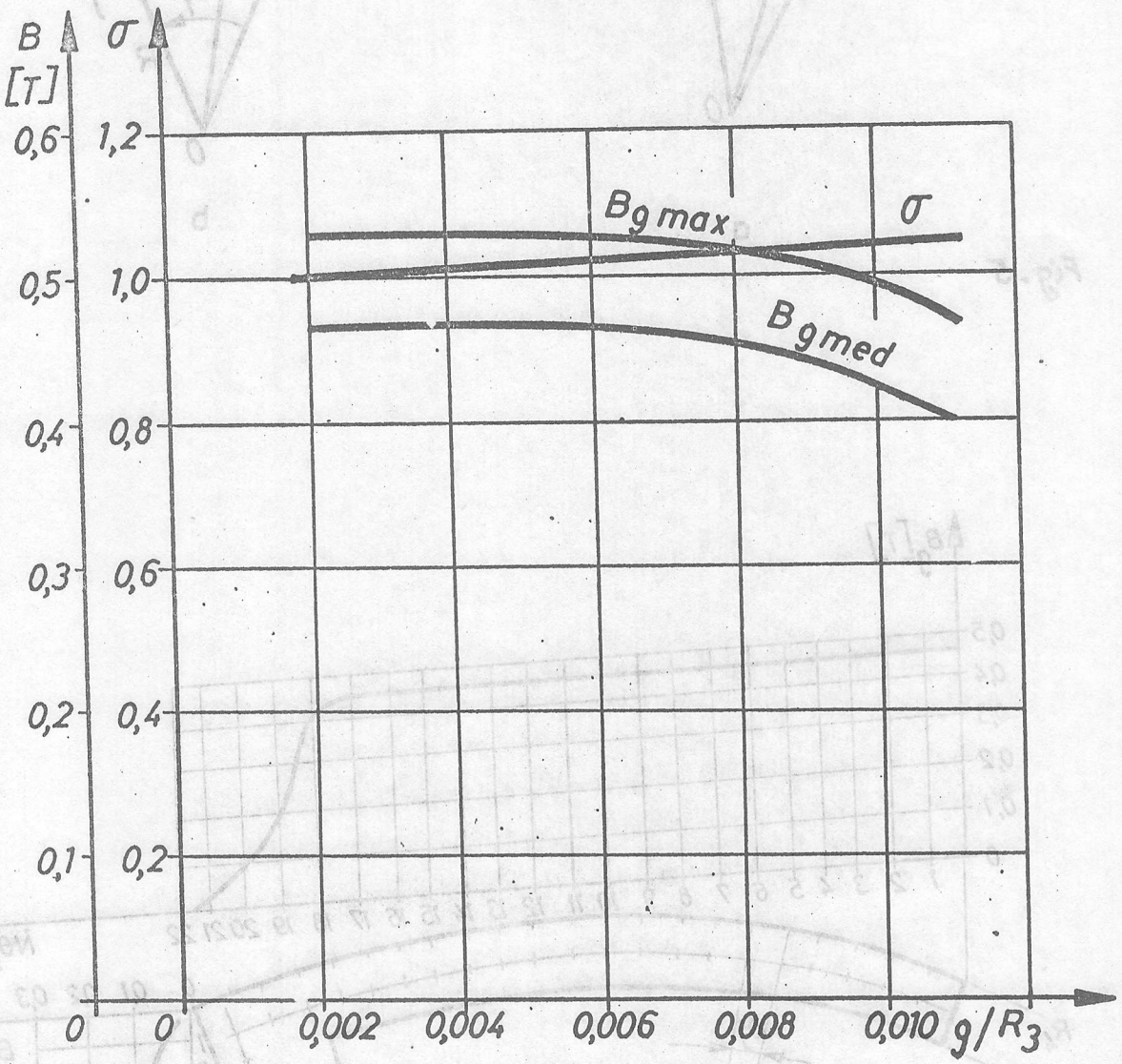
B
[T]
σ
0,6
1,2
0,5
1,0
0,4
0,8
0,3
0,6
0,2
0,4
0,1
0,2
0
0
0,002
0,004
0,006
0,008
0,010
g/R3
Bg max
σ
Bg med

Fig. 7

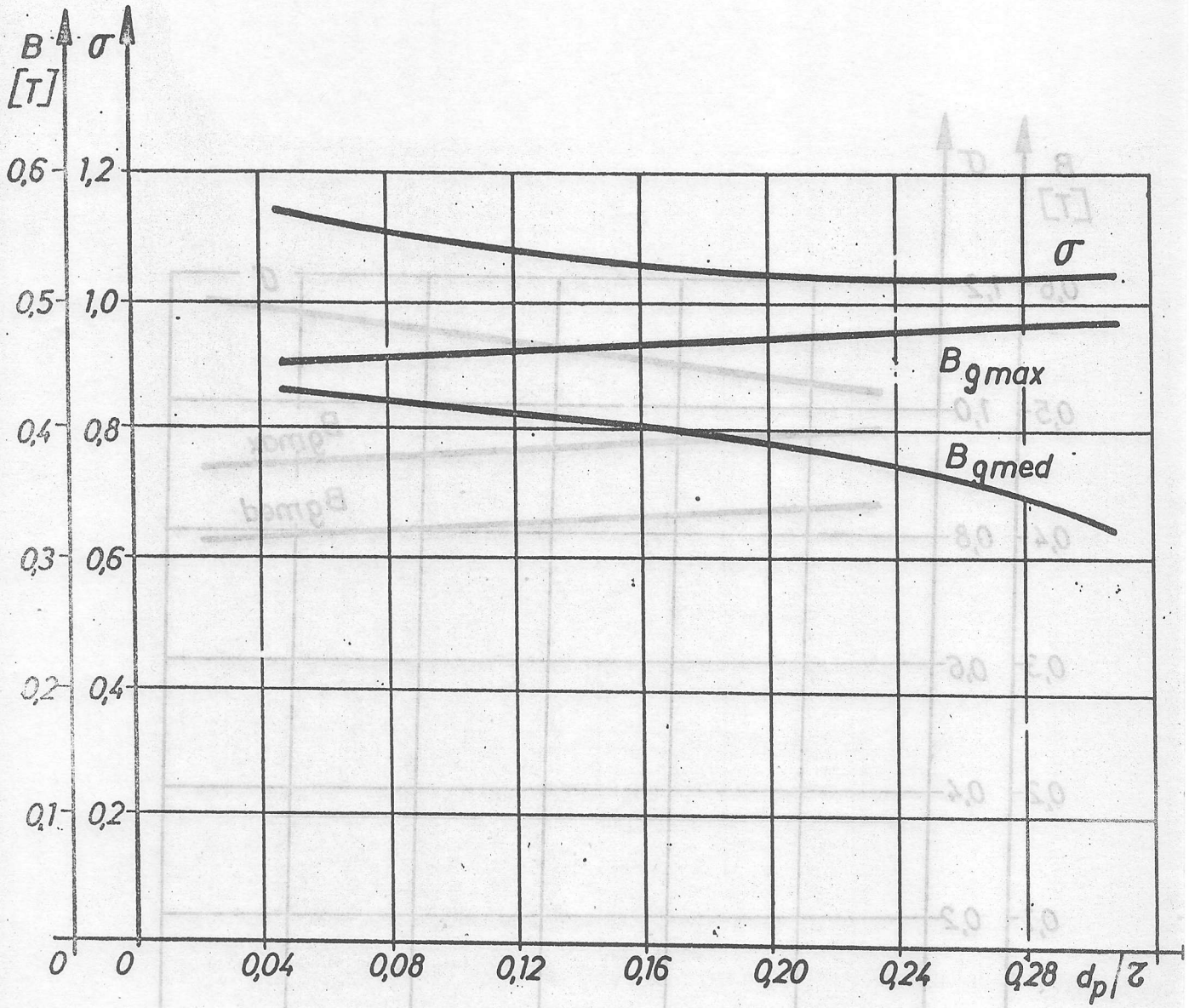
B [T]
σ
0,6
1,2
0,5
1,0
0,4
0,8
0,3
0,6
0,2
0,4
0,1
0,2
0
0
0,04
0,08
0,12
0,16
0,20
0,24
0,28
$d_p/2$
σ
B_{gmax}
B_{gmed}

Fig. 8

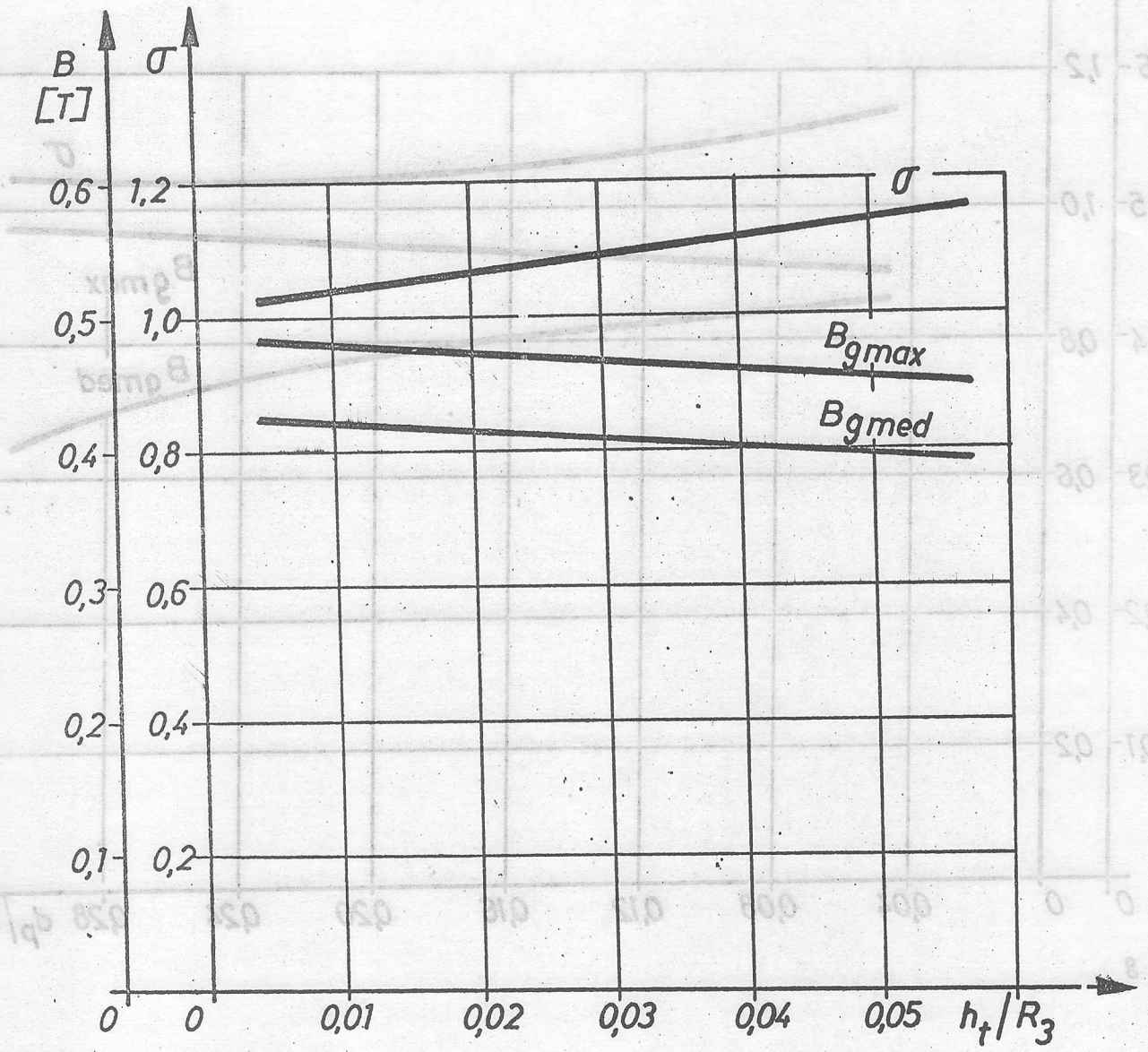
B [T]
σ
0,6
1,2
0,5
1,0
0,4
0,8
0,3
0,6
0,2
0,4
0,1
0,2
0
0
0,01
0,02
0,03
0,04
0,05
h_t/R_3
σ
$B_{g\,max}$
$B_{g\,med}$

Fig. 9

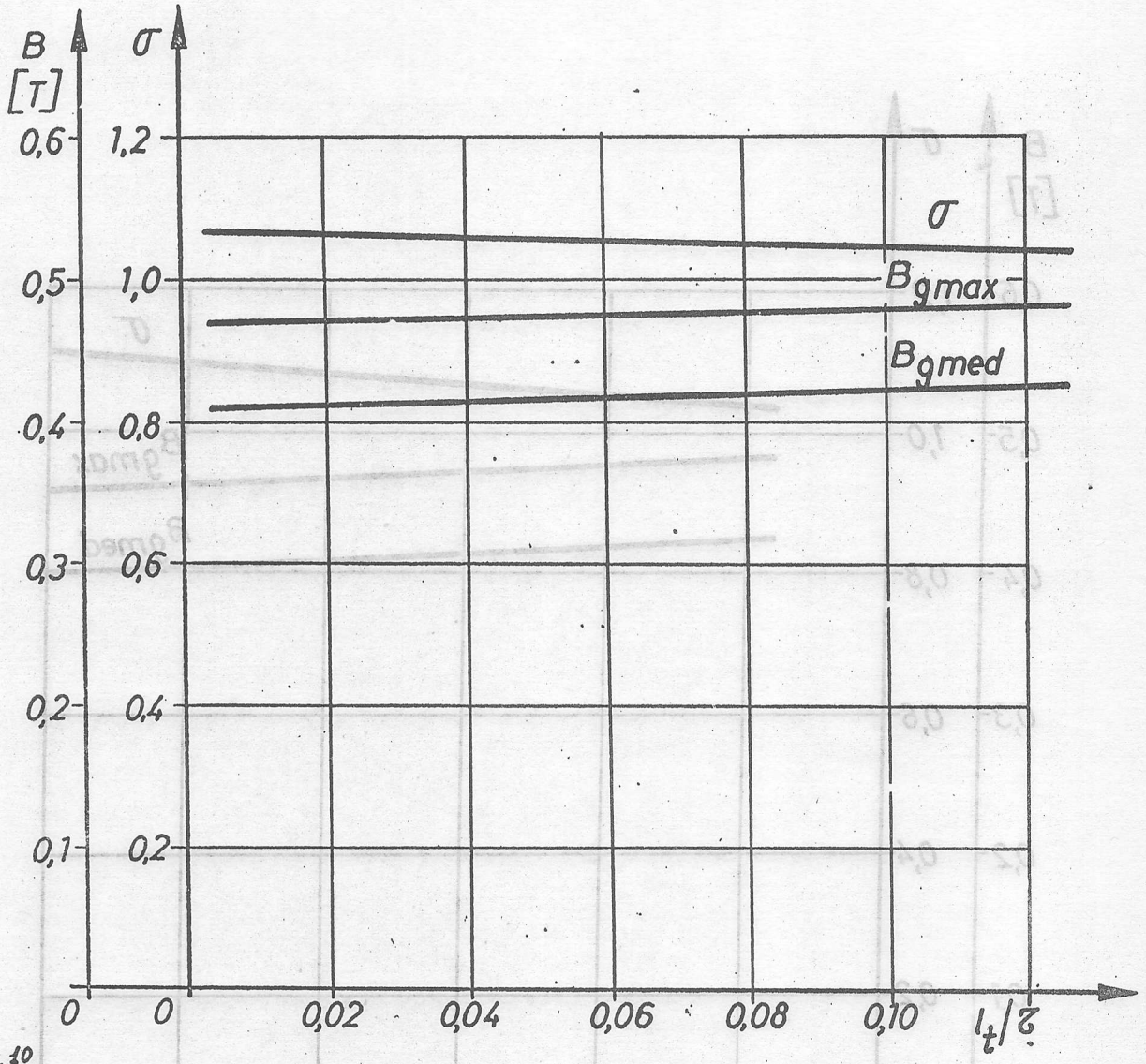
B [T]
σ
0,6
1,2
0,5
1,0
0,4
0,8
0,3
0,6
0,2
0,4
0,1
0,2
0
0
0,02
0,04
0,06
0,08
0,10
$l_t/2$
σ
B_{gmax}
B_{gmed}

Fig. 10

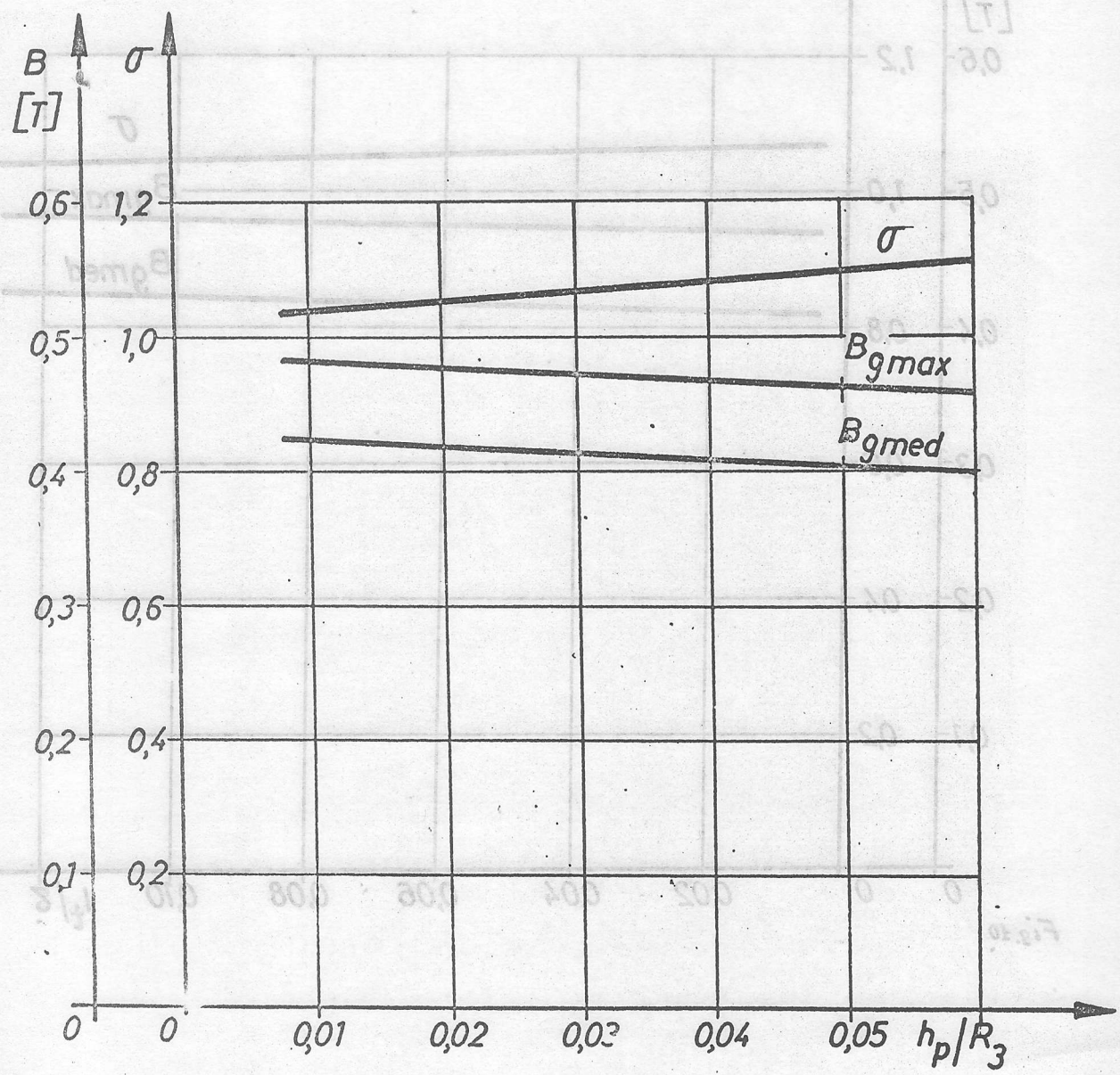
B
[T]
σ
0,6
1,2
0,5
1,0
0,4
0,8
0,3
0,6
0,2
0,4
0,1
0,2
0
0
0,01
0,02
0,03
0,04
0,05
h_p/R_3
σ
B_{gmax}
B_{gmed}

Fig. 11

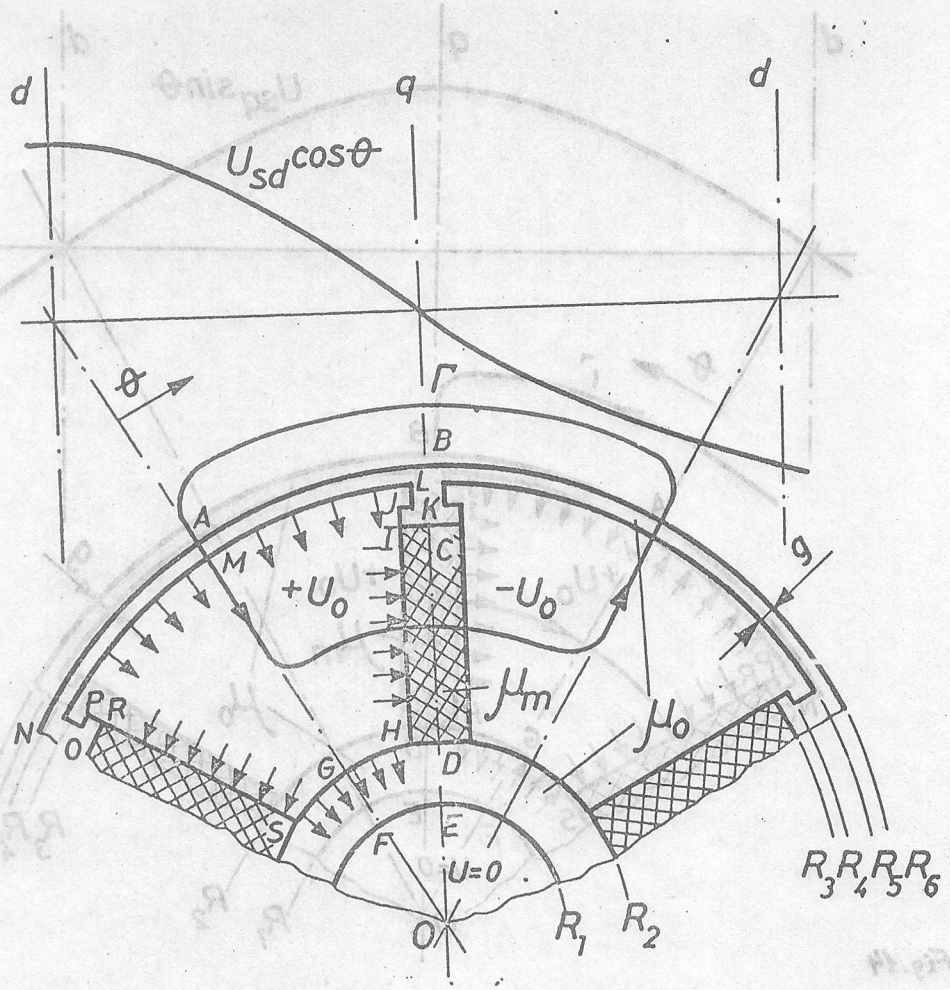
d
q
d
$U_{sd}\cos\vartheta$
ϑ
Γ
B
L
K
A
M
I
C
$+U_0$
$-U_0$
g
μ_m
μ_0
P
R
N
O
H
D
G
S
F
E
U=0
O
R_1
R_2
R_3 R_4 R_5 R_6

Fig. 12

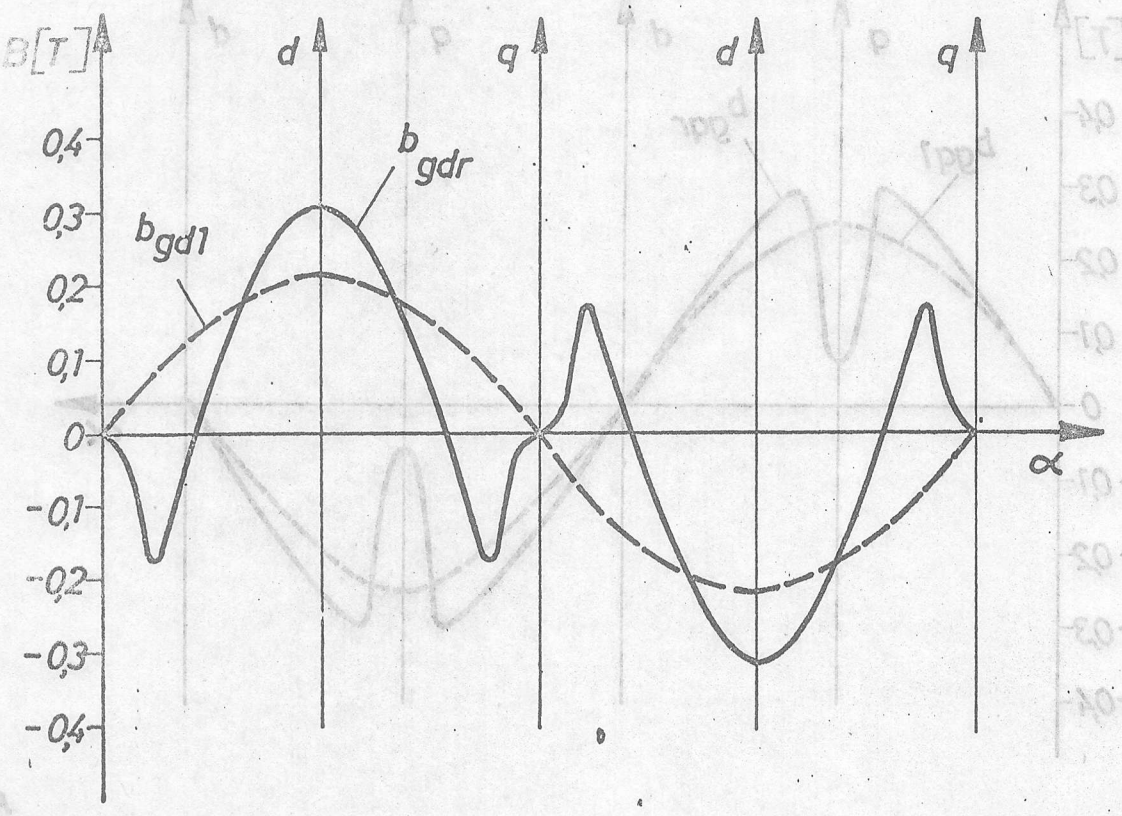
B[T]
d
q
d
q
0,4
0,3
0,2
0,1
0
-0,1
-0,2
-0,3
-0,4
b_{gdr}
b_{gd1}
α

Fig. 13

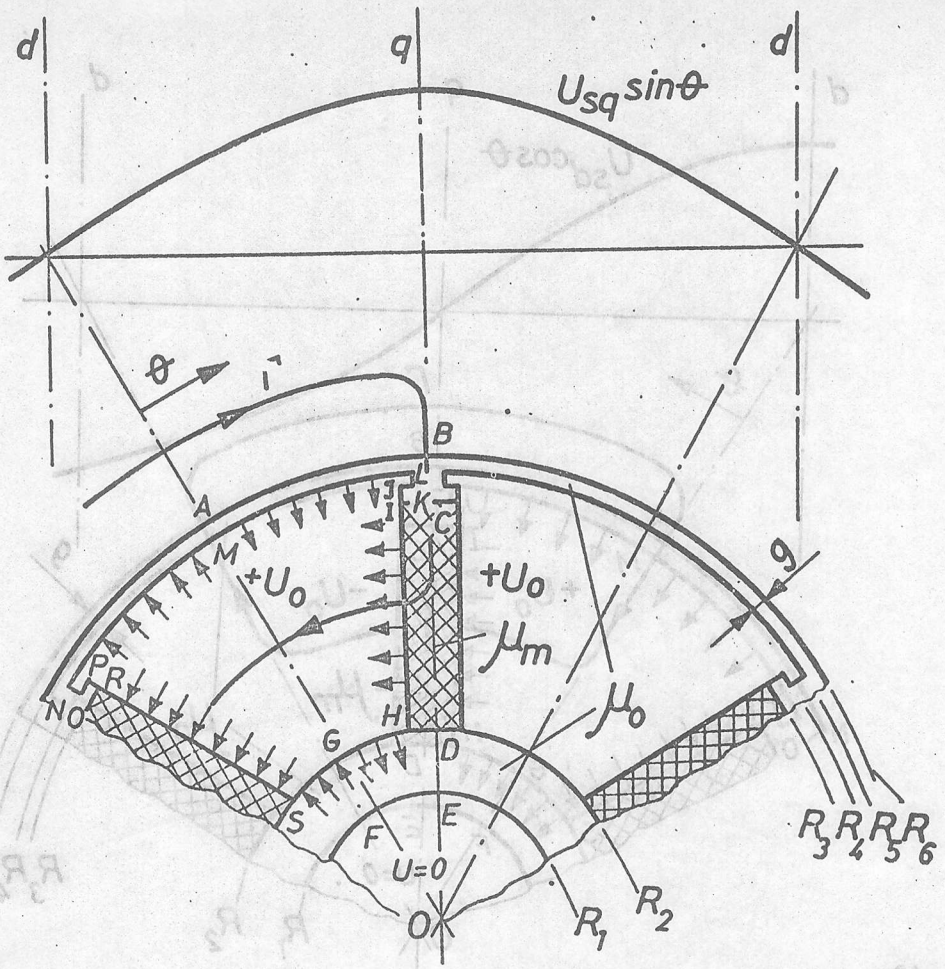
d
q
d
$U_{sq}\sin\vartheta$
ϑ
i
A
B
K
C1
M
$+U_0$
$+U_0$
μ_m
μ_0
g
P
R
N
O
H
G
D
S
F
E
U=0
O
R_1
R_2
R_3 R_4 R_5 R_6

Fig. 14

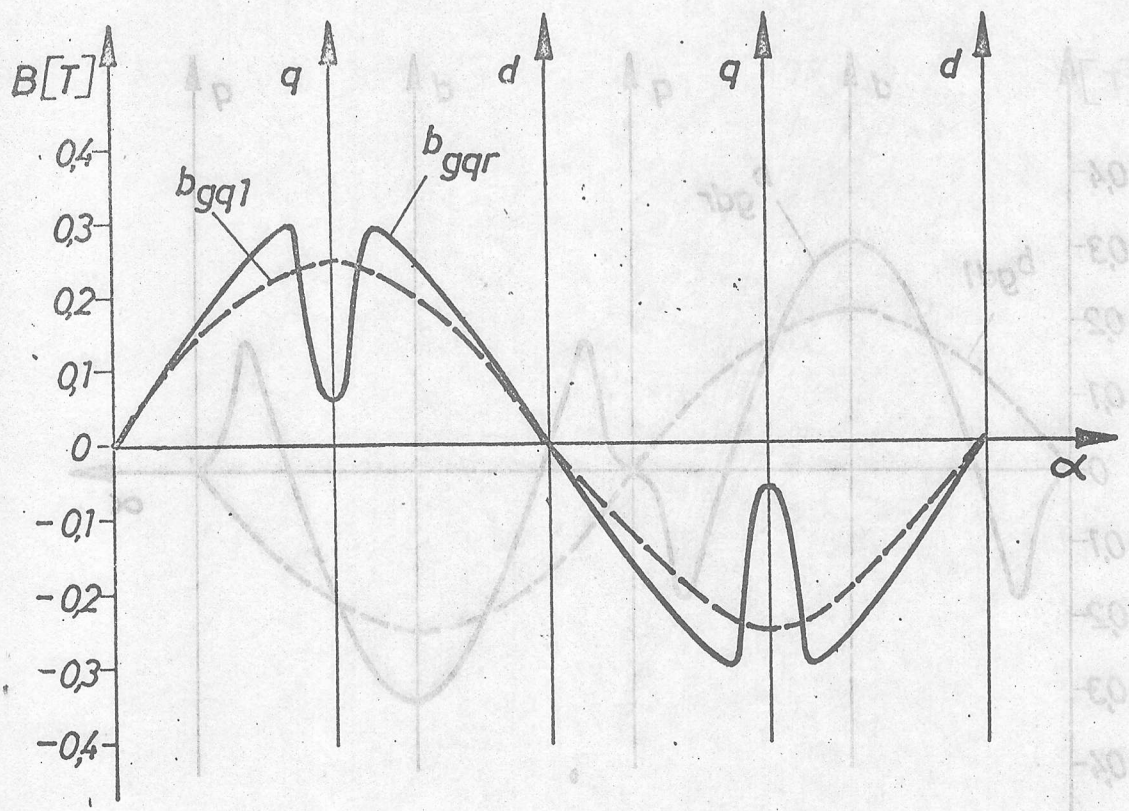
B[T]
q
d
q
d
b_{gq1}
b_{gqr}
0,4
0,3
0,2
0,1
0
-0,1
-0,2
-0,3
-0,4
α

Fig. 15

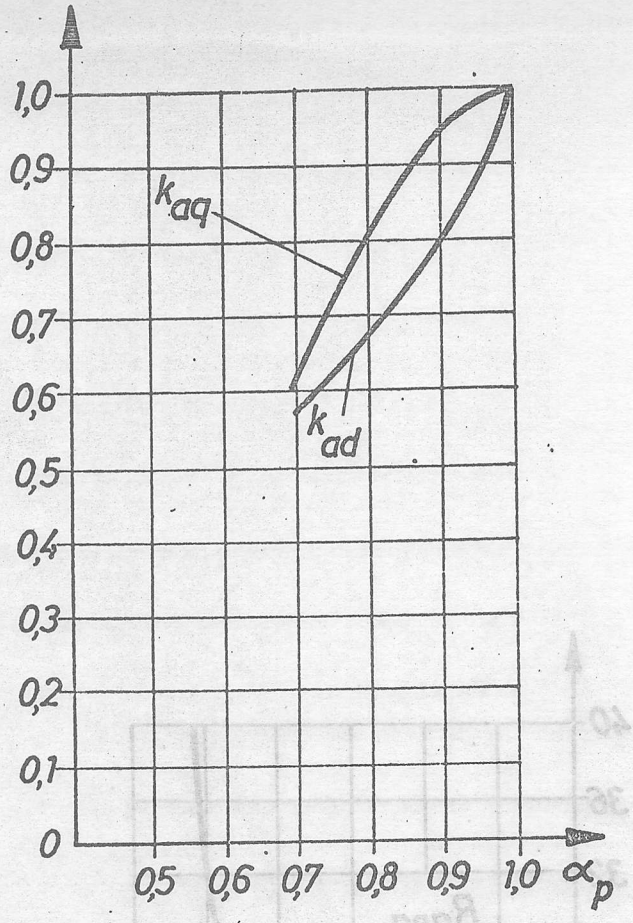
1,0
0,9
0,8
0,7
0,6
0,5
0,4
0,3
0,2
0,1
0
k_{aq}
k_{ad}
0,5 0,6 0,7 0,8 0,9 1,0 α_p

Fig. 16

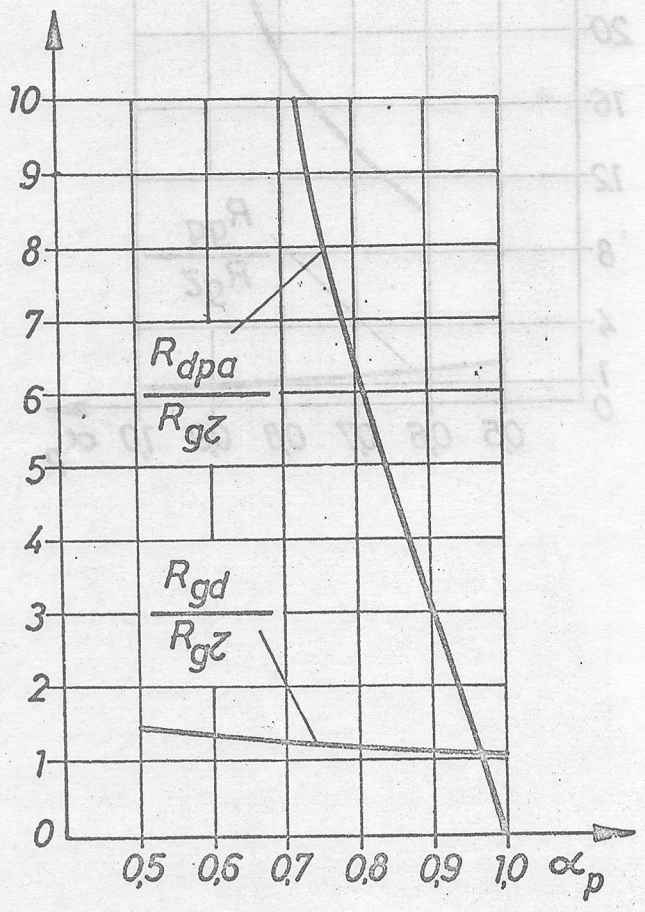
10
9
8
7
6
5
4
3
2
1
0
$\frac{R_{dpa}}{R_{gz}}$
$\frac{R_{gd}}{R_{gz}}$
0,5 0,6 0,7 0,8 0,9 1,0 α_p

Fig. 17

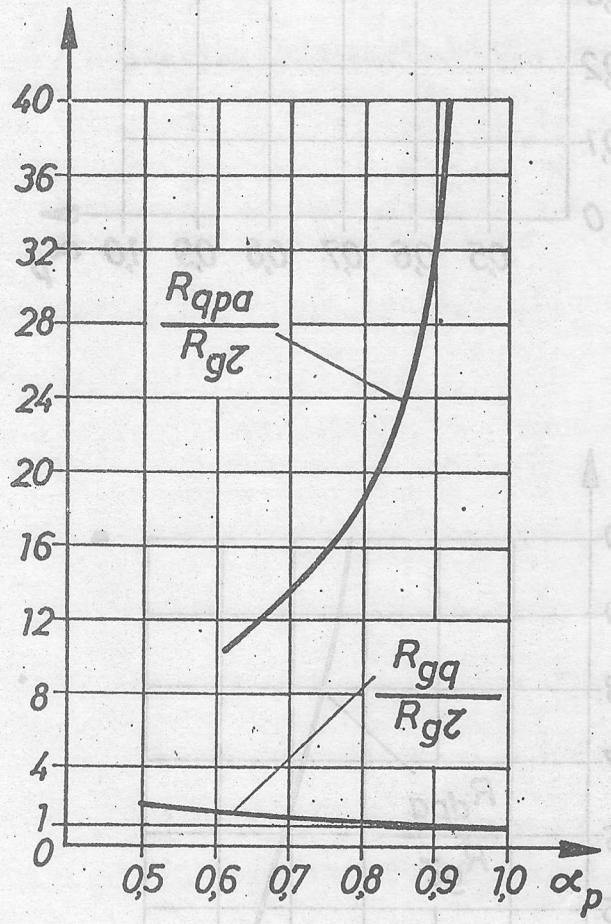
40
36
32
28
24
20
16
12
8
4
1
0
$\frac{R_{qpa}}{R_{gz}}$
$\frac{R_{gq}}{R_{gz}}$
0,5
0,6
0,7
0,8
0,9
1,0
α_p

Fig. 18